

Rochester Institute of Technology

RIT Digital Institutional Repository

Theses

12-1-2002

Response surface methodology of Die-Sink-Electro-Discharge machined surfaces

Bhairav Mehta

Follow this and additional works at: <https://repository.rit.edu/theses>

Recommended Citation

Mehta, Bhairav, "Response surface methodology of Die-Sink-Electro-Discharge machined surfaces" (2002). Thesis. Rochester Institute of Technology. Accessed from

This Thesis is brought to you for free and open access by the RIT Libraries. For more information, please contact repository@rit.edu.

RESPONSE SURFACE METHODOLOGY OF DIE-SINK ELECTRO-DISCHARGE MACHINED SURFACES

BY
BHAIKAV MEHTA

A THESIS SUBMITTED IN PARTIAL FULFILLMENT
OF THE REQUIREMENTS FOR THE MASTER OF SCIENCE DEGREE IN
INDUSTRIAL AND SYSTEMS ENGINEERING IN
KATE GLEASON COLLEGE OF ENGINEERING OF
ROCHESTER INSTITUTE OF TECHNOLOGY

INDUSTRIAL AND SYSTEMS ENGINEERING DEPARTMENT
ROCHESTER INSTITUTE OF TECHNOLOGY
ROCHESTER, NEW YORK

DECEMBER 2002

COMMITTEE MEMBERS

DR. ANDRES CARRANO
ASSISTANT PROFESSOR
INDUSTRIAL AND SYSTEMS ENGINEERING
ROCHESTER INSTITUTE OF TECHNOLOGY

DR. JACQUELINE MOZRALL
DEPARTMENT HEAD
INDUSTRIAL AND SYSTEMS ENGINEERING
ROCHESTER INSTITUTE OF TECHNOLOGY

KATE GLEASON COLLEGE OF ENGINEERING
ROCHESTER INSTITUTE OF TECHNOLOGY
ROCHESTER, NEW YORK

CERTIFICATE OF APPROVAL

MASTER OF SCIENCE DEGREE THESIS

The M.S. Degree Thesis of Bhairav H. Mehta
has been examined and approved by the thesis committee
as satisfactory for the thesis requirement for the
Master of Science degree.

Dr. Andres Carrano, Ph.D. *Advisor*

Dr. Jacqueline Mozrall , Ph.D.

RIT Thesis Binding Procedure

Thesis Reproduction Permission Statement

Permission granted

TITLE OF THESIS:

**RESPONSE SURFACE METHODOLOGY OF DIE-SINK ELECTRO-DISCHARGE
MACHINED SURFACES**

I, **BHAIRAV MEHTA**, hereby **grant permission** to the RIT Library of the Rochester Institute of Technology to reproduce my thesis in whole or in part. Any reproduction will not be for commercial use or profit.

Date: 07/01/03 Signature of Author: _____

ABSTRACT

The performance of most manufacturing processes depends on numerous parameters and their interactions. Most of the time, selection of an appropriate set of machining parameters is done based on experience, trial and error or both. Electro-discharge machining (EDM) process is complicated and random in nature. The large number of parameters and the inherent complexity of removal mechanism taking place in EDM make it even more difficult to select machining conditions for optimal performance. The objective of this study is to provide information on the relationships between the key input variables and resultant surface roughness and to develop a response model for surface roughness optimization utilizing factorial designs, direction of steepest descent method and response surface methodology (RSM). Experiments were setup and executed to understand the individual and combined impact of factors that included the following input variables: gap voltage, depth of penetration, electrode type, and average current and pulse duration. Six iterations were executed in the direction of steepest descent for minimization of surface roughness. Pulse duration and average current have been shown to have significant effect on surface roughness. Depth of penetration was found to be insignificant and was eliminated in the subsequent experiments. Graphite electrode gave better surface finish than copper electrode at given factor level combination. The results shows that graphite electrode can be used in finishing operation while achieving the unprecedented surface quality that was only attainable with copper electrode in such operations. The best surface roughness $0.96\mu\text{m Ra}$ was achieved. Response surface model based on a central composite experimental design was established to give better idea about the relationship between significant parameters, their interactions and surface finish. A higher order model is developed that can relate process inputs to response. The results obtained may be used to recommend process setting to improve process robustness and to get the desired surface roughness.

ACKNOWLEDGEMENT

I am grateful to many people who have contributed to this thesis, and who made my time in the Industrial and Systems Engineering (ISE) Department at Rochester Institute of Technology a great learning and intellectual experience. Many people contributed to the evolution of this research, and it has been enriched because of them.

First I would like to thank my thesis advisor Dr. Andres Carrano for his patience, guidance, offering direction, penetrating criticism and seemingly boundless enthusiasm. His input and direction were invaluable in the creation of this thesis, and the research it contains. I would also like to thank committee member Dr. Jacqueline Mozrall for her inputs and interest. I would like to thank Hardinge Inc., Elmira, New York for providing EDM machine tools for experimental work.

Much of this work was completed at Brinkman Manufacturing Laboratory, Industrial and Systems Engineering Department at Rochester Institute of Technology. I particularly owe a great deal to Mr. Martin Hass, Facilities Manager, Center of Integrated Manufacturing Studies (CIMS) and Mr. Charles Quick, Student Assistant for training me on Electro-discharge machine and their help through out my experimental work. I would also like to thank Mr. Thomas Barker, Assistant Professor and other faculties at Center for Quality and Applied Statistics at Rochester Institute of Technology for their continuous help during analysis phase of this thesis.

Current and former members of manufacturing research group at Industrial and Systems Engineering department at Rochester Institute of Technology in last 2 years have greatly contributed to this thesis, and to making work fun and stimulating: Hitesh Kataria, Bhavin Vora, Patricia Polanco, Luis Alvarez, Deness Vyas, James Cordero and everyone else. I benefited greatly from the weekly meetings of the Manufacturing Research Group.

My love and thanks goes to my parents and siblings for their unwavering encouragement and support through out my graduate studies.

TABLE OF CONTENTS

Abstract.....	i
Acknowledgement.....	ii
List of Figures.....	v
List of Tables.....	vii
1. Introduction.....	1
1.1 Statement of Problem.....	3
2. Background.....	4
2.1 Overview	4
2.1.1 Electro-Discharge Machining (EDM) Process.....	4
2.1.1.1 Overview of production processes.....	4
2.1.1.2 Types of EDM processes.....	5
2.1.1.3 Die-sink EDM Process.....	5
2.1.1.4 The mechanical system.....	7
2.1.1.5 The electrical system.....	8
2.1.1.5.1 Circuit performances and cycles.....	9
2.1.1.6 The dielectric system	12
2.1.1.7 Different phases of discharges.....	13
2.1.1.7.1 The Ignition Phase.....	13
2.1.1.7.2 Formation of plasma channel.....	13
2.1.1.7.3 Melting and evaporation.....	15
2.1.1.7.4 Ejection of the liquid metal	15
2.1.1.8 Major process parameters in die-sink EDM.....	16
2.1.1.9 Surface integrity from die-sink EDM process.....	18
2.1.1.9.1 White layer	19
2.1.1.9.2 Heat affected zone.....	20
2.1.1.9.3 Base material.....	20
2.1.2 Advantages and drawbacks of EDM.....	21
2.1.3 Response surface methodology.....	24
2.1.4 Direction of steepest descent method	25
2.1.2 Iterative response surface methodology.....	28

2.2 Literature review.....	30
3. Methodology.....	35
3.1 Overview of the experiment.....	35
3.2 Experimental Setup.....	35
3.2.1 Specimen	36
3.2.2 Toolings.....	38
3.2.3 Metrology.....	41
4. Experimentation.....	42
4.1 Screening experiment.....	43
4.2 First iteration.....	45
4.3 Second iteration	46
4.4 Third iteration	47
4.5 Fourth iteration	48
4.6 Central composite design	49
5. Results and Analysis	50
5.1 2^5 full factorial design (screening experiment).....	51
5.2 2^4 full factorial design with center point (first iteration experiment).....	60
5.3 2^4 full factorial design with center point (second iteration experiment)	66
5.4 2^4 full factorial design with center point (third iteration experiment)	72
5.5 2^4 full factorial design with center point (fourth iteration experiment)	78
5.6 Central composite design.....	84
6. Conclusion	91
7. Future Work.....	94
8. References.....	95
9. Appendices.....	99
9.1 Hansvedt MS-50C CNC RAM electrical discharge machine manual.....	100
9.2 Heidenhain TNC406 erosion table.....	101
9.3 CNC program for machining.....	102
9.4 Mitutoyo SJ 401 surface roughness profilometer manual.....	103
9.5 Theory for direction of steepest descent step size calculation.....	104
9.6 Surface roughness descriptors.....	105
9.7 Detailed results of experiments.....	107

LIST OF FIGURES

Figure 2.1 Three different types of EDM.....	5
Figure 2.2 EDM System.....	6
Figure 2.3 Schematic of R-C relaxation circuit.....	8
Figure 2.4 Modern type generator.....	9
Figure 2.5 Current –Voltage curves at different stages.....	10
Figure 2.6 Schematic representation of plasma channel.....	11
Figure 2.7 EDM process mechanism.....	14
Figure 2.8 Pulse train.....	16
Figure 2.9 Typical EDM surface.....	18
Figure 2.10 Transverse section of Inconel Alloy 718 EDM surface.....	19
Figure 2.11 Taper effect.....	23
Figure 2.12 A theoretical response surface showing relationship between response “R” and variables “a” and “b”.....	24
Figure 2.13 First order response surface and path of steepest descent.....	25
Figure 2.14 Flowchart for the first phase of experimental optimization procedure.....	27
Figure 2.15 Iterative Response surface methodology.....	29
Figure 3.1 Schematic of parameter and response.....	35
Figure 3.2 5 Axis CNC RAM EDM machine.....	36
Figure 3.3 Experimental specimen setup.....	37
Figure 3.4 Specimen after experimental runs.....	38
Figure 3.3 Graphite and copper electrode properties.....	40
Figure 3.4 Electrodes and tool holder.....	40
Figure 3.5 A typical EDM profile obtained from Mitutoyo SJ 401 profilometer.....	41
Figure 3.6 Evaluation length and measurement procedure for profilometer.....	41
Figure 3.7 Block diagram for experimental order.....	42
Figure 4.1 Experimental setup for screening experiment iteration.....	44
Figure 4.2 Experimental setup for first iteration.....	45
Figure 4.3 Experimental setup for second iteration.....	46
Figure 4.4 Experimental setup for third iteration.....	47
Figure 4.5 Experimental setup for fourth iteration.....	48
Figure 4.6 Experimental setup for Central Composite design.....	49

Figure 5.1 Pareto chart of the standardized effects of screening experiment.....	57
Figure 5.2 Main effects plot for screening experiment.....	57
Figure 5.3 Interaction plots for screening experiment.....	58
Figure 5.4 Pareto chart of the standardized effects of first iteration experiment.....	63
Figure 5.5 Main effects plot for first iteration experiment.....	63
Figure 5.6 Interaction plots for first iteration experiment.....	64
Figure 5.7 Pareto chart of the standardized effects of second iteration experiment.....	69
Figure 5.8 Main effects plot for second iteration experiment.....	69
Figure 5.9 Interaction plots for second iteration experiment.....	70
Figure 5.10 Pareto chart of the standardized effects of third iteration experiment.....	75
Figure 5.11 Main effects plot for third iteration experiment.....	75
Figure 5.12 Interaction plots for third iteration experiment.....	76
Figure 5.13 Pareto chart of the standardized effects of fourth iteration experiment.....	81
Figure 5.14 Main effects plot for fourth iteration experiment.....	81
Figure 5.15 Interaction plots for fourth iteration experiment.....	82
Figure 5.15 Pareto chart of the standardized effects of central composite design experiment.....	86
Figure 5.16 Main effects plot for central composite design experiment.....	86
Figure 5.17 Response surfaces for individual two factor interactions.....	87
Figure 5.18 Contour plots and response surfaces for individual 2 factor interactions.....	88
Figure 5.19 Relative effect of change in response of central composite design experiment.....	100
Figure 9.1 Hansvedt MS-50C 5 Axis CNC RAM EDM machine.....	103
Figure 9.2 Mitutoyo SJ 401 surface roughness profilometer.....	105
Figure 9.4 Arithmetic mean deviation of profile, Ra.....	105
Figure 9.5 Root mean square deviation of profile, Rq.....	106
Figure 9.6 Maximum height of Profile, Ry.....	106
Figure 9.7 Ten-point height of irregularities, Rz.....	107
Figure 9.8 Skewness of profile, Rku.....	107
Figure 9.9 Kurtosis of the profile, Rku.....	107

LIST OF TABLES

Table 3.1 Material specification of workpiece material.....	36
Table 4.1 Factor levels for first iteration experiment.....	43
Table 4.2 Treatment combinations for first iteration experiment.....	44
Table 4.3 Factor levels for second iteration experiment.....	45
Table 4.4 Treatment combinations for second iteration experiment.....	45
Table 4.5 Factor levels for third iteration experiment.....	46
Table 4.6 Treatment combinations for third iteration experiment.....	46
Table 4.7 Factor levels for fourth iteration experiment.....	47
Table 4.8 Treatment combinations for fourth iteration experiment.....	47
Table 4.9 Factor levels for central composite design experiment.....	48
Table 4.10 Treatment combinations for second iteration experiment.....	48
Table 4.11 Factor levels for central composite design experiment.....	49
Table 4.12 Treatment combinations for second iteration experiment.....	49
Table 5.1 Responses of measured parameters for screening experiment.....	51
Table 5.2 Analysis of variance for screening experiment.....	55
Table 5.3 Estimated effects and coefficient (screening Experiment).....	56
Table 5.4 Responses of measured parameters for first iteration experiment.....	60
Table 5.5 Analysis of variance for first iteration experiment.....	61
Table 5.6 Estimated effects and coefficient (first iteration).....	62
Table 5.7 Responses of measured parameters for second iteration experiment.....	66
Table 5.8 Analysis of variance for second iteration experiment.....	67
Table 5.9 Estimated effects and coefficient (second iteration).....	68
Table 5.10 Responses of measured parameters for third iteration experiment.....	72
Table 5.11 Analysis of variance for third iteration experiment.....	73
Table 5.12 Estimated effects and coefficient (third iteration).....	74
Table 5.13 Responses of measured parameters for fourth iteration experiment.....	78
Table 5.14 Analysis of variance for fourth iteration experiment.....	79
Table 5.15 Estimated effects and coefficient (fourth iteration).....	80
Table 5.16 Responses of measured parameters for central composite design experiment....	84
Table 5.17 Analysis of variance for central composite design experiment.....	85
Table 5.18 Estimated effects and coefficient for Ra.....	85

Table 9.1 Specifications for Hansvedt MS 50C RAM electro-discharg machine.....	100
Table 9.2 Heidenhain TNC 406 Erosion table.....	101
Table 9.3 Specifications for Mitutoyo SJ 401 surface roughness profilometer.....	111
Table 9.4 Detailed results of measured response of screening experiment (first replicate)...	108
Table 9.5 Detailed results of measured response of screening experiment (second replicate).....	109
Table 9.6 Detailed results of measured response of first iteration experiment (first replicate).....	110
Table 9.7 Detailed results of measured response of first iteration experiment (second replicate).....	111
Table 9.8 Detailed results of measured response of second iteration experiment (first replicate).....	112
Table 9.9 Detailed results of measured response of second iteration experiment (second replicate).....	113
Table 9.10 Detailed results of measured response of third iteration experiment (first replicate).....	114
Table 9.12 Detailed results of measured response of fourth iteration experiment (first replicate).....	115
Table 9.14 Detailed results of measured response of central composite design experiment (first replicate).....	116
Table 9.15 Detailed results of measured response of central composite design experiment (second iteration).....	117

1. INTRODUCTION

Electro Discharge Machining (EDM) is the most widely recognized and used nontraditional machining process in the industry today. It is a thermal erosion process whereby material is removed from an electrically conductive material immersed in a liquid dielectric with a series of randomly distributed discrete electric sparks or discharges between the shaped tool electrode and the workpiece. It has been used widely in production of medical devices, extrusion dies, fuel injector nozzles, aircraft engine turbine blades and machining of difficult-to-machine materials like tool steel and cemented carbides. It has radically transformed and facilitated the production of tools, dies and molds due to its capability of producing fine details. EDM provides good accuracy and repeatability, however the tradeoff is a very low material removal rate, long machining time, high relative tool wear accompanied by thermal damage of the machined surface due to high heat generated during the discharge pulses. The ever-increasing demands for electro-discharge machining in recent years have turned it into the most prevalent nontraditional machining method in the industry.

An EDM surface is the consequence of random superimposition of roughly spherical craters produced by electric discharge. Each spark erodes a small bit of metal, leaving crater in the surface. As the process progresses and the electrode advances to maintain a constant gap, a hole or cavity is generated in reverse image of the electrode. The electrical discharges generate an enormous amount of heat, which causes local melting and vaporization of the workpiece material. In addition, high local temperatures cause vaporization and cavitations of the dielectric fluid, generating pressure forces and expelling the molten metal in the dielectric fluid. The top surface of the workpiece resolidifies and cools at very high rate. These recurring and continuous moments of high-temperature and high-pressure result in rapid heating and cooling reactions on the workpiece surface. These reactions cause structural changes and surface defects. Surface cracks are developed due to high temperature gradient, which induces fatigue failures in EDM workpieces. Additional plastic deformation may result in residual stresses accumulating in the workpiece, having great influence on the mechanical properties and service life of EDM workpiece such as tools and dies. It is required to understand the change in surface quality with variation in factor levels settings to minimize defects.

The selection of EDM parameters is important in determining accuracy and surface finish obtained for a particular application. Among the numerous parameters affecting EDM performance discussed in past research electrode material, average current, gap voltage and pulse duration has a very important role. As an electrode material graphite and copper electrodes are most widely used in industry. Copper electrode is used because it has high electric and thermal conductivity. It is easily available, consistent in quality and low in cost. Graphite electrode has main advantage of outstanding machinability and the ease with which fine detailed electrodes can be produced. Average current and pulse duration has significant effects on surface roughness of EDM workpiece. Other factors considered during analysis of EDM surfaces are dielectric flushing type, type of dielectric fluid and depth of penetration, which were found to have significant effect on surface quality. Pulse duration is more important as during that time current is generated, gap is bridged and machining is done. Longer the duration more material is removed and resulting craters will be bigger and deeper in size amounting to bad surface quality. Average current plays vital role in this process as higher current produces poor surface quality. Gap voltage is the factor, which control spark gap higher the gap voltage wider is the spark gap between the electrode and workpiece. The interaction effects of these factors are very important for analysis. The surface roughnesses obtained at various factor level combinations are unpredictable as the factors behave unconventionally when they are put together in interaction of each other.

The quality of surface roughness obtained is a factor of importance in the evaluation of any machine tool's productivity. Post finishing operation is addition to production cost and time spent in arriving at an acceptable finish has inevitably reduced manufacturing efficiency of the process. EDM manufacturers and users are always interested in acquiring better stability and higher productivity in the machining process. The higher rate of material removal with desired accuracy and minimal surface damage make the EDM operation less costly and the process more economically viable and affordable. Comprehensive experimental study is required to understand the trend in the surface roughness change with respect to factor level combinations.

1.1 STATEMENT OF PROBLEM

Surface damage due to EDM processes causes adverse effect on the reliability and the performance of components. In current practice the damaged layers of EDMed surfaces are removed either by finishing passes or by chemical milling, which is an added cost to the machining cost. Knowledge of extent of surface damage is essential for the subsequent finishing operations. Due to large number of variables and stochastic nature of the process, even a highly skilled operator is rarely able to achieve the optimal performance. Most of the EDM equipments are probably performing at lower efficiency level. An effective way to solve this problem is to determine the relationship between the performance of the process and its controllable input parameters (i.e. model the process through suitable mathematical techniques).

A quantitative characterization of the surface taking into account the randomness of its generation and reflecting the peculiarities arising from the electrical discharge is needed so that factor level combination can be obtained at which the desired surface finish can be achieved. The execution of this exercise will need understanding of the limits i.e. best possible surface, process robustness against the perturbations on the process parameters, achieving targets by getting the data at what combination of parameters the EDM surface would achieve specific roughness and understanding the interaction between the parameters. The experimental design approach to this problem may give the insight of the process robustness issues. The design of experiment will consider several factors and interaction effects among them pertaining to the process and response measured will be surface roughness. The objective of this research is to develop mathematical models for surface roughness in die-sink electro-discharge machining by response surface methodology in order to optimize the surface finish of the machined surface. The optimum machining condition is obtained by constructing contours of constant surface roughness and used for determining the optimum cutting condition for required surface roughness.

2. BACKGROUND

2.1 OVERVIEW

This chapter reviews the fundamentals as well as research conducted EDM physics and technology. The first section introduces the electro-discharge machining as an important and versatile production tool. The principle of EDM and its operation are discussed. Various process parameters involved in the process and basic R-C (Resistor–Capacitor) relaxation electrical circuits involved in the operation are also overviewed. Lastly, the statistical methods of Direction of Steepest Descent and Response Surface Methodology used in the experimentation are also explained.

2.1.1 Electrical Discharge Machining (EDM)

2.1.1.1 Overview of the production processes

In general, three traditional categories of production processes can be distinguished:

- The process that start from excess of material and that remove part of the material as necessary (removal processes)
- The process that starts from no material and that build up the workpiece layer by layer by adding material only where it is necessary (material accretion processes) or additive processes
- The processes that starts from correct amount of material and that change the shape of the material (deformation processes)

Examples of material accretion processes are stereolithography, laminated object mfg. Casting and forging comes into forming technology and classical metal removal processes are turning, milling, drilling and grinding. More recently non-traditional processes as ultrasonic machining, water jet machining or abrasive jet machining have been developed. A sub-category of non-traditional removal processes is based on thermal effects. Examples of those processes are laser beam machining, plasma beam machining and electro-discharge machining (EDM).

2.1.1.2 Types of EDM

Three different types of EDM processes can be distinguished: wire, Die-sink or RAM and EDM-Milling. In wire EDM, a constantly renewed wire is used to cut a path through the workpiece (fig 2.1). In die-sink EDM, a tool electrode with opposite shape of cavity that is desired “sinks” into the workpiece and erodes the workpiece material. In this type of process, the electrode could process different geometries but only sink downwards. The third type of EDM, the so-called EDM-milling is an evolution of diesinking. In the process of EDM-milling, the desired workpiece shape is machined using standard cylindrical electrodes that describe the necessary paths through the workpiece to obtain finally the desired result. Material removal mechanism in all types of EDM is based on successive electrical discharge that are produced between the electrode and the workpiece, which are both submerged in a fluid dielectric and separated by a small distance. The focus of this research is on die-sink EDM Processes. A detailed discussion of the die-sink EDM process is given in a continuation.

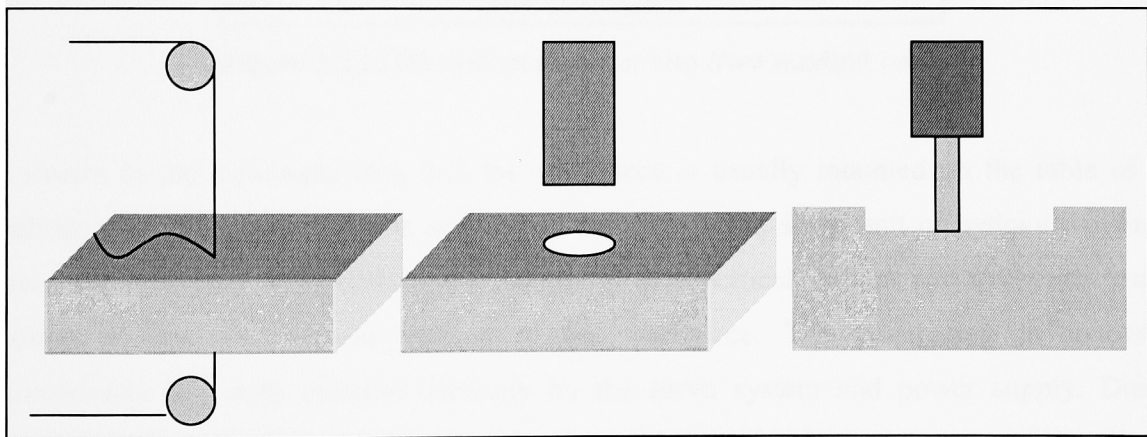


Figure 2.1 The three different types of EDM

Wire cutting EDM (left), Die-sinking (middle), EDM-milling (right)

2.1.1.3 Die-sink EDM process:

Electrical Discharge machining is the process of removing conductive material through the action of a controlled electrical discharge of short duration and high current density. In this case, a series of non-stationary and transient discrete electric sparks or discharges are used to erode a conductive surface. This electrical discharge transferred from a tool, through a dielectric media and into a workpiece creates a localized intense heat on the workpiece. As this

occurs, material melts and/or vaporizes away from the surface of the workpiece, leaving a cavity in the workpiece that is the negative of the tool geometry. As steep temperature gradient develops on the workpiece, rapid quenching occurs through conduction and circulating effects of the dielectric medium.

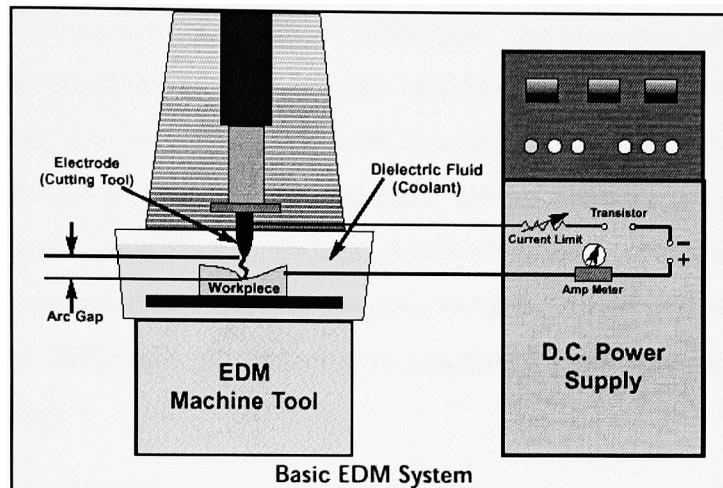


Figure 2.2 EDM system (Source: <http://www.edmtt.com>)

As shown in the schematic (Fig 2.2) the workpiece is usually mounted on the table of the machine tool and the electrode is attached to the ram. A DC servo unit or hydraulic cylinder moves the ram (and consequently the electrode) in a vertical motion and maintains proper position of the electrode in relation to the workpiece. The positioning is controlled automatically and with extreme accuracy by the servo system and power supply. During normal operation the electrode never touches the workpiece, but instead is separated by a small spark gap. During operation, the ram moves the electrode toward the workpiece until the space between them is such that the voltage in the gap can ionize the dielectric fluid and allow an electrical discharge (spark) to pass from the electrode to the workpiece. These spark discharges are pulsed on and off at a high frequency cycle. The spark discharge (arc) always travels the shortest distance across the narrowest gap to the nearest or highest point on the workpiece. The amount of material removed from the workpiece with each pulse is directly proportional to the energy it contains. Each discharge melts or vaporizes a small area of the workpiece surface. This molten metal is then cooled in the dielectric fluid and solidifies into a small spherical particles (swarf), which is flushed away by pressure/motion of the dielectric fluid. The impact

of each pulse is consequently limited to a very localized area, the location of which is determined by the form, position and surface characteristics of both the electrode and workpiece.

In EDM, Both the workpiece and electrode are submerged in a dielectric fluid, which acts as an electrical insulator to help control the spark discharges. the dielectric fluid also performs the function of a coolant medium and reduces the extremely high temperatures in the arc gap. More importantly, the dielectric fluid is pumped through the arc gap to flush away the eroded particles between the workpiece and the electrode. Proper flushing is critical to high metal removal rates and good machining conditions. A relatively soft graphite or metallic electrode can easily machine hardened tool steels or tungsten carbide. This is one of the many attractive benefits of using the EDM process. Rather than machine a workpiece before heat-treating, it can be EDM afterward.

The three main systems in an EDM machine are listed below and explained as continuation:

1. The mechanical system
2. The electrical system
3. The dielectric system

2.1.1.4 The mechanical system

The mechanical system of an EDM machine is responsible for of the relative motion of tool electrode. In simple machines, the X-Y position of the workpiece is controlled via manual system, while in more sophisticated design five or more servo-controlled machines are present. However, the motion in the feed (plunge) direction is always servo controlled. This is necessary to keep the gap between tool and electrode constant. Although there are no cutting forces involved in EDM, some substantial forces can exist especially with high electrode masses or servo accelerations. Additionally, when machining large surfaces hydraulic flushing forces can also become very high. Therefore, a robust machine frame is needed. Nowadays, the machines are equipped with CNC controlled axes and complex movements of the electrode with respect to the workpiece can be realized, as in for example the orbital movement used in

planetary EDM sinking. Automatic machining cycles for obtaining spheres, conical shapes or even threading are available.

2.1.1.5 The electrical system

The electrical system of an EDM comprises the generator, which generates the electrical pulses, the feed control and the cables for the power supply to electrode and workpiece. In the early types of EDM machines, the generator were of the relaxation type, In such generator, the DC power supply charges a capacitor, which increases the electrical tension over the capacitor, which increases the electrical tension over the capacitor and gap simultaneously. At some point when the tension is sufficiently high to provoke discharge, the electrical energy in the capacitor is released via a plasma channel. When the voltage becomes lower than the arc voltage, the discharge is automatically ended.

Resistor-Capacitor Relaxation Circuit:

An outmoded EDM power supplies circuit, uses capacitors to store the charge that produces the spark at the gap. The capacitor is charged through a resistor and discharged across the gap when conditions are correct (gap distance, voltage, etc.). The original EDM circuit and is seldom used in currently available machines.

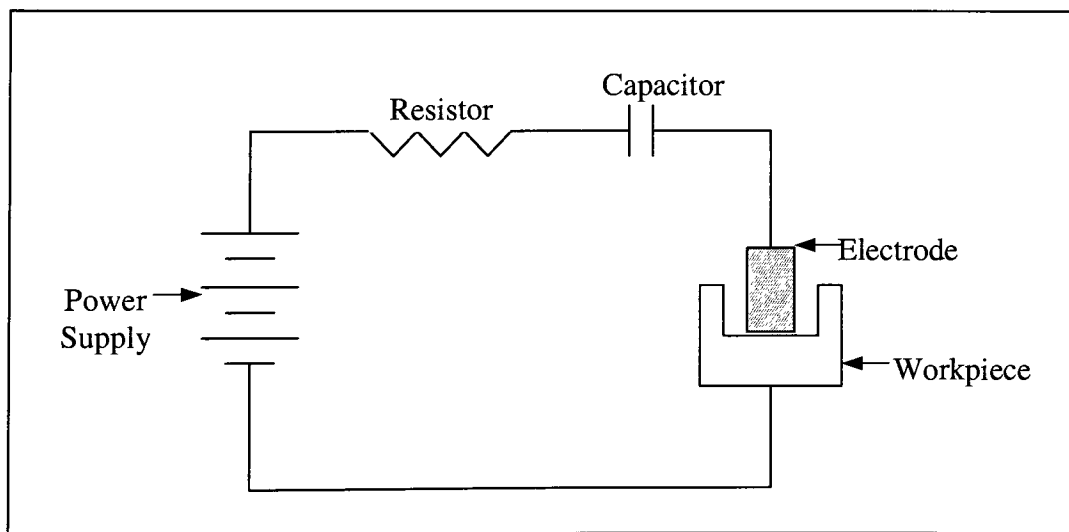


Figure 2.3 Schematic of a R-C Relaxation Circuit

A newer type of generator seen in the figure. 2.3 controls discharges by some switching elements between the gap and a DC voltage and current source.

In the following generator three parts can be seen: the electrode-workpiece system which forms capacitor, a voltage source and a current source. In the first phase of an electrical discharge, A voltage source creates an electrical field between electrode and workpiece, until the discharge breakdown voltage is reached and exceeded. At that moment, a discharge begins, the voltage circuit is opened and current circuit is closed: the current source controls the discharge and a user specified current is maintained for the desired time. After that time has elapsed, the current is stopped, the plasma channel collapses and generator pauses for sometime to allow the dielectric to reorganize. Then the entire cycle is repeated.

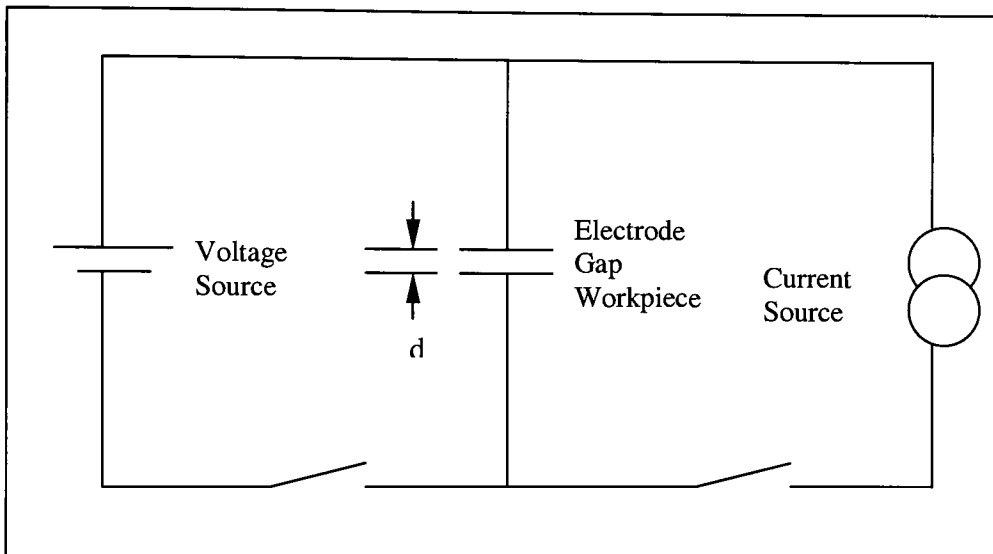


Figure 2.4 Modern type of generator

This kind of generators allows the user to choose discharge current, time frequency, polarity and open circuit voltage. A much better control of the EDM-process is thus possible with this configuration.

2.1.1.5.1 Circuit performances and cycles:

Pulse trains are generated through the circuit and completion of each cycle takes place. These pulses are defined in 4 different shapes, which directly affect the performance of the circuit.

1. Effective Discharge,
2. Arcing,
3. Short Circuit
4. Open Circuit

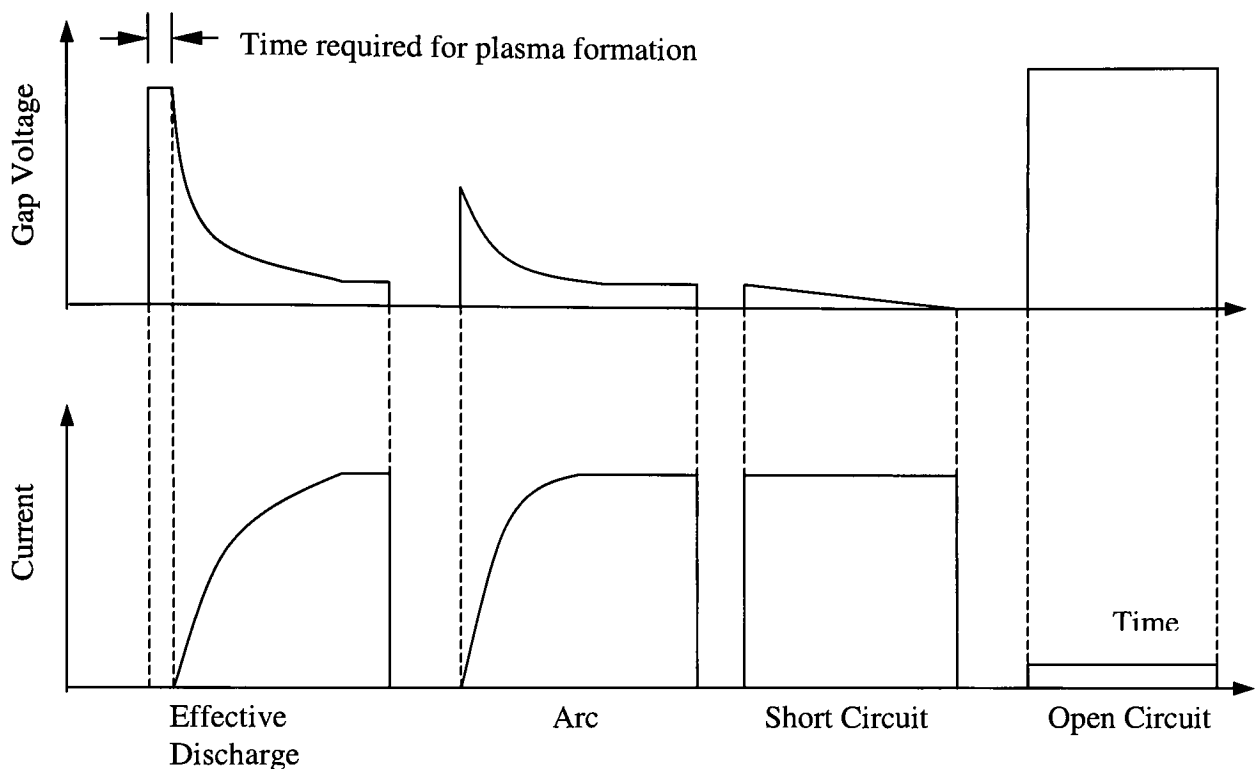


Figure 2.5 Current-Voltage curves at different stages

An electrical discharge is the passage of electrical current through a material, which normally would not conduct electricity. Otherwise, Consider, for example, a simple experiment. If two wires are held, each connected to one pole of a battery, a few millimeters apart, no perceptible electrical current flows through the air, because the air is insulating. However if this wire were connected to a high voltage source of several thousand volts, “sparks” will fly. The normally insulating air was transformed into a conductor, a process called electrical breakdown, and the “sparks”, which we would see, are a form of an electrical discharge. During the breakdown process, some of the negatively charged electrons are separated from their host atoms, leaving them with a positive charge. The negatively charged electrons, and the positively charged atoms (known as positive ions) are then free to move separately under the influence of the applied voltage. Their movement constitutes an electrical current. The collection of ions and electrons is known as plasma, and one of its more important properties is that plasma can conduct electrical current. The Arc is a high current, low voltage discharge, which occurs when

the plasma channel of the previous pulse is not fully deionized (ineffective discharge or arc) the current during the following pulse will flow by preference along the same current path. Therefore, in such a case, no time is required to form a new gaseous current path. The formation of the gaseous channel is normally considered to be necessary to initiate a new spark breakdown. Arcing also occurs when successive discharges occur at the same place or even combine to one discharge that continues for a longer time. It can be caused by too high local concentration of debris particles in the gap or when the pause between two successive discharges is not long enough. Arcing usually results in a very poor surface quality.

Open circuits, occurring when the distance between both electrodes is too large, obviously do not contribute to any material removal or electrode wear. On the other end when contact between tool and workpiece takes place, a short circuit occurs which does not contribute to material removal. The range of the electrode distances in between these two extreme cases can be considered to be a practical working gap yielding actual discharges, i.e., sparks and arcs. Both pulse types do show a characteristic voltage drop across the gap during a pulse.

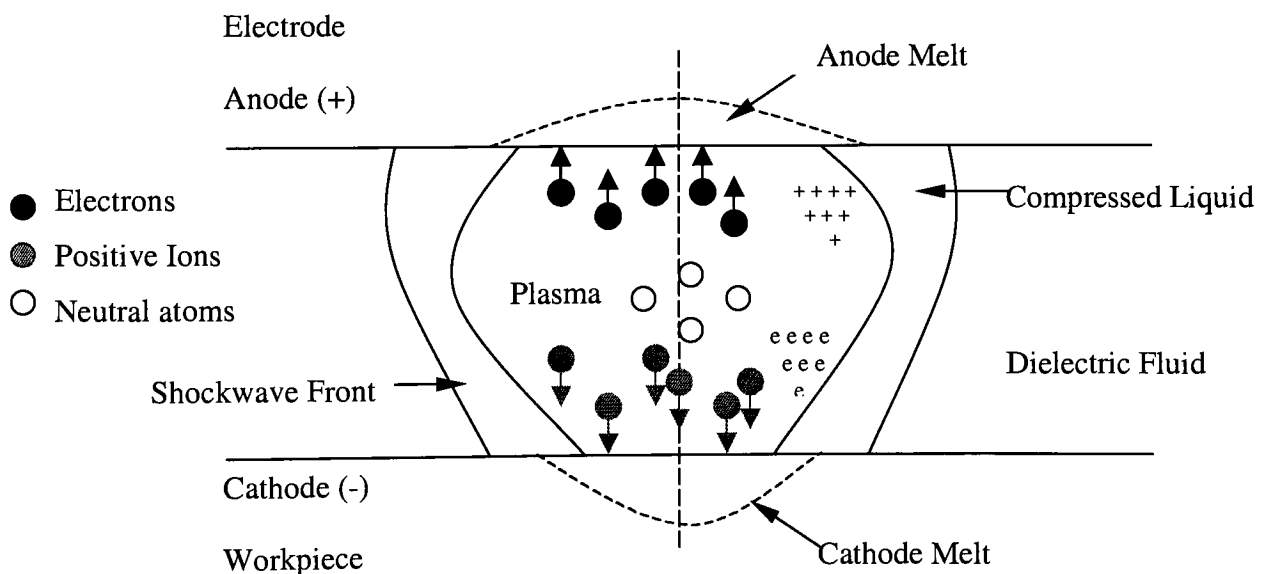


Figure 2.6 Schematic representation of the plasma channel

2.1.1.6 The Dielectric System

Although it is also possible to machine without dielectric. In most die-sinking EDM machines, tool electrode and workpiece are submerged in a dielectric fluid.

Briefly mentioned before, the dielectric has three main functions:

1. Concentration of the discharge energy

A sufficiently high concentration of the discharge energy is required to melt the material of the workpiece. The presence of the dielectric helps to canalize and concentrate the discharge on a single spot, also the high inertia of the liquid dielectric prevents the occurrence of a rapid expansion of the plasma channel and that would cause rapid drop of energy density.

2. Removal of debris by flushing

During machining, not only debris from the workpiece and the electrode are formed, but cracking of the dielectric due to the high temperature also creates some small particles in the gap. All these particles have to be removed to prevent short circuit and arcing. This is done by means of flushing and filtering.

There exist different kinds of flushing. In the particular case of die-sinking EDM, both injection and suction flushing can be applied. In many cases, a simple lateral flushing between electrode and work piece is enough. To remove debris particles from dielectric, filter is added to the dielectric system. In many cases, some sort of paper filters is applied.

3. Cooling of electrode and workpiece

Especially when using higher power, a cooling system is needed to evacuate the heat produced by the EDM-process. The applied electrical energy is transformed into heat, the electrode and the workpiece and must be dissipated by dielectric medium

2.1.1.7 The different phases of discharge

Currently, no complete model of EDM that explains in all detail the different processes that take place is available. However, some explanations and theories that are accepted by most researchers in the field. According to these, an electrical discharge between the tool electrode and the workpiece proceeds in four successive steps:

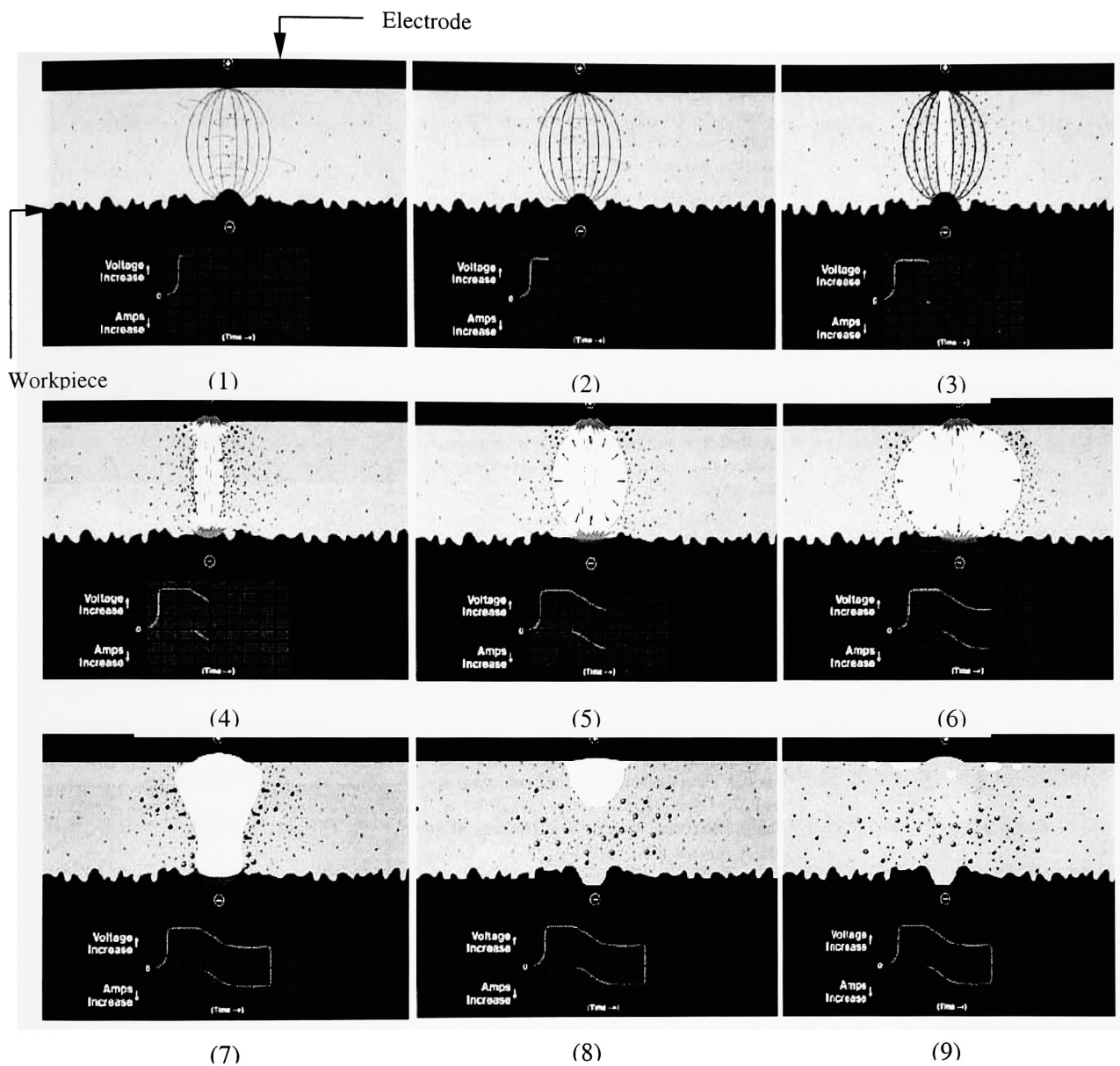
1. The ignition phase
2. Formation of the plasma channel
3. Melting and evaporation of a small amount of workpiece material
4. Ejection of the liquid molten material

2.1.1.7.1 The ignition phase

Whenever an electrical tension is applied between electrode and workpiece, it creates an electrical field, which is characterized by the voltage gradient. This voltage expressed by the ratio of tension to distance as well as some other relationships. These electrons are called the primary electrons. The primary electrons are those attracted by anode and starts moving towards it. On their way through the dielectric atoms split up in positive ions and electrons. These newly generated electrons are called the secondary electrons.

2.1.1.7.2 Formation of the plasma channel

The positive ions originating from the dielectric fluid are attracted towards the cathode. When they hit cathode, additional electron are freed. This process is called the secondary emission. These electrons also move towards the anode and split up some more neutral dielectric atoms. The current, created by both the electron and the ions increases drastically and the dielectric starts heating locally. This decreases the electrical resistance and the current increases further. The dielectric continues heating and vapor and even a plasma channel are created. The plasma channel is characterized by high pressure and temperature. The formation of the plasma channel is also called the voltage breakdown because when the plasma channel is created, the voltage drops from the higher; user specified open circuit tension to the breakdown voltage which is characterized by the material combination of electrode and workpiece.



- (1) Charged electrodes brought near the workpiece. Potential (voltage) is increasing and current is zero.
- (2) Insulating property of dielectric fluid decreases. Voltage reaches peak.
- (3) Current establishes as fluid becomes less of insulator and Voltage begins to decrease.
- (4) Discharge channel begins to form between the electrode and workpiece. Heat builds up as current increases.
- (5) Ions are attracted by the extremely intense electromagnetic field that has built up. Current rises and voltage drops
- (6) At the end of on-time Voltage and Current stabilizes and heat and pressure reaches maximum. Discharge channel consists of superheated plasma made of vaporizing metal and dielectric oil with intense current passing through it.
- (7) Beginning of off time, current and voltage drops to zero.
- (8) Dielectric oil quenches the workpiece surface. Unexpelled molten metal solidifies forming recast layer.
- (9) Expelled metal resolidifies into tiny spheres dispersed in dielectric oil.

Figure 2.7 EDM process Mechanism (Courtesy. EDM Tech. Manual, Poco Graphite Inc.)

The time which elapses between applying the voltage and the breakdown is called ignition delay time. When the distance between electrode and workpiece enlarges, the ignition delay time increases. Thus the value of ignition delay time can be used to measure the gap width to control the motion.

The description is valid for clean dielectrics. During machining however, debris particles caused by machining and other particles caused by the decomposition of the dielectric due to the high temperatures, are present in the dielectric. In these cases, the particles form discharge paths with increase in voltage gradient. Consequently, the discharges take place more easily as the gap is increased.

2.1.1.7.3 Melting and evaporation

The plasma channel is maintained by the EDM machine for a user specified time. During this time, the anode and cathode are bombarded by electrons and ions respectively. When an electron or an ion collides with a surface, its kinetic energy is transformed in heat. This heat induces melting and a partial evaporation of surface. The amount of material that is molten depends on other things from the number of electrons or ions that collide with the surface. The number of colliding particles per discharge depends on the current of the discharge and discharge time.

There is an important difference in mass between electron and ions. Metal ions are much heavier than electrons and so their kinetic energy is much higher. But due to higher inertia of ions, it takes more time to bring them to a certain speed.

2.1.17.4 Ejection of molten material

At the end of the user specified discharge time, the EDM machine stops the current abruptly. As a consequence, the plasma channel collapses and so the pressure on the molten cathode and anode surface suddenly. This makes the molten material at both electrode and workpiece to boil violently and small droplets of liquid metal are ejected from the molten metal pool. The removed material is evacuated by the flow of the dielectric fluid. This is the main material removal process in EDM. A small part of the material is removed by evaporation, but the main part is removed by the sudden and intense boiling at the end of the discharge.

2.1.1.8 Major Process Parameters in Die-sink EDM:

Pulse-Duration: Pulse duration is the duration of each pulse both ontime and offtime. When the spark gap is bridged, current is generated and the work is accomplished. The longer the spark is sustained the more is the material removal. Consequently the resulting craters will be broader and deeper and the surface finish will be rougher. With shorter duration of sparks the surface finish will be better. With a positively charged work piece the spark leaves the tool and strikes the work piece resulting in the machining. More sparks (interactions) accelerates tool-wear, hence this process behaves quite opposite to normal processes in which the tool wears more during finishing. While most of the machining takes place during on time of the pulse, the off time during which the pulse rests and the reionization of the dielectric takes place, can affect the speed of the operation in a large way. The off time also governs the stability of the process. An insufficient off time can lead to erratic cycling and retraction of the advancing servo, slowing down the operation cycle.

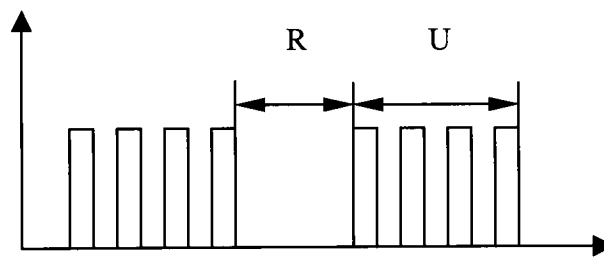


Figure 2.8 A pulse train, followed by a pause

Average Current: The average current is the average of the amperage in the spark gap measured over a complete cycle. This is read on the ampmeter during the process. Average current is an indication of the machining operation efficiency with respect to material removal rate. Current is responsible for the ionization of dielectric medium.

Gap Voltage: The preset gap-voltage determines the width of the spark gap between the leading edge of the electrode and the workpiece. High voltage settings increase the gap and hence the flushing and machining. However when using graphite electrodes, high open gap voltage drastically increases the electrode wear.

Dielectric Fluid: The EDM setup consists of a power supply whose one lead is connected to the workpiece immersed in a tank having dielectric oil. The tank is connected to a pump, an oil

reservoir and a filter system. The pump provides pressure for flushing the work area and moving the oil while the filter system removes and traps the debris in the oil. The oil reservoir restores the surplus oil and provides a container for draining the oil between the operations. There exist different types of dielectric fluid. For Die-sink EDM process basically there are 3 types of Die-electric fluid namely synthetic, semi-synthetic and petroleum based oils. Selection of Dielectric Fluid is done based on many factors as Aromatic Content, Viscosity, Evaporation rate, fire and flash point, oxidation rate, dielectric strength.

Depth of penetration: Depth of penetration is the measurement of depth of machining. Bruzzone and Lonardo (1999) mentioned in their research that depth of penetration affects the workpiece surface roughness by doing one factor at a time experiments. Depth of penetration is the amount of depth to which the workpiece material is machined in a single run.

Electrode Type: There are two major types of electrode materials - graphites and metallics. Each material has its own unique properties and will fit certain applications better than others. When EDM first became a reality, the primary choice for electrode material was copper. As improvements in equipment made EDM more feasible for everyday applications, the physical limitations of straight copper became evident. With EDM spark temperatures many times higher than copper's melting point, certain applications using copper electrodes were no longer cost effective due to unacceptable wear. In metallic electrode materials used with respect to the desired application is namely brass, tellurium copper, copper tungsten, tungsten carbide, silver tungsten and tungsten. In graphite, density and grain size will be a key factor in its performance. If the application does not require good finish or fine detail, then satisfactory results can be obtained with a graphite electrode with higher grain size. If good finish and fine details are the primary considerations, then a material with small grain size and high density should be used.

Hence, a study of the technological parameters to further extrapolate this integrated approach to regular EDM, it is necessary to employ some statistical technique, which will account for the inherent randomness in the process.

2.1.1.9 Surface Integrity from Die-sink EDM Process:

The quality of machined surfaces has becoming more and more important because of the increasing demands of sophisticated component performance, and reliability. Surface integrity is defined as the inherent or enhanced condition of a surface produced in a machining or other surface generating operation. Surface integrity consists of two parts. The first is surface texture, which describes surface roughness, which essentially is a measure of surface topography. The second is surface metallurgy, which is a study of the nature of the surface layer produced as a consequence of machining. Surface integrity of a surface produced by a metal removal operation includes the nature of both surface topography as well as surface metallurgy on the mechanical and physical properties of a material in its chosen environment.

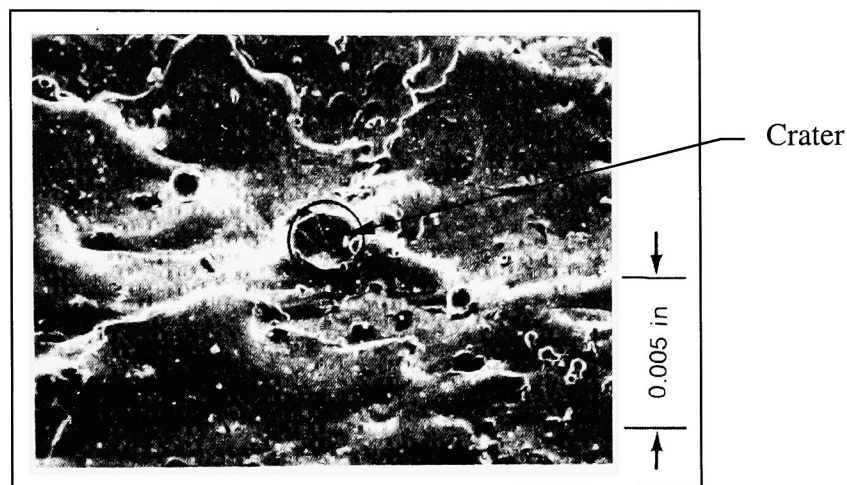


Figure 2.9 Typical EDM Surface (Source: <http://www.unl.edu/nmrc>)

Especially in EDM process the surface integrity issues are more concerning as it is a thermal material removal process, which utilizes a variety of heat sources to melt, vaporize or sublime the workpiece surface. The surface texture reflects the impingement of the heat source and the molten state that occurred is shown in the figure (Fig.2.9).

EDM has a completely different effect on working material than customary methods of processing. The electrical spark hitting the work piece heats up the outer layer of the workpiece material so much (about 10,000° C) that the material evaporates. The metal gases formed then condense in the dielectric, usually in the form of hollow balls, open on one side and having a sharp edge. In the work piece itself, depressions, shaped like craters, are formed.

Due to EDM processes, the chemical composition and the metallographic structure of the surface of the machined workpiece is changed. Different zones can be distinguished. At the top of the workpiece, a molten and resolidified zone, the base material is situated. Figure (fig.2.10) shows the different zones in a transverse section of inconel alloy 718.

A description of each layer is found as continuation:

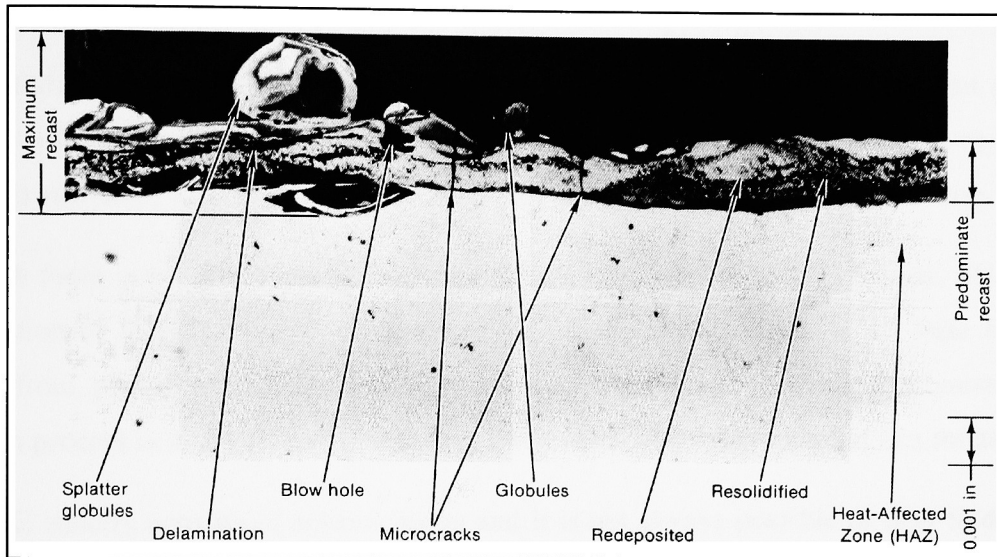


Figure 2.10 Transverse section of Inconel alloy 718 EDM surface
(Source: <http://www.unl.edu/nmrc>)

2.1.1.9.1 White layer or recast layer:

The white layer is the top layer of the workpiece. This layer has undergone a change in metallographic structure as well as composition. The material in this zone has been molten, but not removed consequently has resolidified. Due to interaction with the dielectric and with small wear particles of electrode material, the chemical composition has been changed. The name white layer is also often used for this layer because in the case of tool steels, etching of this layer is rather difficult, so the layer remains white after standard etching. Normally the white layer has a very non-homogeneous composition and the structure and it can present mechanical characteristics, which greatly differ from those of the base material. The hardness and the toughness of the white layer may change as well as the resistance against corrosion and wear. Especially during roughing regime, a lot of microcracks, microholes, globules and delaminations are created in the white layer. It is only during the later use of workpiece that the

cracks may grow and continue the underlying layers. The melted zone shows clearly that it has solidified very quickly have grown vertically up out of the metal surface during solidification. A crack that has formed in this layer runs inward along the line of crystals. The melted layer is usually about 15-30 μm thick after normal rough work. In the hardened zone the temperature rose above that needed for hardening.

2.1.1.9.2 Heat affected zone (HAZ)

The heat-affected zone (HAZ) is situated just below the white layer. An important difference with the white layer is that material in the HAZ has not been molten. The heat of the EDM process is sufficient to change the structure of this zone, but not to cause any melting.

Although there is no direct interaction with the dielectric or with the electrode, the chemical composition of the HAZ might be changed too. A diffusion process is the base for such a change from places from a high concentration to places with a lower concentration. The diffusion process is much slower than that in the process of mixing material in a molten state.

The HAZ usually consists of several layers and It is not always possible or easy to distinguish them. Sometimes, the layers are very thin, or they have the same color when looked at with a light microscope.

2.1.1.9.3. Base Material

The base material is the part of the workpiece that has not been influenced by the EDM process. It still possesses the same composition and structure as before machining. The temperature might have risen, but not enough to induce metallographic changes in the workpiece.

Apart from metal removal, surface roughness and electrode wear, the effect on the surface quality of the working material is of utmost importance.

2.4. Advantages and Drawbacks of EDM

Advantages of EDM

One of the main advantages of EDM is a consequence of the thermal process it is based on: removing material by melting, so the hardness of the workpiece is no limitation for machining. Even the hardest steel grades can be machined and this with almost the same machining speed as for softer steels.

- **Machining hard material**

Since EDM erodes metal with electrical discharges instead of with chip machining cutting tools, the hardness of the workpiece does not determine whether or not a material can be machined by EDM. The capacity of the machining hard material is a major benefit as most tools and moulds are made of hard materials to increase their lifetime. The recent development in cutting tools for turning and milling and the processes of the high speed machining allow machine harder materials than before, but EDM still remains the only available process for machining many hard material (e.g. carbides).

- **Absence of forces**

As the EDM process is based on a thermal principle, almost no mechanical forces are applied to the workpiece. This allows to machine very thin and fragile structure. It should be noticed that some small mechanical, electrical and magnetic forces are produced by EDM process and that, as already mentioned, flushing and hydraulic forced may become large for some workpiece geometry. The large cutting forces of the mechanical material removal processes however remain absent.

- **Machining complex shapes**

Complex cavities can often be machined without difficulties by die-sinking EDM, provided an electrode is available, having the opposite shape of the cavity. In most cases, the soft electrode (Cu, graphite, or W-cu) can be machined rather easily by conventional processes as milling and turning or by wire cutting EDM. In this way, complex cavities can be eroded, even on simple die-sinking machines which can only erode in downward direction.

EDM is one of the only processes capable of machining three dimensional micro workpieces. A large growth of application for so called micro electro mechanical systems is predicted for the near future.

- **High degree of automation**

The high degree of automation and the use of tool and workpiece changers allows to let the machines work unattended for overnight and during weekends.

- **Accuracy of the process**

EDM is very accurate machining process. Especially in the case of wire EDM, where the tool electrode is constantly renewed (no effect of tool wear and other tool inaccuracies). In the case of workpieces with a higher thickness, the accuracy and the fine surface quality remains the same over the whole process condition over the total workpiece height. Processes like laser beam or water jet machining can also achieve a high surface finish, but only for workpieces with a limited thickness. When the thickness increases, focusing problems induce a loss of quality.

Drawbacks of EDM

- **The need for electrical conductivity**

To be able to create discharges, the workpiece has to be electrically conductive. Isolators, like plastics, glass and most ceramics, can not be machined by EDM, although some exceptions like for example diamond are known, Machining of partial conductors like Si semiconductors, partially conductive ceramics is also possible.

- **Predictability of the gap**

The dimensions of the gap are not always easily predictable, especially with intricate workpiece geometry. In these cases, the flushing conditions and the contaminations and the contaminations state of the dielectric are uncertain and this can cause the final workpiece dimension to differ from the specified one. In the case of die-sinking EDM, the tool wear also contributes to the deviation of the desired workpiece geometry and it could reduce the

achievable accuracy. Intermediate measuring of the workpiece or some preliminary tests can often solve problem.

- Optimization of electrical parameters

The choice of the electrical parameters of the EDM-process depends largely on the material combination of electrode and workpiece and EDM manufacturer only supply these parameters for a limited amount of material combination. When machining special alloys, the user has to develop his own technology.

- Low material removal rate

The material removal of the EDM process is rather low, especially in the case of diesinking EDM, where the total volume of a cavity has to be removed by melting and evaporating the metal. This problem can be solved by removing already part of the material by conventional processes before hardening the workpiece.

- Taper effect at the edge of machined cavity

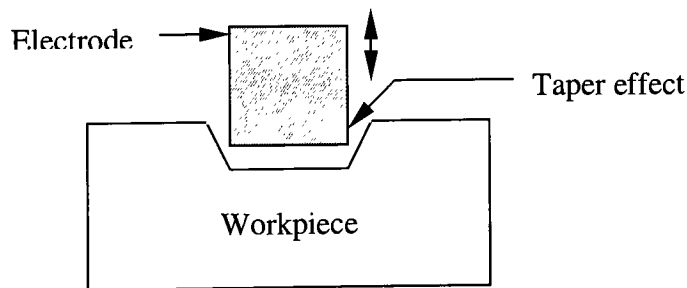


Figure 2.11 Taper effect

The taper effect developed between the electrode and workpiece is due to the undue machining done at the diametric edges of the electrode. As the electrode progresses downwards the original diameter of the hole is more than the required one. This defect often causes dimensional defects in the EDM machined workpieces.

2.1.2 Response Surface Methodology:

Response surface methodology is a collection of statistical and mathematical techniques useful for developing, improving and optimizing processes. In some industrial processes several input variables potentially influence some performance measures or quality characteristic of the product or process. This measure is called response. The input variables are called independent variables.

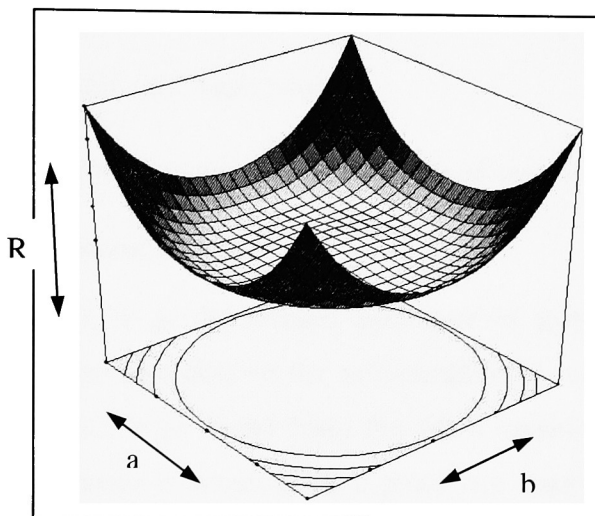


Figure 2.12 A theoretical response surface showing the relationship between Response “R” and variables “a” and “b”

Figure shows graphically the relationship between the response variable (R) in a chemical process and the 2 process variables “a” and “b”. Note that for each value of a and b there is a corresponding value of yield as a surface lying above the a-b plane. As shown in the figure basically it’s a graphical perspective of the problem environment that has led to the term response surface methodology.

Most of the application of response surface methodology is iterative and sequential in nature. That is, at first some ideas are generated and concerning which factor or variables are likely to be important in the response surface study. A screening experiment is designed and executed to understand the nature of the process and eliminate the unimportant variables from the process. After screening experiment the focus will be on the important variables. The iterative experiments are done and the trend and behavior of response is observed. As explained in the

prior section the direction of steepest ascent or descent is determined taking into consideration the area of interest (i.e. maximization or minimization). As we approach the region of interest the experiments are designed with center point to get

The experiment is designed to allow us to estimate interaction and even quadratic effects, and therefore give us an idea of the (local) shape of the response surface we are investigating. For this reason they are termed response surface method (RSM) designs. RSM designs are used to:

1. Find improved or optimal process settings
1. Troubleshoot process problems and weak points.
2. Make a product or process more *robust* against external and non-controllable influences.

2.1.3 Direction of steepest descent method:

Direction of steepest descent is gradient-based optimization technique. Experiments are executed in the direction of steepest descent for minimization of response when the area of interest is minimization. Direction is found from the fitted equation. The experiments are iterated until the desired response is acquired. The procedure basically starts at the current operating conditions then linear model is fitted after that direction of steepest descent is determined and experiments are iterated until the no improvement is observed in the response- then iterate the process. The direction of steepest descent is determined by the gradient of the fitted model and depends on the scaling convention.

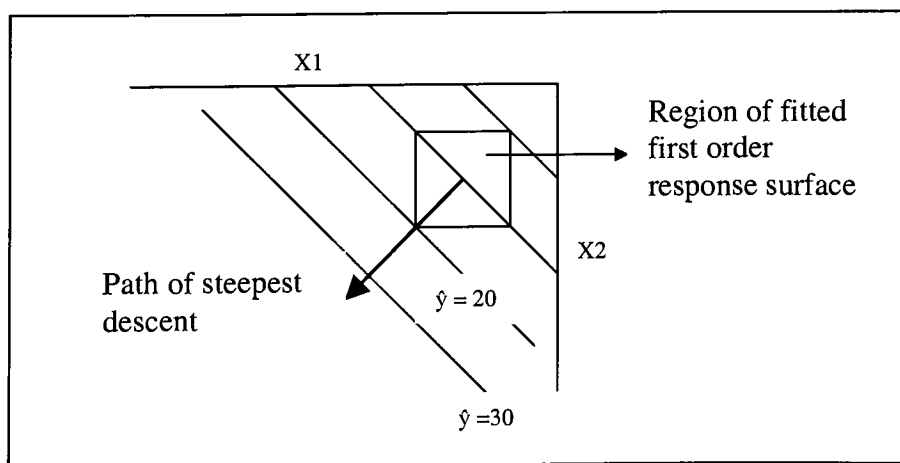


Figure 2.13 First order response surface and path of steepest ascent

If experimentation is initially performed in a new, poorly understood production process, chances are that the initial operating conditions $\chi_1, \chi_2, \dots, \chi_k$ are located far from the region where the factors achieve a minimum for the response of interest Y . A first order model will serve as a good local approximation in a small region close to the initial operating conditions and far from where the process exhibits curvature. If the response is well modeled by a linear functions of the independent variables, then the approximating function is the first order model.

$$y = \beta_0 + \beta_1\chi_1 + \beta_2\chi_2 + \beta_3\chi_3 + \dots + \beta_k\chi_k + \varepsilon$$

If there is curvature in the system, then a polynomial of higher degree must be used, such as second order model.

$$Y = \beta_0 + \sum_{i=1}^k \beta_i \chi_i + \sum_{i=1}^k \beta_{ii} \chi_i^2 + \sum_{i=1}^k \sum_{j=1}^k \beta_{ij} \chi_i \chi_j + \varepsilon$$

Procedure at this stage is to keep experimenting along the direction of steepest descent until there is no further improvement in the response. At that point, a new fractional factorial experiment with center runs is conducted to determine a new search direction. This process is repeated until at some point significant curvature in Y is detected. This implies that the operating conditions X_1, X_2, \dots, X_k are close to where the minimum of Y occurs. When significant curvature, or lack of fit, is detected, the experimenter should proceed with response surface designs.

The process of steepest ascent is a significant process of finding the direction of steepest descent and finding step size in the direction of steepest descent is most important of this method. It is a process for moving sequentially along the path of steepest descent, that is, in the direction of the minimization of response. Experiments are conducted in along the path of steepest descent until no further decrease in response is observed.

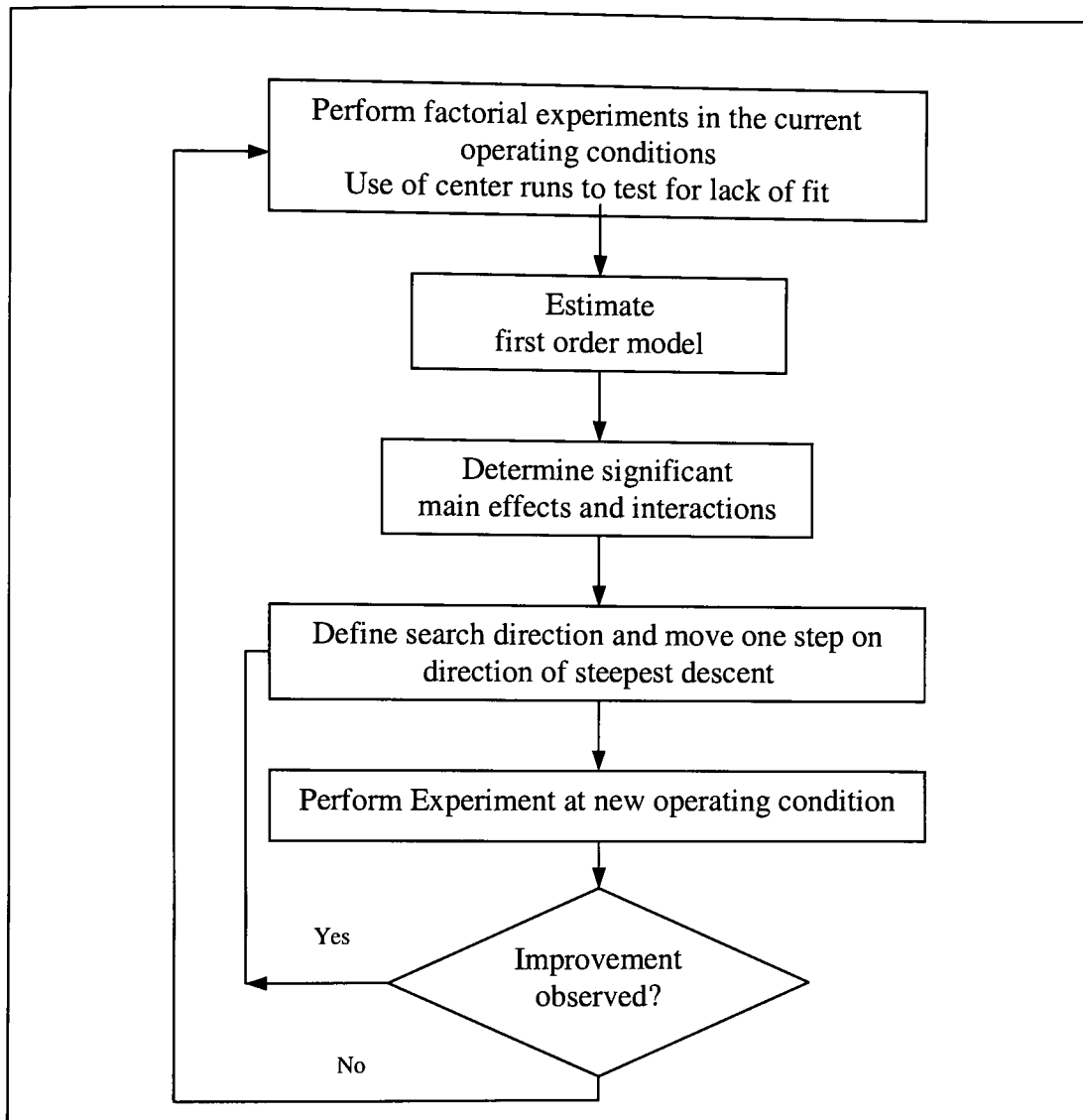


Figure 2.14 Flow Chart for the First Phase of the Experimental Optimization Procedure in the path of steepest of descent

This coding convention is recommended since it provides better parameter estimates, and therefore, a more reliable search direction. The coordinates of the factor settings on the direction of steepest ascent separated a distance ρ from the origin are given by:

$$\text{Minimize } b_0 + b_1x_1 + b_2x_2 + \dots + b_kx_k$$

$$\text{Subject to: } \sum_{i=1}^k x_i^2 \leq \rho^2$$

The direction of the gradient, g , is given by the values of the parameter estimates, that is, $g' = (b_1, b_2, \dots, b_k)$

The coded factors x_i in the original units of measurement, X_i are obtained from the relation:

$$x_i = \frac{X_i - (X_{low} + X_{high})/2}{X_{high} - X_{low}/2} \quad i = 1, 2, 3, \dots, k$$

The solution is a simple equation, which yields the coordinates, This coding convention is recommended since it provides parameter estimates that are scale independent, generally leading to a more reliable search direction.

$$x_i = \rho \frac{b_i}{\sqrt{\sum_{i=1}^k b_i^2}} \quad i = 1, 2, \dots, k$$

An engineer can compute this equation for different increasing values of ρ and get different factor settings all on the steepest descent direction.

Iterative Response Surface Methodology:

Iterative Response Surface Methodology is the process of sequential experimentation. The objective here is to lead the experiment rapidly and efficiently along the path of improvement toward the general vicinity of the optimum. Once the region of the optimum has been found, a more elaborate model, such as the second order model, may be employed, and an analysis may be performed to locate the optimum.

Following figure depicts the exact procedure where first the 2 level full factorial experiments are executed to understand the behavior of the process and to eliminate the insignificant factors this experiment is called screening experiments. After screening experiment the full factorial design with center point is designed using only significant factors from the screening experiment. After each design the phases are changed and first order model is determined for the response. As explained in the previous section of direction of steepest descent method step sizes and direction is found. The experiments are executed in the path of steepest descent for the minimization of response. At some point in this iterative process the response reaches the minimum value after which it starts increasing. At that stage the Central composite design is executed to get the exact behavior of the optimal level of the factors involved in the

experiment. The eventual objective of RSM is to determine the optimum operating conditions for the system or to determine a region of the factor space in which operating requirements are satisfied

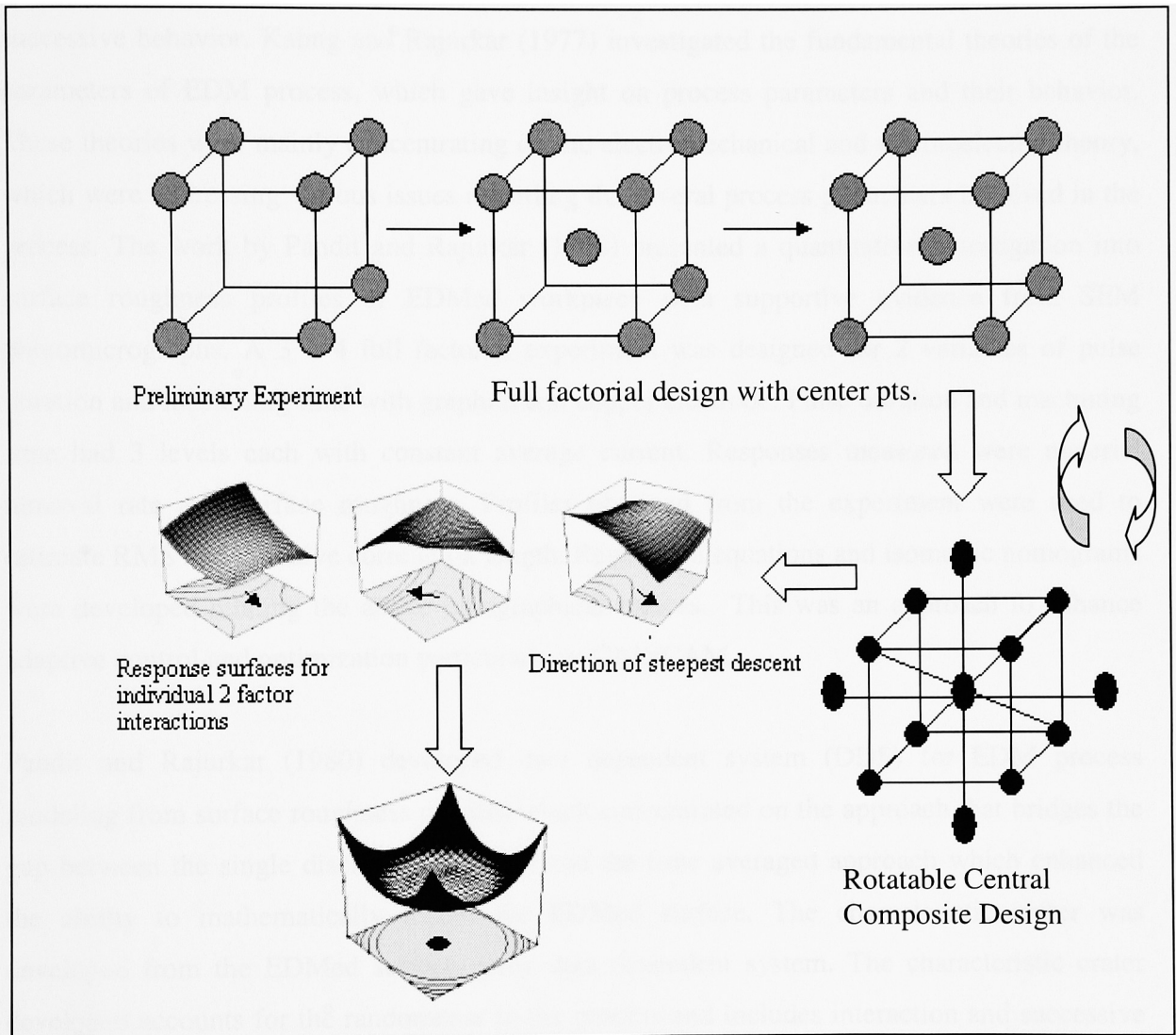


Figure 2.15 Iterative response surface methodology
(Source: <http://www.itl.nist.gov/div898/handbook>)

2.2. LITERATURE REVIEW

Extensive studies concerning the electro discharge machining process and its optimization are available. Cooke and Crookall (1973) analyzed electro-discharge machining in a statistical way by considering various factors to optimize the responses. In this study the objective was to follow in the succession of rapid discharges and to observe their statistical distribution and successive behavior. Kahng and Rajurkar (1977) investigated the fundamental theories of the parameters of EDM process, which gave insight on process parameters and their behavior. These theories were mainly concentrating on the electromechanical and thermoelectric theory, which were addressing various issues regarding the several process parameters involved in the process. The work by Pandit and Rajurkar (1978) presented a quantitative investigation into surface roughness profiles of EDMed workpiece with supportive evidence from SEM photomicrographs. A 3 x 4 full factorial experiment was designed for 2 variables of pulse duration and machining time with graphite and copper electrode. Pulse duration and machining time had 3 levels each with constant average current. Responses measured were material removal rate and surface roughness. Profiles obtained from the experiment were used to estimate RMS and effective correlation length. Regression equations and isometric nomograms were developed relating the above topographical indices. This was an approach to enhance adaptive control and optimization particularly in CAD/CAM.

Pandit and Rajurkar (1980) developed data dependent system (DDS) for EDM process modeling from surface roughness profiles which concentrated on the approach that bridges the gap between the single discharge approach and the time averaged approach which enhanced the ability to mathematically model the EDMed surface. The characteristic crater was developed from the EDMed surface using data dependent system. The characteristic crater developed accounts for the randomness in the process and includes interaction and successive dependencies with in discharges in EDM. It was proved with experimental evidence that calculation of erosion rate using a characteristic crater provides a better quantitative agreement with experimental results than those obtained from single discharge. Rajurkar and Pandit (1982) worked on prediction of metal removal rate and surface roughness in electrical discharge machining. Successful integration of optimization techniques and adaptive control of EDM and published work on the developments of quantitative relationship between output

parameters and controllable input variables. The experiments were done on the development of expressions for radius and depth of melting crater in terms of material properties and machining conditions using the predictions regarding surface roughness and metal removal rate were done. The expressions obtained were utilized to predict metal removal rate and surface roughness parameters under working condition. Experimental verifications of these predictions useful in shop practice were presented. Rajurkar (1985) published significant work in surface damage and shock waves in EDM. The paper discussed the possibility of a single measure of surface damage based on the comparison of different measures of surface integrity. The effect of shockwave was integrated with surface damage due to single discharge to bridge the effect gap between single discharge and multiple discharge results. Singh, Miller and Urquhart (1985) investigated into the influence of electro-discharge machining parameters on machining characteristic. The influence of various electro-discharge machining parameters such as, the gap voltage, gap current, dielectric fluid pressure, electrode material and pulse frequency are discussed. It was found that these parameters have a significant influence on machining characteristics such as metal removal rate, dimensional accuracy and surface finish. Among electrode materials used (Graphite, Copper and Brass), graphite exhibits superior quality, with respect to machining characteristics except surface finish. Low voltage exhibit high metal removal rate with poor surface finish while high gap voltage gives lower metal removal rate, fine surface finish and good dimensional accuracy.

Jain and Rajurkar (1990) in their work introduced multi-objective optimization techniques in a EDM process. The factors considered were depth of penetration, tool diameter, and gap voltage and pulse duration. Responses measured were machining rate, tool wear rate, surface roughness etc. Mathematical optimization techniques were used while developing the non-linear model. Non-linear goal programming (NLGP) technique was used considering main technological constraints for getting the optimal results. NLGP methodology allowed for viewing the effect of varying the targets or the goals and its priorities in EDM process. Luo and Chen (1990) published a paper describing the effect of a pulsed electromagnetic field on the surface roughness in EDM process. The paper states that the discharge energy could be reduced by setting small electric parameter of the pulse generator. Very smooth surface can be achieved by applying very short discharge pulses.

William and Rajurkar (1991) investigated wire electrical discharge machined surface characteristics. This research work concentrated in detailed study of the complex and random nature of erosion process in wire EDM. The work concluded that it is required to have the application of deterministic as well as stochastic modeling and analysis methodology to better understand the complexity of the process. The main parameter in consideration was the average current at 4 levels. Scanning electron microscope and energy depressive spectrometry were used to analyze the process. The surface integrity of wire electro-discharge machining was studied. Under these conditions higher peak current resulted in rougher surfaces.

Indurkha and Rajurkar (1992) used the artificial neural networks (ANN) to model EDM process. The experiments were carried out with a 9-9-2-size back-propagation neural network. Machining depth, tool radius, orbital radius, radial step, vertical step, offset depth, pulse ontime, pulse offtime and discharge current were selected as input parameters. The material removal rate (MRR) and surface roughness (Ra) were output parameters for the model. Results of the neural network model were compared with estimates obtained by multiple regression analysis. Experiments were also performed to check the validity of the neural network model. It was concluded that the artificial neural network model for EDM provides faster and more accurate results. Soni and Chakraverti (1997) published their research in performance evaluation of rotary EDM by experimental design technique. The response surface technique was used to compare the performance of rotary EDM. The response surfaces and the corresponding response functions were determined for machining indices for metal removal rate, surface finish and micro-hardness. Spedding and Wang (1997) worked in the field of modeling of wire EDM machine using artificial neural networks (ANN) and response surface methodology (RSM). The parameters tested were wire tension, wire-breaking rate the pulse-width, the time between two pulses, the wire mechanical tension and the injection set-point are selected as the factors and responses measured were surface roughness and cutting speed. The two models were compared for goodness of fit. Verification experiments were carried out to check the validity of the developed models. A RSM model and a 4-16-3 back propagation. Results showed that both the models fit the process successfully but ANN can predict more accurately

Wong, Lim and Lee (1995) studied in the effects of flushing on electro-discharge machined surfaces under a one factor at a time approach. Different flushing types, different pressure settings and types of dielectric was used to investigate their implication on the process and surface roughness. Different types of workpiece material were examined after EDM was performed (e.g. 98% iron, C steel, and AISI 01 tool steel) and it was found that 13ml/s was optimal flushing rate where the crack density and average thickness of the recast layer were at the minimum for all three materials. Scheller, Kanadi and Irawan published research in examining the relationship between grainsize and surface finish in graphite EDM electrodes. Significant differences were shown between the surface finishes produced fine grain (2 and 5 μ m) and coarse grain electrodes (10 and 20 μ m). Bruzzone and Lonardo (1999) investigated influence of electrode material, flushing, electrode dimension, depth of cut and planetary on EDM performance. The observed results showed the importance of electrode material, injection flushing and geometry of cutting on removal rate, electrode wear and surface quality. Chen and Mahdavian (1999) did some work into parametric study into erosion wear in Computer numerical controlled EDM process. Experiments with different values of discharge current, pulse duration and interval time in electro-discharge machining were conducted to investigate their effects on the material removal rate, surface quality and dimensional accuracy of the tool and product. Optimum pulse duration and pulse interval values in EDM that either produce highest erosion rate or fine surface finish have been shown to have significant importance to the machining process. Lee and Yur (2000) published research in characteristic analysis of EDMed surfaces using the Taguchi approach. The factors under consideration were specimen material, gap voltage, pulse current, pulse-on duration, pulse-off duration, servo gap, servo gain, servo noise rejection, jump down, arc sensitivity and arc protection degree. Responses measured were hole enlargement rate, surface roughness and thickness of white layer. L12 orthogonal array was selected as experimental layout. Analyzed results showed that the main influencing factor in the surface roughness was pulse current, pulse on-time, and specimen material, while gap voltage was found to have very negligible effect. Pulse current, pulse on duration and gap voltage are significant factors to improve hole enlargement. In the case of white layer thickness pulse current and pulse on-time was significant factor.

There are extensive efforts done in modeling of electro-discharge machining process. Most of the work is in the area of modeling the process using data dependent system and multi-objective optimization techniques. Major research is done concentrating on Wire EDM process. The factors considered in Wire EDM are not common in RAM edm process. The recent developments in EDM-related technology have opened new avenues of a broad spectrum of EDM applications, which needs more work in this field. There is a need for concentration on surface roughness improvement and to get the factor level combination at which the best surface finish can be achieved. The approach followed in most of the work is purely related to experimental design. It is required to follow factorial design approach combined with response surface methodology to investigate into this complex process. There is need for a mathematical model, which can aid to achieving desired targets (i.e. combination of process parameters that would achieve a specific roughness).

3. METHODOLOGY

3.1 Overview of the Experiment:

The objective of experimentation was to perform a series of experiments in order to estimate the impact of set of process parameters on the EDM surface roughness. The experiments were executed on Hansvedt MS-50C 5 Axis CNC Ram EDM machine (see figure) located in Brinkman Machine tool laboratory at Rochester Institute of Technology. The experiments were planned using statistical design of experiments and run order were completely randomized. The factors involved were (1) inputs factors: Pulse Duration, average current, electrode material, Gap Voltage, Depth of penetration. (2) Response: surface roughness

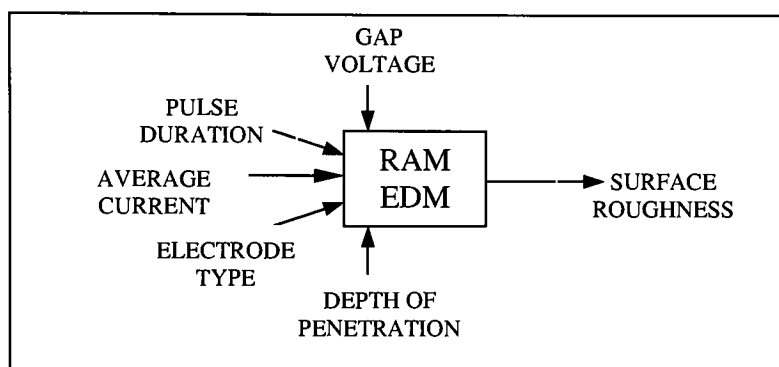


Fig 3.1 Schematic of parameters and response

This study intended to answer questions related to individual main effects and interactions of parameters involved in the Electrical discharge machining (EDM) to determine the robustness of applications for surface quality and to aid in proper parameter setting for process control and optimization.

3.2. Experimental setup:

HANSVEDT 5 axis CNC Ram EDM machine was used to execute the experiments. the machining was done using simple CNC code. The factor levels were set on the machine on factor-by-factor bases. There was a particular set of steps settings in which the levels of various parameters were controlled. Each steps in the machine control designated to increment of the each factor by some units. There were several parameters, which were controllable on real-time basis during machining. IONOPLUS dielectric was used as dielectric material. Direct

Flushing was used and dielectric jets were located directly at the workpiece and electrode interface.

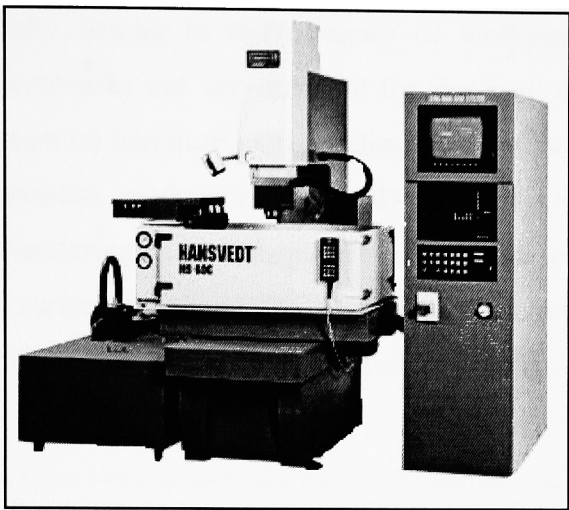


Figure 3.2 5 Axis CNC RAM EDM machine

3.2.1 Specimen:

Aluminum 6061-T3 was used as Specimen material. The non-corrosive and surface retaining property lead to the selection of Aluminum as the workpiece material. The rectangular blocks were cut using hacksaw from same barstock. The average sizes of bar stock was 7” x 4”x 2” The specimens were end milled to desired size and both the faces were used for experimentation. After the experimentation the surface was cleaned using Iso-propyl alcohol and air jet. The resultant surface after experimentation was then measured.

Material Aluminium 6061	Si	Fe	Cu	Mn	Mg	Cr	Zn	Ti	Other	Al
Max %	0.4	0.7	0.15	0.15	0.8	0.04	0.25	0.15	0.05	Balance
Min %	0.8		0.4		1.2	0.35				

Table 3.1 Specification of work piece material

T3: Solution heat-treated, cold worked, and naturally aged to a substantially stable condition. Applies to products that are cold worked to improve strength, or in which the effect of cold work associated with flattening or straightening is recognized in applicable specifications.

Due to the lower hardness and strength of aluminium compared to steel, aluminium is not very suitable for making dies (except for small product series). Machining of aluminium workpieces with EDM is especially used for manufacturing delicate, accurate and/or complex structures. Such workpieces usually belong to the category of workpieces, which are exposed to mechanical forces. Microcracks are very harmful for this kind of application and should be avoided. Currently, almost no literature exists dealing with the influence on the surface quality when machining aluminium workpieces with EDM. In this research work selection of aluminium is done considering the availability issues, tenure of research work and as the response of interest is surface roughness the non-corrosive nature of aluminum is also taken into account for retaining surface finish for longer period of time.

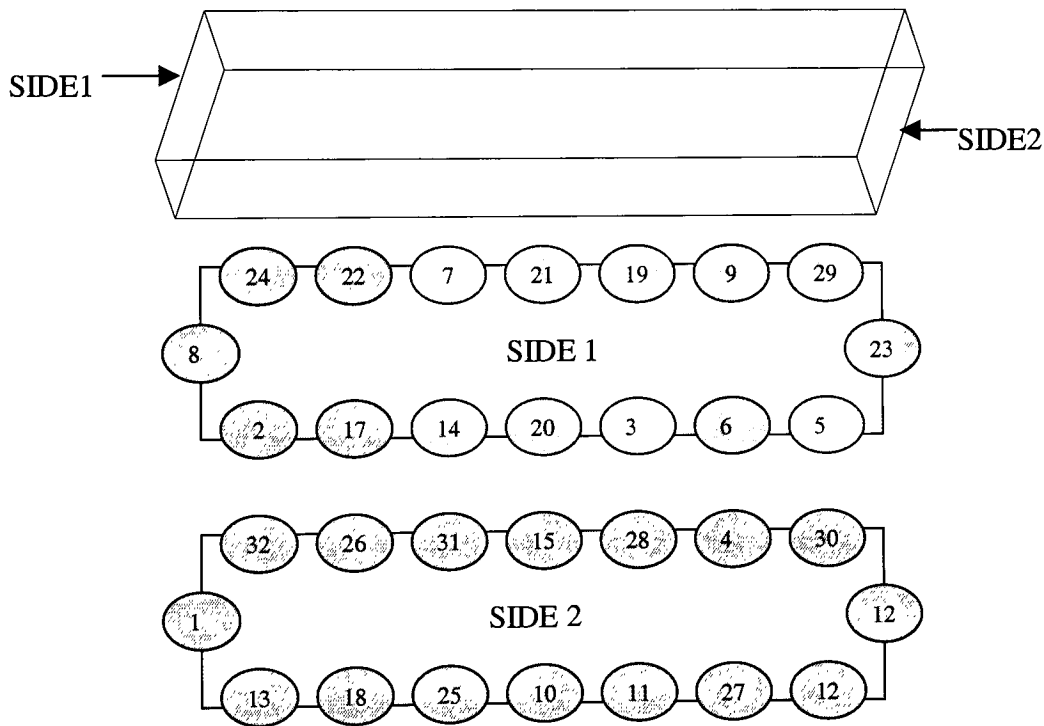


Figure 3.3 Experimental specimen set up

The experimental specimen set up is as shown above. Experiments are set up in such a way that there is enough clearance for access for the surface profilometer to measure the surface roughness. Due to negligible forces involved while machining no clamping and fixturing was considered while setting up the experiments. The experiments are executed on the 2 sides of

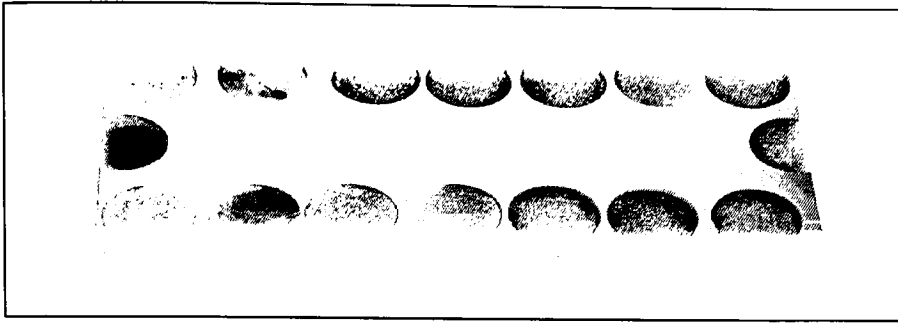


Figure 3.4 Specimen after experimental runs

the specimen on the edges of the rectangular workpiece. The positioning of the electrode with respect to the workpiece is done using Heidenhan TNC406 controller by manual adjustments using handheld controller. The CNC program as shown in Appendix 9.3 is used for machining and controls once the positioning is finalized. Each experimental run is 1" spaced appropriately to facilitate handling and measurement. After each experimental run the machined surface was cleaned and conditioned to remove traces of dielectric material and eroded electrode material accumulated on the machined surface.

3.2.2 Tooling:

Graphite and copper electrodes were used as tools. As shown in figure 3.3 Sakura graphite EC-110 and Tellurium copper electrodes were used. The exact specifications for the electrodes are displayed in the following table. Graphite and copper electrodes were obtained in the form of 1" diameter rod and were prepared for experiments. The copper electrode was cut using hacksaw to required length then turned to get parallel surfaces and graphite electrode was filed to remove distortion present on the electrode surface in contact with the workpiece. The electrodes were filed at regular interval to remove the irregularity during machining. Characteristics of electrodes are explained in the following table 3.5.

The response of interest is surface roughness and good surface finish is obtained by combination of the proper electrode material and good flushing condition. As appropriate settings of the above parameters produces less defined craters in the work metal, the final surface finish will be mirror image of the electrode's surface, The characteristic of electrode surface is very important. In the case of graphite electrode considering the powdery nature the

grain size of the electrode is very important. Low grain sized graphite electrodes are best choices for getting better surfaces. We selected the grainsize of 7 μ m because of the availability issues.

Copper electrode was selected on the basis of literature review and industrial practices. This is a good electrode material that is readily available and gives a good erosion rate. Slender electrodes can be difficult to machine and may suffer from heat distortion during machining. Available in most forms including plate, sheet, bar, tube from most nonferrous material suppliers (specify halfhard or hard when ordering). Small tubes (below 3mm dia.) available from specialist EDM electrode suppliers. Wear rate on high power higher than graphite. A polished copper electrode will give the best EDM finish available on steels. Use of high voltage circuit reduces electrode wear.

Graphite electrode is readily machined without the problems of distortion evident in copper but has a tendency to chip and is fragile to handle. Dust extraction is required when machining graphite electrodes (listed as nuisance particulate note a major health hazard). dust problems can be minimised by soaking in dielectric before machining. EDM graphites are only available from specialist EDM electrode suppliers. The graphite is available in many forms including blocks, sheets, bars, plates and tubes. High-density graphites and copper impregnated graphites are expensive but useful for fine detailed work where wear resistance is important. Graphite is almost exclusively used for large work such as large die block cavities and blow moulds. It has low wear and high metal removal rates.

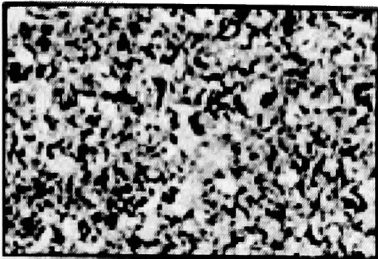
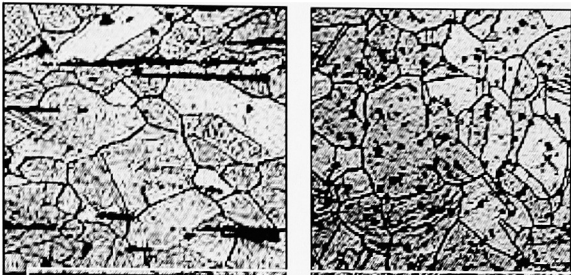
<p>SAKURA GRAPHITE ECT-110</p> 	<p>TELLURIUM COPPER</p>  <p>Transverse section Longitudinal Section</p>
<p>Grain Size: 7 μm Flexure Strength: 13000psi Hardness: 60 Shore, Electrical Conductivity: 1.95e-3/$\mu\text{ohm-inch}$ Electrical Resistivity: 512 $\mu\text{ohm-inch}$</p>	<p>ISO- CuTe (Te-Tellurium) Composition %: Cu+Ag = 99.4% Te = 0.4-0.7 %, P = 0.004-0.012 % Electrical Conductivity: 0.2110/$\mu\text{ohm-inch}$ Electrical Resistivity: 4.72 $\mu\text{ohm-inch}$</p>

Figure 3.5 Graphite and Copper Electrode Properties (Source: Poco Graphite Inc.)

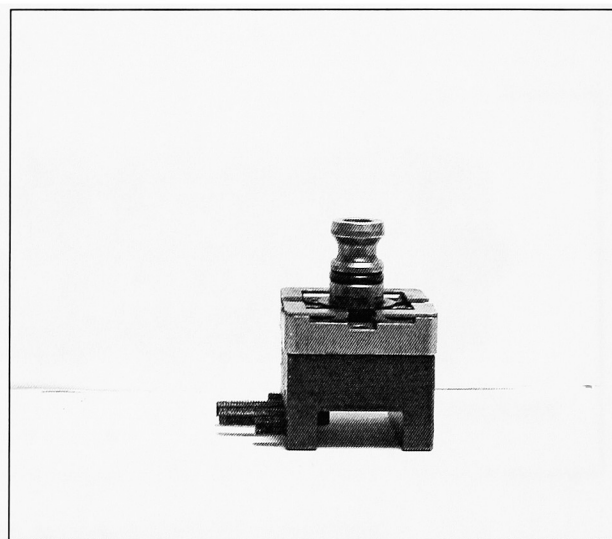
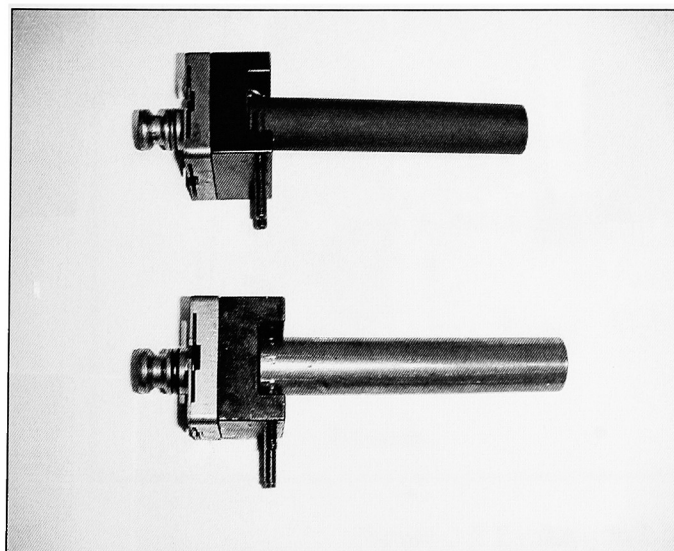


Figure 3.6 Electrodes and Tool Holder for electrodes
(Top) Graphite Electrode (Bottom) Copper Electrode

3.2.3 Metrology:

After machining the experimental run was measured using MITUTOYO SJ 401 surface roughness profilometer. The surface was measured 3 times on each experimental run as shown in the following figure. The measurement was done and profile was obtained which was the replicate of the surface on which the stylus moved. Six surface roughness descriptors were measured for analysis. The evaluation length (i.e. the distance traveled by the stylus during each measurement) was 4 mm, which was kept constant for all the runs. The profile obtained as shown the following figure was used to analyze the surface.

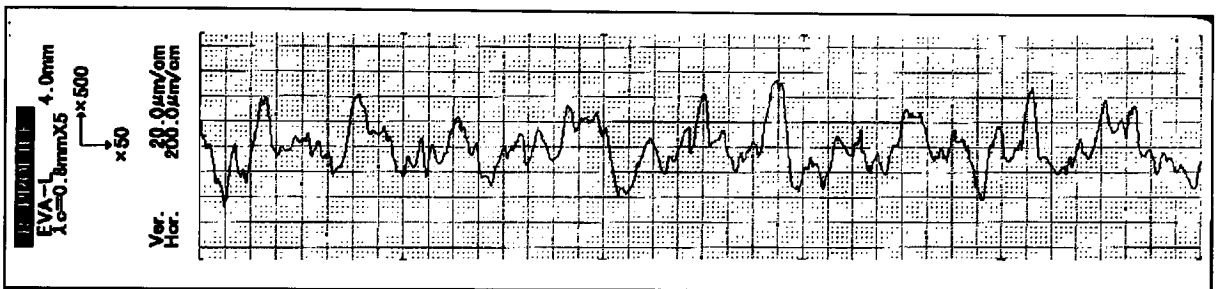


Figure.3.7 A Typical EDM Profile obtained from Mitutoyo SJ 401 profilometer

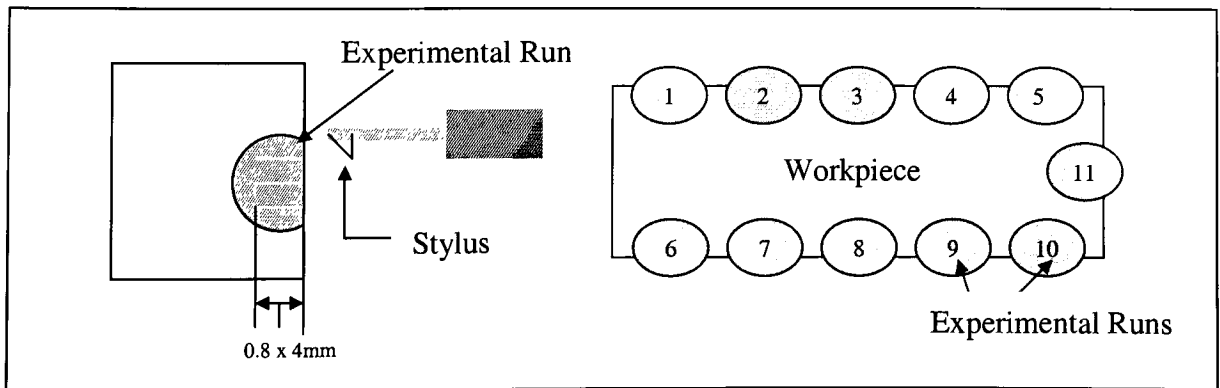


Figure 3.8 Evaluation Length and measurement procedure

4. EXPERIMENTATION:

Experimentation is done in 6 steps and each step is followed by analysis and stepsize calculation for the next experiment. The following figure 3.9 explains the flow of experiments and the elimination of insignificant factors during the experiments.

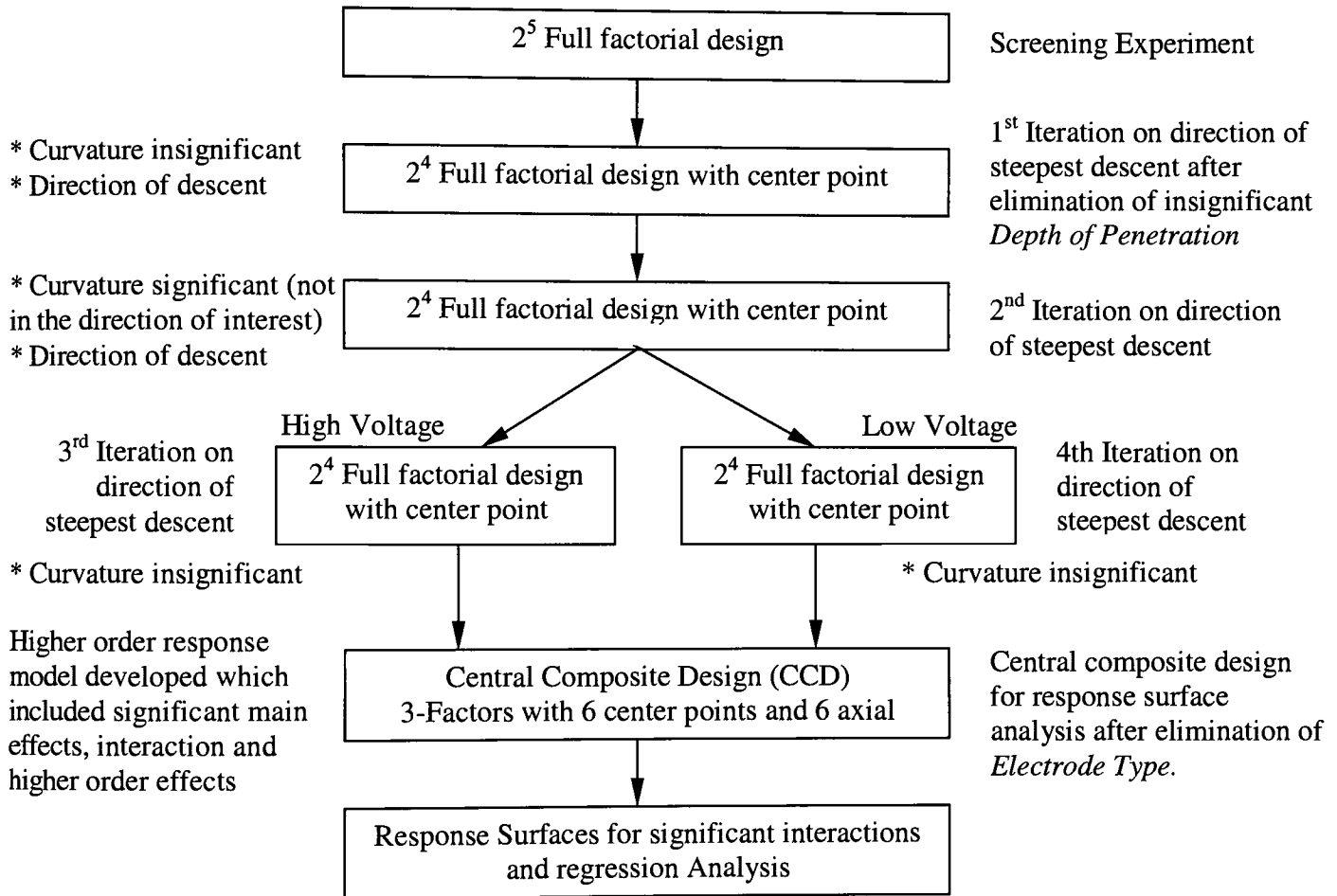


Figure 3.9 Experimentation block diagram

The factors considered and factor levels for experimentation were identified after exhaustive literature review, observation of current industrial practices and results of some one factor at a time experiments. Experiments involved 2 replicates each. As shown in figure 3.9 the screening experiment, first iteration experiment, second iteration experiments were executed in direction of steepest descent. The insignificant factors were eliminated subsequently when

identified. Total six experiments were executed in the path of steepest descent, which included the central composite design experiment for testing higher order effects and experiments with center points for test of curvature.

Screening experiment was executed to observe the trend and effect of factors on surface roughness. It included 5 major factors gap voltage, average current, pulse duration, depth of penetration and electrode type. Depth of penetration was identified as insignificant and was removed from further experiments. Rests of the factors were carried over for subsequent experimentation. The center point was introduced in remaining experiments to identify significant curvature effects in the results. The next first iteration experiment was designed in the path of steepest descent for minimization of response. The factor levels were calculated from the first order model obtained from the previous screening experiment. Second iteration experiment was executed for further investigation into the trend followed by the response in the direction of interest. Third and fourth iterations were carried out to study the effect of Gap voltage on the surface roughness keeping rest of the factors constant only gap voltage was changed. Finally electrode type was eliminated from the design and central composite design experiment was executed to identify higher order effects.

Results and analysis section discusses the design transition issues and step size calculation and limitations faced in the experimental process. The remaining part of this section displays the designed experiments with factor level combination and experimental setup.

4.1. 2⁵ full factorial experimental design (Screening Experiment):

Table 4.1 Factor levels for screening experiments

Factor	Code	Low level (-)	High level (+)
Gap Voltage	A	40V	80V
Pulse Duration	B	36 μ s	300 μ s
Average Current	C	30Amp	50Amp
Electrode Type	D	Graphite	Copper
Depth of Penetration	E	1mm	4mm

Table 4.2 Treatment combinations for screening experiment

#	Treatments	A (V)	B (μ s)	C (Amp)	D	E (mm)
1	(1)	40	36	30	Graphite	1
2	a	80	36	30	Graphite	1
3	b	40	300	30	Graphite	1
4	ab	80	300	30	Graphite	1
5	c	40	36	50	Graphite	1
6	ac	80	36	50	Graphite	1
7	bc	40	300	50	Graphite	1
8	abc	80	300	50	Graphite	1
9	d	40	36	30	Copper	1
10	ad	80	36	30	Copper	1
11	bd	40	36	30	Copper	1
12	abd	80	36	30	Copper	1
13	cd	40	300	50	Copper	1
14	acd	80	300	50	Copper	1
15	bcd	40	36	50	Copper	1
16	abcd	80	36	50	Copper	1
17	e	40	300	30	Graphite	4
18	ae	80	300	30	Graphite	4
19	be	40	36	30	Graphite	4
20	abe	80	36	30	Graphite	4
21	ce	40	36	50	Graphite	4
22	ace	80	36	50	Graphite	4
23	bce	40	300	50	Graphite	4
24	abce	80	300	50	Graphite	4
25	de	40	36	30	Copper	4
26	ade	80	36	30	Copper	4
27	bde	40	300	30	Copper	4
28	abde	80	300	30	Copper	4
29	cde	40	36	50	Copper	4
30	acde	80	36	50	Copper	4
31	bcde	40	300	50	Copper	4
32	abcde	80	300	50	Copper	4

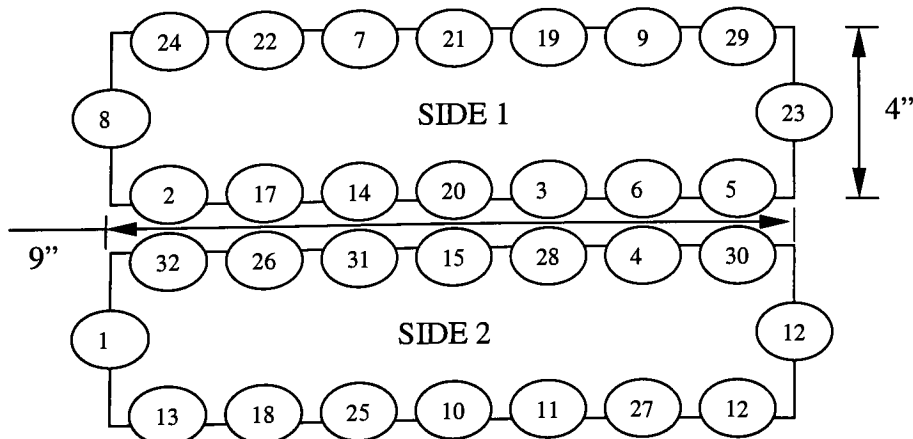


Figure 4.1 Experimental set up for screening experiment

4.2. 2⁴ Full factorial experiment (First Iteration)

Table 4.3 Factor levels for first iteration experiments

Factor	Code	Low Level(-)	Zero (0)	High Level(+)
Gap Voltage	A	20V	30V	40V
Pulse Duration	B	18μs	36μs	50μs
Average Current	C	20A	30A	40A
Electrode Type	D	Graphite		Copper

Table 4.4 Treatment combinations for first iteration experiment

#	Treatments	A (V)	B(μs)	C (Amp)	D
1	(1)	20	18	20	Graphite
2	a	40	18	20	Graphite
3	b	20	50	20	Graphite
4	ab	40	50	20	Graphite
5	c	20	18	40	Graphite
6	ac	40	18	40	Graphite
7	bc	20	50	40	Graphite
8	abc	40	50	40	Graphite
9	d	20	18	20	Copper
10	ad	40	18	20	Copper
11	bd	20	50	20	Copper
12	abd	40	50	20	Copper
13	cd	20	18	40	Copper
14	acd	40	18	40	Copper
15	bcd	20	50	40	Copper
16	abcd	40	50	40	Copper
17	0	30	36	30	Graphite
18	0	30	36	30	Copper
19	0	30	36	30	Graphite
20	0	30	36	30	Copper
21	0	30	36	30	Graphite
22	0	30	36	30	Copper

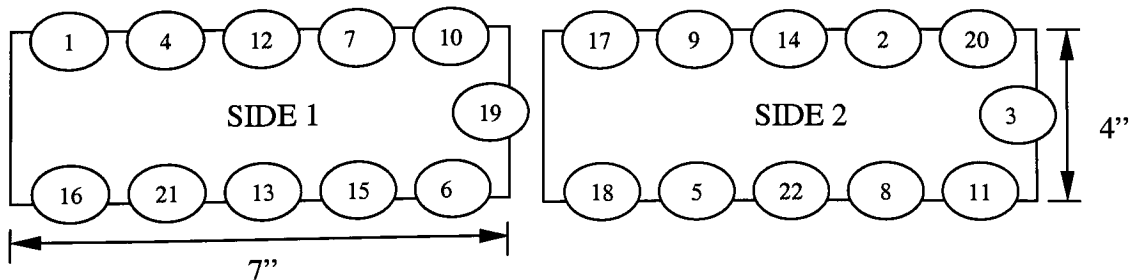


Figure 4.2 Experimental set up for first iteration experiment

4.3. 2⁴ Full factorial experiment (Second Iteration)

Table 4.5 Factor levels for second iteration experiments

Factor	Code	Low Level(-)	Zero (0)	High Level(+)
Gap Voltage	A	20V	70V	120V
Pulse Duration	B	10 μ s	14 μ s	18 μ s
Average Current	C	12A	15A	20A
Electrode Type	D	Graphite		Copper

Table 4.6 Treatment combinations for second iteration experiments

#	Treatments	A (V)	B	C (μ s)	D (Amp)
1	(1)	20	10	12	Graphite
2	a	120	10	12	Graphite
3	b	20	18	12	Graphite
4	ab	120	18	12	Graphite
5	c	20	10	20	Graphite
6	ac	120	10	20	Graphite
7	bc	20	18	20	Graphite
8	abc	120	18	20	Graphite
9	d	20	10	12	Copper
10	ad	120	10	12	Copper
11	bd	20	10	12	Copper
12	abd	120	10	12	Copper
13	cd	20	18	20	Copper
14	acd	120	18	20	Copper
15	bcd	20	10	20	Copper
16	abcd	120	10	20	Copper
17	0	70	14	15	Graphite
18	0	70	14	15	Copper
19	0	70	14	15	Graphite
20	0	70	14	15	Copper
21	0	70	14	15	Graphite
22	0	70	14	15	Copper

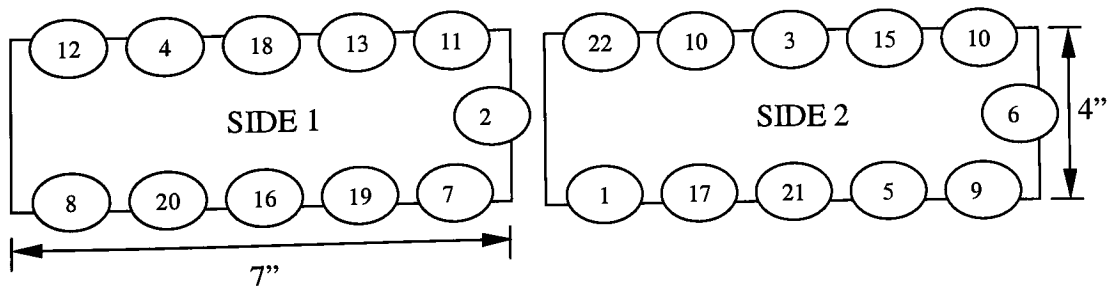


Figure 4.3 Experimental set up for second iteration experiment

4.4 2⁴ Full factorial experiment (Third Iteration)

Table 4.7 Factor levels for third iteration experiments

Factor	Code	Low Level(-)	Zero (0)	High Level(+)
Gap Voltage	A	10V	15V	20V
Pulse Duration	B	3 μ s	5 μ s	7 μ s
Average Current	C	4.5A	6A	8A
Electrode Type	D	Graphite		Copper

Table 4.8 Treatment combinations for third iteration experiments

#	Treatments	A (V)	B	C (μ s)	D (Amp)
1	(1)	10	3	4.5	Graphite
2	a	20	3	4.5	Graphite
3	b	10	7	4.5	Graphite
4	ab	20	7	4.5	Graphite
5	c	10	3	8	Graphite
6	ac	20	3	8	Graphite
7	bc	10	7	8	Graphite
8	abc	20	7	8	Graphite
9	d	10	3	4.5	Copper
10	ad	20	3	4.5	Copper
11	bd	10	7	4.5	Copper
12	abd	20	7	4.5	Copper
13	cd	10	3	8	Copper
14	acd	20	3	8	Copper
15	bcd	10	7	8	Copper
16	abcd	20	7	8	Copper
17	0	15	5	6	Graphite
18	0	15	5	6	Copper
19	0	15	5	6	Graphite
20	0	15	5	6	Copper
21	0	15	5	6	Graphite
22	0	15	5	6	Copper

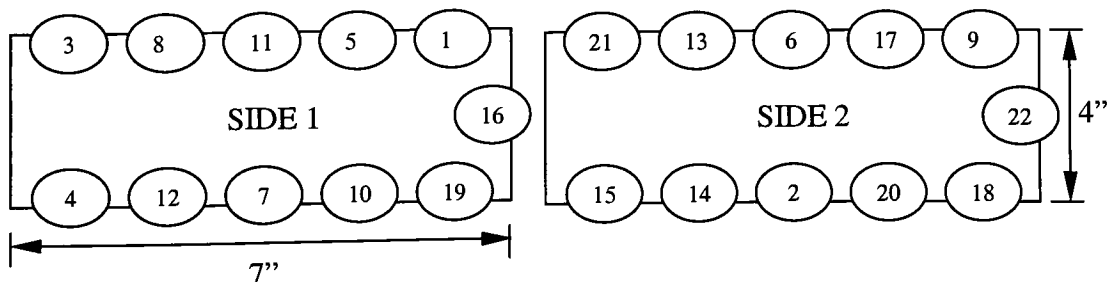


Figure 4.4 Experimental set up for third iteration experiment

4.5. 2⁴ Full factorial experiment (Fourth Iteration)

Table 4.9 Factor levels for fourth iteration experiments

Factor	Code	Low Level(-)	Zero (0)	High Level(+)
Gap Voltage	A	120V	130V	150V
Pulse Duration	B	3μs	5μs	7μs
Average Current	C	4.5A	6A	8A
Electrode Type	D	Graphite		Copper

Table 4.10 Treatment combinations for fourth iteration experiments

#	Treatments	A (V)	B (μs)	C (Amp)	D
1	(1)	120	3	4.5	Graphite
2	a	150	3	4.5	Graphite
3	b	120	7	4.5	Graphite
4	ab	150	7	4.5	Graphite
5	c	120	3	8	Graphite
6	ac	150	3	8	Graphite
7	bc	120	7	8	Graphite
8	abc	150	7	8	Graphite
9	d	120	3	4.5	Copper
10	ad	150	3	4.5	Copper
11	bd	120	7	4.5	Copper
12	abd	150	7	4.5	Copper
13	cd	120	3	8	Copper
14	acd	150	3	8	Copper
15	bcd	120	7	8	Copper
16	abcd	150	7	8	Copper
17	0	130	5	6	Graphite
18	0	130	5	6	Copper
19	0	130	5	6	Graphite
20	0	130	5	6	Copper
21	0	130	5	6	Graphite
22	0	130	5	6	Copper

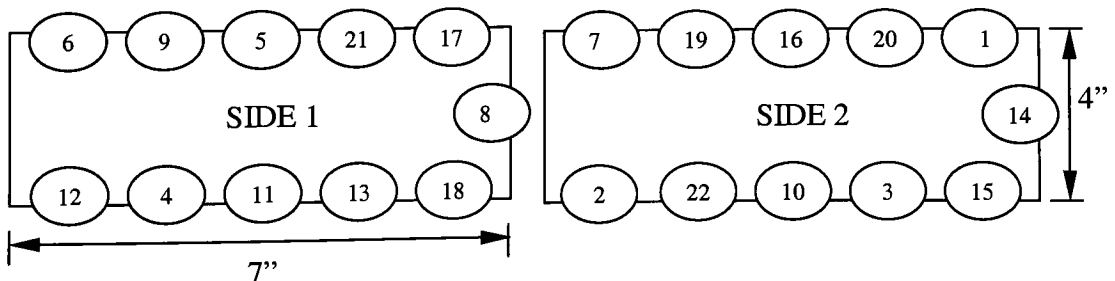


Figure 4.5 Experimental set up for fourth iteration experiment

4.6. Central Composite Design

Table 4.11 Factor levels for central composite design experiments

Factor	Code	-1.68	-1	0	+1	+1.68
Gap Voltage	A	140	150	160	170	180
Pulse Duration	B	1.5	2	3	4	4.5
Average Current	C	0.5	1.5	2	3	4.5

Table 4.12 Treatment combination for central composite design experiments

#	Treatments	A (V)	B (μ s)	C (Amp)
1	(1)	150	2	1.5
2	a	170	2	1.5
3	b	150	4	1.5
4	ab	170	4	1.5
5	c	150	2	3
6	ac	170	2	3
7	bc	150	4	3
8	abc	170	4	3
9	$-\alpha a$	140	3	2
10	$+\alpha a$	180	3	2
11	$-\alpha b$	160	1.5	2
12	$+\alpha b$	160	4.5	2
13	$-\alpha c$	160	3	0.5
14	$+\alpha c$	160	3	4.5
15	0	160	3	2
16	0	160	3	2
17	0	160	3	2
18	0	160	3	2
19	0	160	3	2
20	0	160	3	2

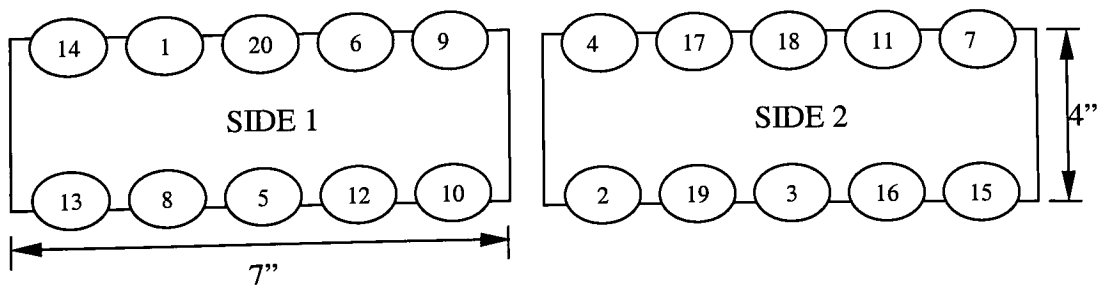


Figure 3.15 Experimental set up for central composite design experiment

5. RESULTS AND ANALYSIS :

Direction of steepest descent method, response surface methodology and analysis of variance were used to analyze the effect of various parameters from the factorial designs on surface roughness. The effects of significant parameters on outputs were analyzed with set of experimental runs. A total of six experiments were executed which included an initial screening experiment and a final central composite design experiment. Experiments were designed following the direction of steepest descent. Gap voltage, average current, pulse duration, electrode type and depth of penetration were the factors involved in the experimentation. Results are in the form of response table showing responses for each iteration followed by analysis of variance table, pareto chart showing standardized effects of each main effects and interaction as well as main effects and interactions plot. Detailed data containing all replicates can be found in appendix 9.6. Detailed calculation and formulae are presented for iterations after each design.

5.1. 2⁵ Full factorial design (Screening Experiment)

Factor	Code	Low level (-)	High level (+)
Gap Voltage	A	40V	80V
Pulse Duration	B	36μs	300μs
Average Current	C	30Amp	50Amp
Electrode Type	D	Graphite	Copper
Depth of Penetration	E	1mm	4mm

Table 5.1 Responses of measured parameters for screening experiment

#	Treatments	A	B	C	D	E	Ra Avg (μm)	Ra Avg (μm)	Ra Avg.
							Replicate 1	Replicate 2	(μm)
1	(1)	-1	-1	-1	-1	-1	6.94	5.00	5.97
2	a	+1	-1	-1	-1	-1	6.80	7.33	7.07
3	b	-1	+1	-1	-1	-1	9.18	8.33	8.76
4	ab	+1	+1	-1	-1	-1	9.59	8.49	9.04
5	c	-1	-1	+1	-1	-1	14.00	17.64	15.82
6	ac	+1	-1	+1	-1	-1	15.88	15.25	15.57
7	bc	-1	+1	+1	-1	-1	18.33	14.93	16.63
8	abc	+1	+1	+1	-1	-1	20.33	15.18	17.76
9	d	-1	-1	-1	+1	-1	6.35	8.20	7.28
10	ad	+1	-1	-1	+1	-1	7.76	8.28	8.02
11	bd	-1	+1	-1	+1	-1	8.71	8.89	8.80
12	abd	+1	+1	-1	+1	-1	8.38	7.18	7.78
13	cd	-1	-1	+1	+1	-1	12.50	13.21	12.86
14	acd	+1	-1	+1	+1	-1	15.83	15.31	15.57
15	bcd	-1	+1	+1	+1	-1	15.17	16.53	15.85
16	abcd	+1	+1	+1	+1	-1	17.08	19.55	18.32
17	e	-1	-1	-1	-1	+1	7.73	7.74	7.74
18	ae	+1	-1	-1	-1	+1	8.24	6.62	7.43
19	be	-1	+1	-1	-1	+1	10.34	9.96	10.15
20	abe	+1	+1	-1	-1	+1	10.09	8.30	9.20
21	ce	-1	-1	+1	-1	+1	15.23	13.22	14.23
22	ace	+1	-1	+1	-1	+1	17.98	16.51	17.25
23	bce	-1	+1	+1	-1	+1	17.98	20.50	19.24
24	abce	+1	+1	+1	-1	+1	16.43	18.04	17.24
25	de	-1	-1	-1	+1	+1	7.24	6.60	6.92
26	ade	+1	-1	-1	+1	+1	7.22	7.92	7.57
27	bde	-1	+1	-1	+1	+1	9.11	9.09	9.10
28	abde	+1	+1	-1	+1	+1	8.70	8.74	8.72
29	cde	-1	-1	+1	+1	+1	15.81	16.37	16.09
30	acde	+1	-1	+1	+1	+1	16.12	17.27	16.70
31	bcde	-1	+1	+1	+1	+1	18.26	19.78	19.02
32	abcde	+1	+1	+1	+1	+1	21.58	21.05	21.32
								Overall Avg.	12.47

The analysis of the above responses is done using analysis of variance. The following calculations show the coded formulae to find the contrasts for each main effects of experimental factors and their respective two, three and four factor interactions. The sum of squares and mean square are also determined. These same formulae can be applied to any experimental designs.

Analysis of Main Effects:

$$A = (1/4n) \{a-(1)+ab-b+ac-c+abc-bc+ad-d+abd-bd+acd-cd+abcd-bcd+ae-e+abe-be+ace-ce+abce-bce+ade-de+abde-bde+acde-cde+abcde-bcde\}$$

$$B = (1/4n) \{b+ab+bc+abc+bd+bcd+abcd+be+abe+bce+bde+abde+bcde+abcde-(1)-a-c-ac-d-ad-cd-acd-e-ae-ce-ace-de-ade-cde-acde\}$$

$$C = (1/4n) \{c+ac+bc+abc+ac+bc+acd+ce+ace+cde+acde+bcd+abcd+bce+bcde+abcde-(1)-a-b-ab-ad-d-e-ae-de-ade-bd-abd-be-abe-bde-abde\}$$

$$D = (1/4n) \{acd+cde+acde+bcd+abcd+bcde+abcde+ad+d+de+ade+bd+abd+bde+abde-c-ac-ce-ace-bc-abc-ac-bc-bce-(1)-a-b-ab-e-ae-be-abe\}$$

$$E = (1/4n) \{cde+acde+bcde+abcde+de+ade+bde+abde+ce+ace+bce+e+ae+be+abe-(1)-a-b-ab-bc-abc-ac-bc-c-ac-acd-bcd-abcd-ad-d-bd-abd\}$$

Analysis of two factor interactions:

Interaction effects of AB

<u>B</u>	<u>Average A Effect</u>
High (+)	$[(abc-bc)+(ab-b)+(abd-bd)+(abcd-bcd)+(abe-be)+(abce-bce)+(abde-bde)+(abcde-bcde)]/2n$
Low (-)	$\{[(ac-c)+(ad-d)+(acd-cd)+(ae-e)+(ace-ce)+(ade-de)+(acde-cde)+[a-(1)]]/2n$
Difference	$\{[(abc-bc+ab-b)+(abd-bd)+(abcd-bcd)+(abe-be)+(abce-bce)+(abde-bde)+(abcde-bcde)]-[(ac-c)+(a-(1))+(ad-d)+(acd-cd)+(ae-e)+(ace-ce)+(ade-de)+(acde-cde)]\}/2n$
AB interaction is 1/2 of above difference	$= \{[(abc-bc+ab-b)+(abd-bd)+(abcd-bcd)+(abe-be)+(abce-bce)+(abde-bde)+(abcde-bcde)]-[(ac-c)+(a-(1))+(ad-d)+(acd-cd)+(ae-e)+(ace-ce)+(ade-de)+(acde-cde)]\}/4n$

Interaction effects of AC

<u>C</u>	<u>Average A Effect</u>
High (+)	$[(abc-bc) + (ac-c) + (abcd-bcd) + (abce-bce) + (abcde-bcde) + (acd-cd) + (ace-ce) + (acde-cde)]/2n$
Low (-)	$\{[(ad-d) + (ae-e) + (ade-de) + [a- (1)] + (abd-bd) + (abe-be) + (abde-bde) + (ab-b)]\}/2n$
Difference	$\{[(abc-bc) + (ac-c) + (abcd-bcd) + (abce-bce) + (abcde-bcde) + (acd-cd) + (ace-ce) + (acde-cde)] - \{[(ad-d) + (ae-e) + (ade-de) + [a- (1)] + (abd-bd) + (abe-be) + (abde-bde) + (ab-b)]\}\}/2n$
AC interaction is 1/2 of the above difference	$= \{[(abc-bc) + (ac-c) + (abcd-bcd) + (abce-bce) + (abcde-bcde) + (acd-cd) + (ace-ce) + (acde-cde)] - \{[(ad-d) + (ae-e) + (ade-de) + [a- (1)] + (abd-bd) + (abe-be) + (abde-bde) + (ab-b)]\}\}/4n$

Interaction effects of AD

<u>D</u>	<u>Average A Effect</u>
High (+)	$[(abcd-bcd) + (abcde-bcde) + (acd-cd) + (acde-cde) + (ad-d) + (ade-de) + (abd-bd) + (abde-bde)]/2n$
Low (-)	$\{[(ae-e) + [a- (1)] + (abe-be) + (ab-b) + (abc-bc) + (ac-c) + (abce-bce) + (ace-ce)]\}/2n$
Difference	$\{[(abcd-bcd) + (abcde-bcde) + (acd-cd) + (acde-cde) + (ad-d) + (ade-de) + (abd-bd) + (abde-bde)] - \{[(ae-e) + [a- (1)] + (abe-be) + (ab-b) + (abc-bc) + (ac-c) + (abce-bce) + (ace-ce)]\}\}/2n$
AD interaction	$= \{[(abcd-bcd) + (abcde-bcde) + (acd-cd) + (acde-cde) + (ad-d) + (ade-de) + (abd-bd) + (abde-bde)] - \{[(ae-e) + [a- (1)] + (abe-be) + (ab-b) + (abc-bc) + (ac-c) + (abce-bce) + (ace-ce)]\}\}/4n$

Analysis of three factor interactions:

ABC interaction = $1/4n [abc-cde-acde-bcde-abcde-de-ade-bde-abde-ce-ace-bce-e-ae-be-abe-(1)+a+b-ab-bc-abc-ac-bc+c-ac-acd-bcd-abcd-ad-d-bd-abd]$

Similarly all 3 factor interactions can be explained.

Analysis of four factor interactions:

ABCD interaction = $1/4n[a-cde-acde-bcde-abcde-de-ade-bde-abde-ce-ace-bce-e-ae-be-abe-(1)+b-ab-bc-abc-ac-bc+c-ac-abc-ac`d-bcd+abcd-ad-d-bd-abd]$

Similarly all 4 factor interactions can be explained.

ABCDE interaction = $1/4n[a-cde-acde-bcde+abcde-de-ade-bde-abde-ce-ace-bce-e-ae-be-abe-(1)+b-ab-bc-abc-ac-bc+c-ac-abc-acd-bcd-abcd-ad-d-bd-abd]$

Sum of Squares (SS) : $(\text{Contrast})^2 / 8n$,

Mean Square (MS) : SS_i / DF_i (Where i = any treatment and DF is degrees of freedom)

These values can be determined and used in the analysis of variance to obtain the significant main effects and interactions. The significance level considered through out this work is 5%. For example, hypothesis will be rejected if the test statistic exceeds the critical value (for $\alpha = 0.05$) or analogously fail to reject the null hypothesis if the p -value is smaller than 0.05. The analysis of variance is followed by pareto chart for standardized effects, main effect plot and interaction plot. The Pareto chart allows you to look at both the magnitude and the importance of an effect. It displays the absolute value of the effects, and draws a reference line on the chart. Any effect that extends past this reference line is significant. Similar to the regression output (since DOE is a regression on the design matrix), analysis also displays t statistics for the estimated coefficients portion of the output (titled Estimated Effects and Coefficients for response) and F statistics for the ANOVA part of the output. t squared equals F . For the exact depiction of the pareto plot displayed and for more elaborate analysis of the data both ANOVA and estimated effects table is shown after each experimental analysis. The reference dotted line is drawn where t is the $(1 - \alpha/2)$ quantile of a t -distribution with degrees of freedom equal to the degrees of freedom for the error term.

Table 5.2 Analysis of variance for screening experiment

TCs	Sum of Squares	DF	Mean Square	F value	P value
Main Effects					
A	6.98	1	6.98	4.58	0.040
B	1232.60	1	1232.60	808.26	0.000
C	73.66	1	73.66	48.30	0.000
D	16.61	1	16.61	10.89	0.002
E	0.01	1	0.01	0.00	0.946
Two Factor Interactions					
AB	6.73	1	6.73	4.41	0.044
AC	3.03	1	3.03	1.99	0.168
AD	1.41	1	1.41	0.92	0.345
AE	1.95	1	1.95	1.28	0.268
BC	3.30	1	3.30	2.16	0.152
BD	4.10	1	4.10	2.69	0.111
BE	0.44	1	0.44	0.29	0.595
CD	2.09	1	2.09	1.37	0.251
CE	0.14	1	0.14	0.09	0.769
DE	1.98	1	1.98	1.30	0.264
Three factor Interactions					
ABC	0.15	1	0.15	0.10	0.756
ABD	0.02	1	0.02	0.01	0.914
ABE	2.12	1	2.12	1.39	0.247
ACD	0.59	1	0.59	0.38	0.539
ACE	1.13	1	1.13	0.74	0.396
ADE	0.10	1	0.10	0.07	0.800
BCD	0.51	1	0.51	0.34	0.568
BCE	6.41	1	6.41	4.20	0.049
BDE	9.15	1	9.15	6.00	0.020
CDE	0.51	1	0.51	0.34	0.568
Four Factor Interactions					
ABCD	1.46	1	1.46	0.96	0.333
ABCE	2.99	1	2.99	1.96	0.171
ABDE	1.62	1	1.62	1.06	0.309
ACDE	4.41	1	4.41	2.89	0.098
BCDE	0.68	1	0.68	0.45	0.506
Five Factor Interactions					
ABCDE	3.30	1	3.30	2.16	0.151
Error	48.79	32	1.53		
Total	1438.16	63			

Table 5.3. Estimated Effects and Coefficient for Ra

Term		Effect	Coefficient	SE Coefficient	T	P
Main Effects						
A	A	0.6612	0.3306	0.1543	2.14	0.040
B	D	8.7750	4.3875	0.1543	28.43	0.000
C	E	2.1469	1.0734	0.1543	6.95	0.000
D	C	1.02	0.51	0.1543	3.30	0.002
E	B	0.0213	0.0106	0.1543	0.07	0.946
Two Factor Interactions						
AB	AD	0.6469	0.3243	0.1543	2.10	0.044
AC	AE	-0.4350	-0.2175	0.1543	-1.41	0.168
AD	AC	-0.2956	-0.1478	0.1543	-0.96	0.345
AE	AB	0.3481	0.1741	0.1543	1.13	0.268
BC	DE	0.4525	0.2263	0.1543	1.47	0.152
BD	CD	0.5056	0.2528	0.1543	1.64	0.111
BE	BD	0.1656	0.0828	0.1543	0.54	0.595
CD	CE	0.3612	0.1806	0.1543	1.17	0.251
CE	BE	0.0913	0.0456	0.1543	0.30	0.769
DE	BC	0.3506	0.1753	0.1543	1.14	0.264
Three Factor Interactions						
ABC	ADE	0.0969	0.0484	0.1543	0.31	0.756
ABD	ACD	-0.0338	-0.0169	0.1543	-0.11	0.914
ABE	ABD	0.3637	0.1819	0.1543	1.18	0.247
ACD	ACE	-0.1919	-0.0959	0.1543	-0.62	0.539
ACE	ABE	0.2656	0.1328	0.1543	0.86	0.396
ADE	ABC	0.0787	0.0394	0.1543	0.26	0.800
BCD	CDE	0.1781	0.0891	0.1543	0.58	0.568
BCE	BDE	0.6319	0.3159	0.1543	2.05	0.049
BDE	BCD	0.7563	0.3781	0.1543	2.45	0.020
CDE	BCE	0.1781	0.0891	0.1543	0.58	0.568
Four Factor Interactions						
ABCD	ACDE	-0.3038	-0.1519	0.1543	-0.98	0.333
ABCE	ABDE	0.4325	0.2162	0.1543	1.40	0.171
ABDE	ABCD	-0.3194	-0.1597	0.1543	-1.03	0.309
ACDE	ABCE	0.5262	0.2631	0.1543	1.70	0.098
BCDE	BCDE	-0.2075	-0.1038	0.1543	-0.67	0.506
Five Factor Interactions						
ABCDE	ABCDE	0.4544	0.2272	0.1543	1.47	0.151

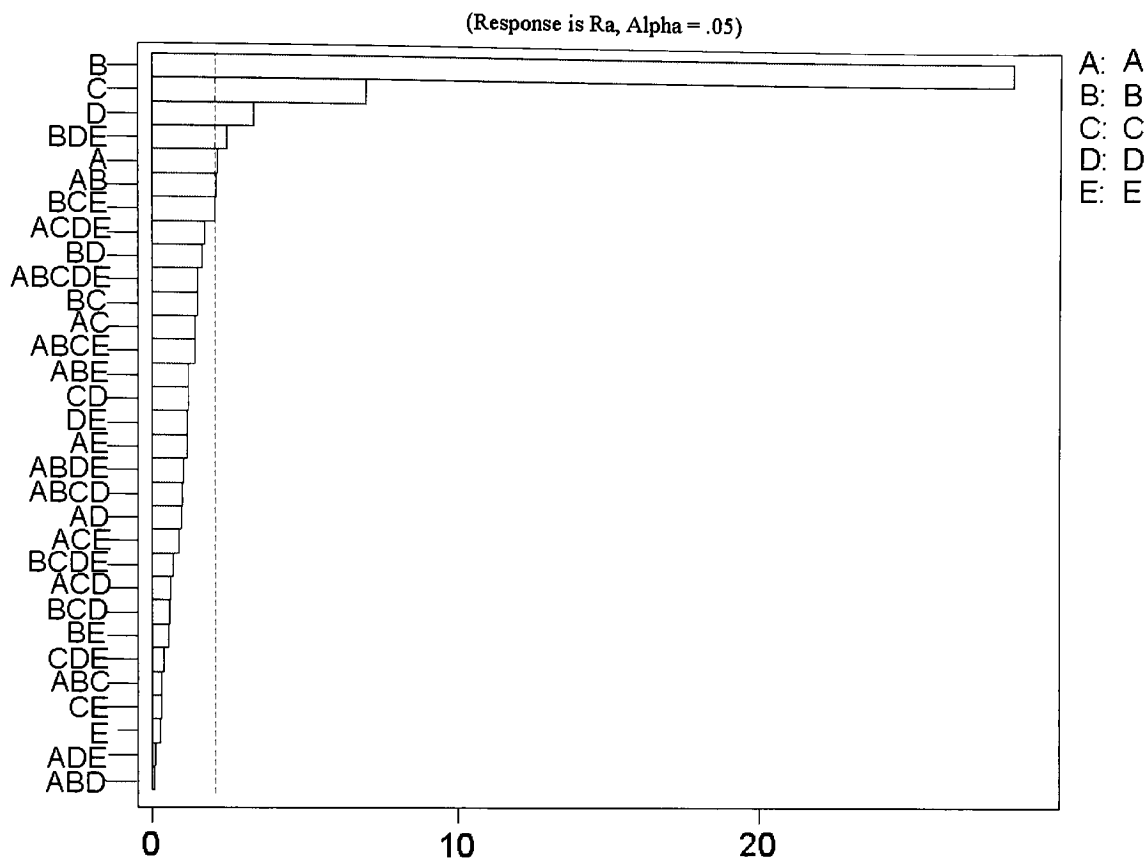


Figure 5.1 Pareto Chart of Standardized Effects (Screening Experiment)

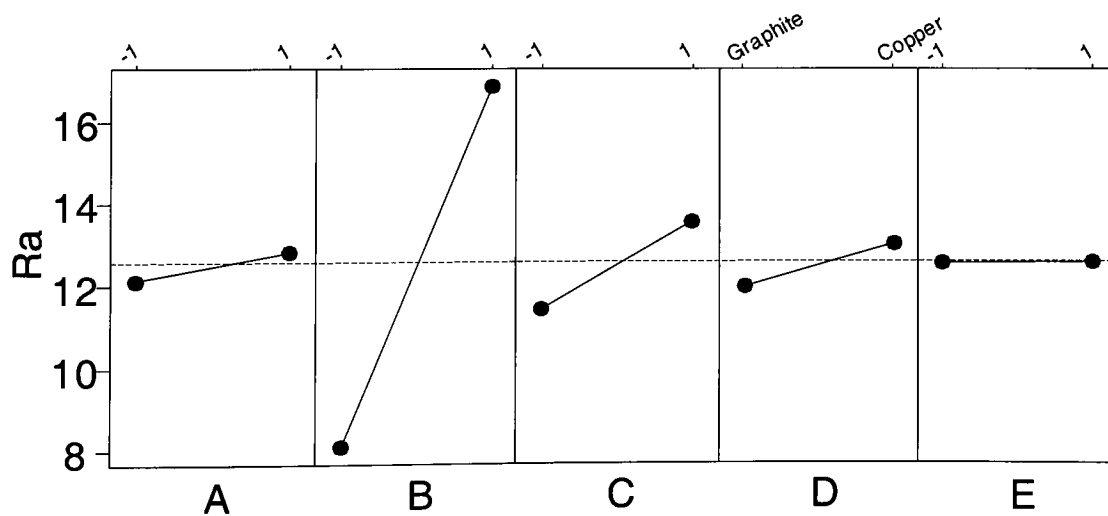


Figure 5.2 Main Effects Plot (data means) for Ra (Screening Experiment)

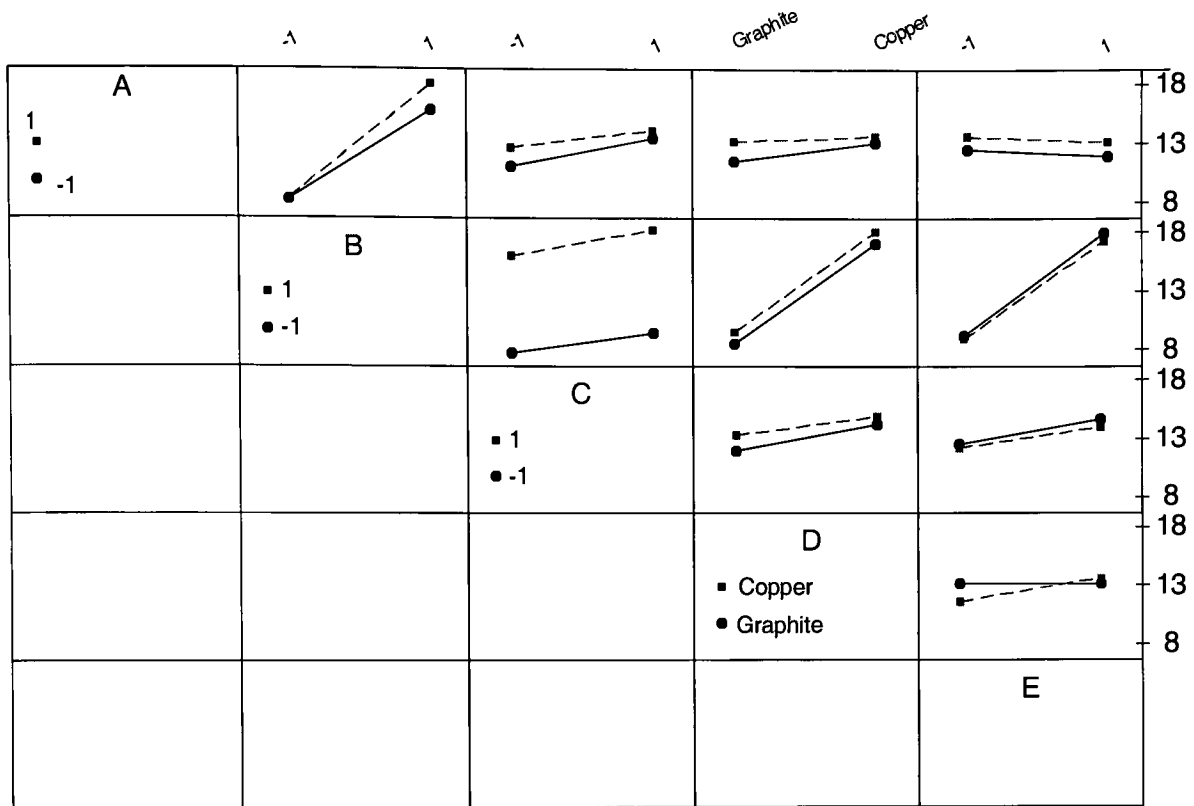


Figure 5.3 Interaction Plots (Data means) (Screening experiment)

The screening experiment was intended to observe the trend in the change in surface roughness at various factor level combinations and to eliminate factors, which are insignificant. Screening experimentation involved 5 major parameters in die-sink EDM (gap voltage, pulse duration, average current, type of electrode and depth of penetration). 2^5 full factorial experiment was executed. As seen from the plots and analysis of variance among the 5 factors: gap voltage, pulse duration, average current and electrode type are significant and depth of penetration is insignificant factor. There are no 2-factor interactions, which are significant. We can observe that there is a 3-factor interaction, which is significant. Three-factor interaction involves pulse duration, electrode type and depth of penetration. Considering scope of research the three-factor interaction is not analyzed in this study. The results show the positive slopes for the all the factors (i.e. Lower response is observed at lower levels of factors) Depth of penetration is insignificant factor and is discarded from further experimentation.

It can be seen from the ANOVA table that there is no significant lack of linear fit due to an interaction term. Furthermore, there is evidence that the first-order model is significant. Using

the DESIGN EXPERT statistical software, we obtain the resulting model (in the coded variables) as

$$\text{Response} = 12.49 + 0.32 \times \text{Gap Voltage} + 04.36 \times \text{Pulse Duration} \\ + 1.10 \times \text{Average current} + 0.54 \times \text{Electrode type}$$

The usual diagnostic checks show conformance to the regression assumptions, although the R^2 value is not very high: $R^2 = 0.9322$.

To *Minimize*, we use the direction of steepest descent. The engineer selects $\rho = 1$ since a point on the steepest descent direction one unit (in the coded units) from the origin is desired. Then from the equation above for the predicted Y response, the coordinates of the factor levels for the next run are given by. As explained in Appendix 9.5 :

$$x_1 = \rho \frac{b_1}{\sqrt{\sum_{i=1}^k b_i^2}} = \frac{(1)(0.32)}{\sqrt{(0.32)^2 + (4.36)^2 + (1.10)^2 + (0.54)^2}} = 0.074$$

Similarly,

$$x_2 = 0.9601, \quad x_3 = 0.2421, \quad x_4 = 0.1189$$

Now we have orthogonally coded factors :

$$x_1 = \frac{X_1 - 60}{20}, \quad x_2 = \frac{X_2 - 168}{132}, \quad x_3 = \frac{X_3 - 40}{10}$$

To minimize the surface roughness descriptor, Ra

for every (0.074) (20) = 1.48V voltage should be decreased per step

for every (0.96) (132) = 126.32μs pulse duration should be decreased per step

for every (0.24) (10)=2.4A Average Current should be decreased per step

The step sizes calculated from the preliminary design were not feasible to be used for the next design as the values were not balanced and there were machine-setting limitation issues. Hence, next experiment was designed considering factor-levels in literature-reviewed and results from the screening experiment. Center points were added for testing the response for curvature.

2. 2⁴ full factorial experiment with center point (First Iteration)

Factor	Code	Low Level(-)	Zero (0)	High Level(+)
Gap Voltage	A	20V	30V	40V
Pulse Duration	B	18μs	36μs	50μs
Average Current	C	20A	30A	40A
Electrode Type	D	Graphite		Copper

Table 5.3 Responses of measured parameters for first iteration experiment

#	Treatments	A	B	C	D	Ra Avg	Ra Avg	Ra Avg.
						Replicate 1	Replicate 2	
1	(1)	-1	-1	-1	-1	4.80	4.29	4.55
2	a	+1	-1	-1	-1	5.20	5.37	5.29
3	b	-1	+1	-1	-1	8.77	7.98	8.38
4	ab	+1	+1	-1	-1	7.86	7.48	7.67
5	c	-1	-1	+1	-1	7.11	7.12	7.12
6	ac	+1	-1	+1	-1	6.64	6.80	6.72
7	bc	-1	+1	+1	-1	9.77	10.01	9.89
8	abc	+1	+1	+1	-1	9.89	9.09	9.49
9	d	-1	-1	-1	+1	6.29	6.29	6.29
10	ad	+1	-1	-1	+1	5.50	6.19	5.85
11	bd	-1	+1	-1	+1	8.35	9.66	9.01
12	abd	+1	+1	-1	+1	8.10	6.87	7.49
13	cd	-1	-1	+1	+1	8.00	7.12	7.56
14	acd	+1	-1	+1	+1	8.05	7.74	7.90
15	bcd	-1	+1	+1	+1	10.95	10.15	10.55
16	abcd	+1	+1	+1	+1	10.05	11.79	10.92
17	0	0	0	0	-1	7.66	7.54	7.60
18	0	0	0	0	+1	8.62	9.41	9.02
19	0	0	0	0	-1	7.35	7.39	7.37
20	0	0	0	0	+1	7.95	9.45	8.70
21	0	0	0	0	-1	8.15	8.65	8.40
22	0	0	0	0	+1	8.80	9.71	9.26
							Overall Avg.	7.96

As mentioned earlier, we add centerpoint runs interspersed among the experimental setting runs for two purposes:

1. To provide a measure of process stability and inherent variability.
2. To check for curvature.

Table 5.4 Analysis of variance for first iteration experiment

TCs	Sum of Squares	DF	Mean Square	F value	P value
Main effects					
A	0.51	1	0.51	1.56	0.2222
B	61.24	1	61.24	187.69	0.0000
C	30.57	1	30.57	93.70	0.0000
D	9.20	1	9.20	28.20	0.0000
Two factor interactions					
AB	0.77	1	0.77	2.37	0.1350
AC	0.42	1	0.42	1.30	0.2650
AD	0.03	1	0.03	0.10	0.7590
BC	0.11	1	0.11	0.35	0.5570
BD	0.24	1	0.24	0.74	0.3970
CD	0.11	1	0.11	0.35	0.5570
Three factor interactions					
ABC	0.82	1	0.82	2.50	0.1260
ABD	0.02	1	0.02	0.06	0.8020
ACD	1.54	1	1.54	4.71	0.0390
BCD	0.01	1	0.01	0.04	0.8400
ABCD	0.01	1	0.01	0.04	0.8400
Curvature	3.14	1	3.14	9.61	0.0040
	0.0102	27	0.3263		
	118.223	43			

Table 5.3. Estimated Effects and Coefficient for Ra

Term	Effect	Coefficient	SE Coefficient	T	P
Main Effects					
A	-0.2525	-0.1262	0.101	-1.25	0.2222
B	2.7663	1.3831	0.101	13.70	0.0000
C	1.9550	1.9775	0.101	9.68	0.0000
D	0.9145	0.4573	0.101	5.31	0.0000
Two Factor Interactions					
AB	-0.3113	-0.1556	0.101	-1.54	0.1350
AC	0.2300	0.1150	0.101	1.14	0.2650
AD	-0.0625	-0.0312	0.101	-0.31	0.7590
BC	0.1238	0.0619	0.101	0.59	0.5570
BD	-0.1738	0.0869	0.101	-0.86	0.3970
CD	0.1200	0.0600	0.101	0.59	0.5570
Three Factor Interactions					
ABC	0.3188	0.1594	0.101	1.58	0.1260
ABD	0.0512	0.0256	0.101	0.25	0.8020
ACD	0.4375	0.2187	0.101	2.17	0.0390
BCD	0.2913	0.1456	0.101	-0.20	0.8400
Four Factor Interactions					
ABCD	-0.0412	-0.0206	0.101	-0.20	0.8400
Curvature		0.6	0.1934	3.10	0.0040

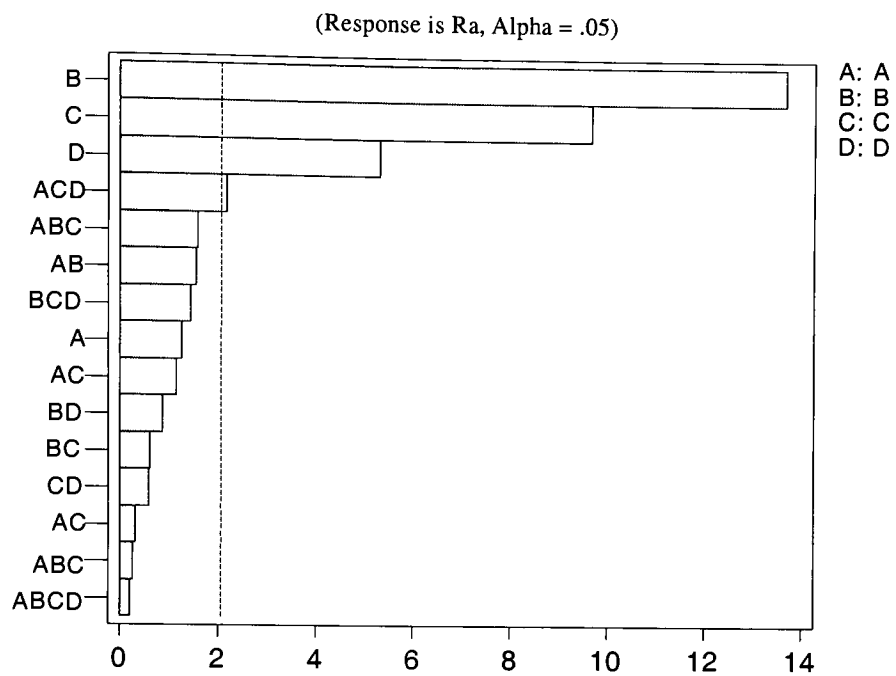


Figure 5.7 Pareto Chart of the Standardized effects (First Iteration)

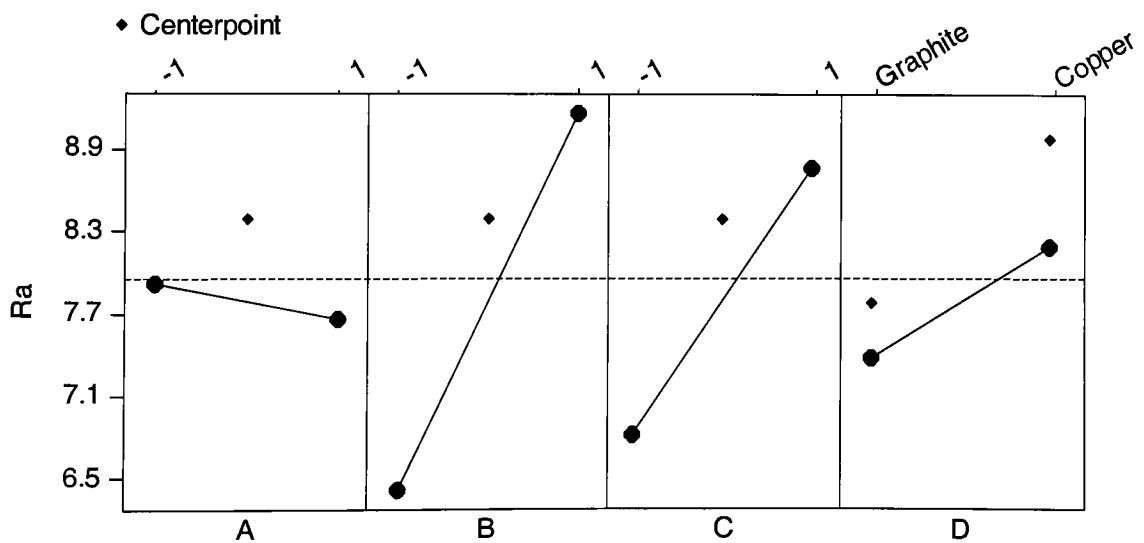


Figure 5.11 Main Effects plots (First Iteration)

◆ Centerpoint

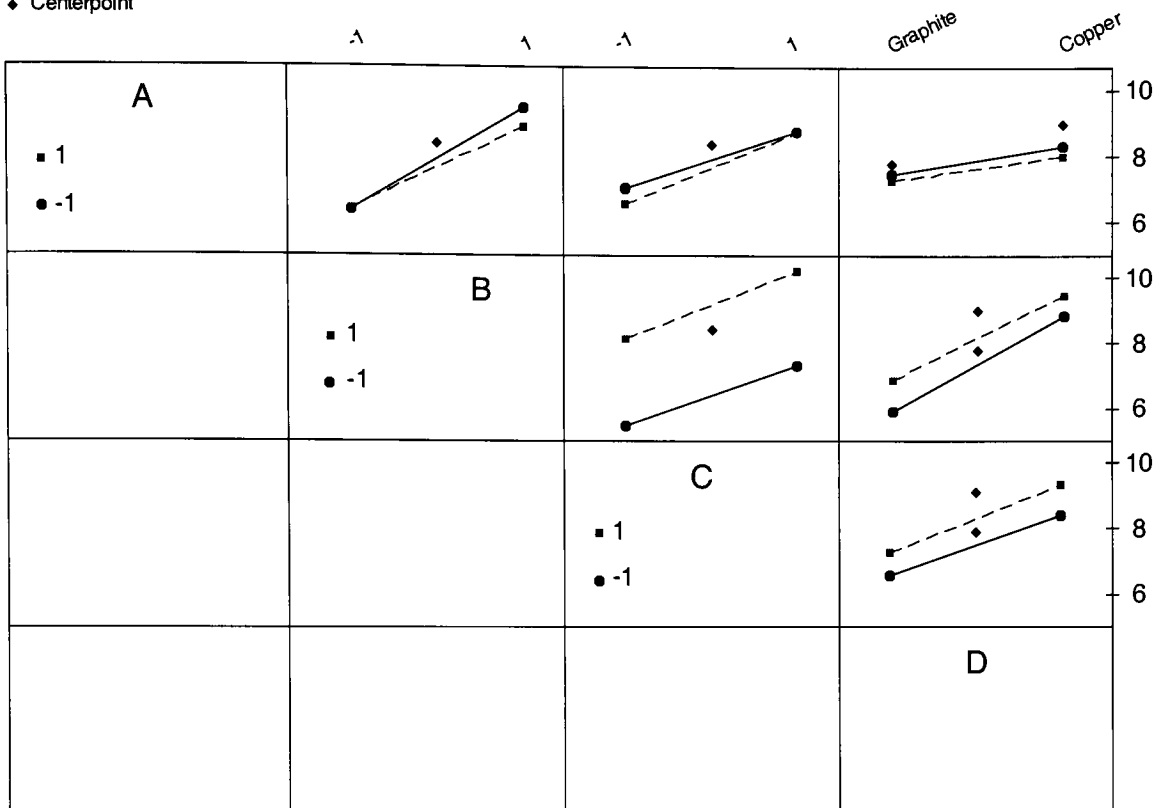


Figure 5.6 Interaction Plots (Data Means) (First Iteration)

After first iteration experiment it was observed that pulse duration, average current and electrode type were significant factors and gap voltage was insignificant. Electrode type is a qualitative factor so; the center point run was replicated 3 times for graphite and copper electrode both to get the goodness-of-fit of the planar two-level factorial model. The average response value from the actual center points was compared to that estimated value of the center point that comes from averaging all the factorial points. If there would be curvature of the response surface in the region of the design, the actual center point value would be higher than predicted by the factorial design points. The curvature was significant in this design but it wasn't significant in the direction of interest i.e. minimization. In the precedence of significance level pulse duration was most significant followed by average current and electrode type. Graphite electrode produced better surface finish than copper electrode. There were no significant 2-factor interactions. Despite the fact that gap voltage was not significant there was an important observation, which showed better surface at higher gap voltage setting.

Furthermore, there is evidence that the first-order model is significant. Using the DESIGN EXPERT statistical software, we obtain the resulting model (in the coded form)

$$\text{Response} = +7.79 - 0.13 \times \text{Gap Voltage} + 0.40 \times \text{Pulse Duration} + 1.38 \times \text{Average Current} + 0.98 \times \text{Electrode Type}$$

The usual diagnostic checks show conformance to the regression assumptions, although the R^2 value is not very high: $R^2 = 0.8270$.

To *minimize*, we use the direction of steepest descent. The engineer selects $\rho = 1$ since a point on the steepest descent direction one unit (in the coded units) from the origin is desired. the coordinates of the factor levels for the next run are given by:

$$x_1 = \rho \frac{b_1}{\sqrt{\sum_{i=1}^k b_i^2}} = \frac{(1)(-0.13)}{\sqrt{(0.13)^2 + (0.40)^2 + (1.38)^2 + (0.98)^2}} = 0.077$$

Similarly,

$$x_2 = 0.234, \quad x_3 = 0.793, \quad x_4 = 0.560$$

Now we have orthogonally coded factors :

$$x_1 = \frac{X_1 - 30}{10}, \quad x_2 = \frac{X_2 - 36}{18}, \quad x_3 = \frac{X_3 - 30}{10}$$

To minimize the surface roughness descriptor, Ra

for every (0.077) (10) = 0.77 V gap voltage should be decreased per step

for every (0.234) (18) = 4.21 μ s pulse duration should be decreased per step

for every (0.793) (10)=7.93 A Average Current should be decreased per step

From the regression equation obtained it is observed that coefficient of gap voltage is negative. Gap voltage is insignificant in the design but to understand the above mentioned variation it has been retained in the next design. As we see the step sizes are balanced and it can be used for the next design. Step size for gap voltage in the second iteration design is decided considering wider interval between low and high levels to understand the nature of trend in . Other factor- levels are decided taking into account single step decrement of the levels. The adjustment is done in the levels after subtraction of step size because of machine setting limitation. Refer (Appendix 10.2)

5.3. 2⁴ Full factorial experiment with center points (Second iteration)

Factor	Code	Low Level(-)	Zero (0)	High Level(+)
Gap Voltage	A	20V	70V	120V
Pulse Duration	B	10μs	14μs	18μs
Average Current	C	12A	15A	20A
Electrode Type	D	Graphite		Copper

Table 5.5 Responses of measured parameters for second iteration

#	Treatments	A	B	C	D	Ra Avg		Ra Avg.
						Replicate 1	Replicate 2	
1	(1)	-1	-1	-1	-1	3.62	3.65	3.64
2	a	+1	-1	-1	-1	3.91	3.51	3.71
3	b	-1	+1	-1	-1	4.80	4.70	4.75
4	ab	+1	+1	-1	-1	4.73	4.82	4.78
5	c	-1	-1	+1	-1	3.83	4.70	4.27
6	ac	+1	-1	+1	-1	4.70	5.20	4.95
7	bc	-1	+1	+1	-1	5.54	5.41	5.48
8	abc	+1	+1	+1	-1	5.77	5.58	5.68
9	d	-1	-1	-1	+1	4.06	3.94	4.00
10	ad	+1	-1	-1	+1	4.25	4.18	4.22
11	bd	-1	+1	-1	+1	5.51	5.23	5.37
12	abd	+1	+1	-1	+1	4.76	5.24	5.00
13	cd	-1	-1	+1	+1	5.00	4.94	4.97
14	acd	+1	-1	+1	+1	4.84	4.70	4.77
15	bcd	-1	+1	+1	+1	5.64	5.27	5.46
16	abcd	+1	+1	+1	+1	6.84	5.74	6.29
17	0	0	0	0	-1	4.52	4.42	4.47
18	0	0	0	0	+1	4.72	4.54	4.63
19	0	0	0	0	-1	4.68	4.47	4.58
20	0	0	0	0	+1	5.45	4.73	5.09
21	0	0	0	0	-1	5.37	5.74	5.56
22	0	0	0	0	+1	4.72	5.12	4.92
							Overall Avg.	4.85

Table 5.6 Analysis of variance for second iteration

TCs	Sum of Squares	DF	Mean Square	F value	P value
Main effects					
A	0.697	1	0.697	3.06	0.2170
B	3.844	1	3.844	16.89	0.0180
C	4.072	1	4.072	17.89	0.0163
D	1.574	1	1.574	6.92	0.0482
Two factor interactions					
AB	0.059	1	0.059	0.26	0.7453
AC	0.055	1	0.055	0.24	0.7140
AD	0.361	1	0.361	1.59	0.3600
BC	0.561	1	0.561	2.46	0.2607
BD	0.118	1	0.118	0.52	0.5883
CD	0.023	1	0.023	0.10	0.8091
Three factor interactions					
ABC	0.014	1	0.014	0.06	0.8521
ABD	0.001	1	0.001	0.00	0.9571
ACD	0.322	1	0.322	1.42	0.3842
BCD	0.168	1	0.168	0.74	0.5220
Four factor interaction					
ABCD	1.052	1	1.052	4.62	0.0840
Curvature	0.093	1	0.093	0.41	0.6310
Pure Error	0.084	27			
Total	14.143	43			

Table 5.3. Estimated Effects and Coefficient for Ra

Term	Effect	Coefficient	SE Coefficient	T	P
Main Effects					
A	0.4163	0.2081	0.1193	1.75	0.2170
B	0.9804	0.4902	0.1193	4.11	0.0180
C	1.0079	0.5040	0.1193	4.23	0.0160
D	0.5348	0.2647	0.1193	2.63	0.0480
Two Factor Interactions					
AB	0.1221	0.0610	0.1193	0.51	0.7000
AC	0.1163	0.0581	0.1193	0.49	0.7140
AD	-0.2996	-0.1498	0.1193	-1.26	0.3600
BC	0.3754	0.1877	0.1193	1.57	0.2600
BD	0.1729	0.0865	0.1193	0.72	0.5880
CD	-0.0762	-0.0381	0.1193	-0.32	0.8090
Three Factor Interactions					
ABC	0.0588	0.0294	0.1193	0.25	0.8520
ABD	-0.0171	-0.0085	0.1193	-0.07	0.9570
ACD	0.2838	0.1419	0.1193	1.19	0.3840
BCD	-0.2054	-0.1027	0.1193	-0.86	0.5220
Four Factor Interactions					
ABCD	0.5129	0.2565	0.1193	2.15	0.0840
Curvature		0.1463	0.2892	0.64	0.6310

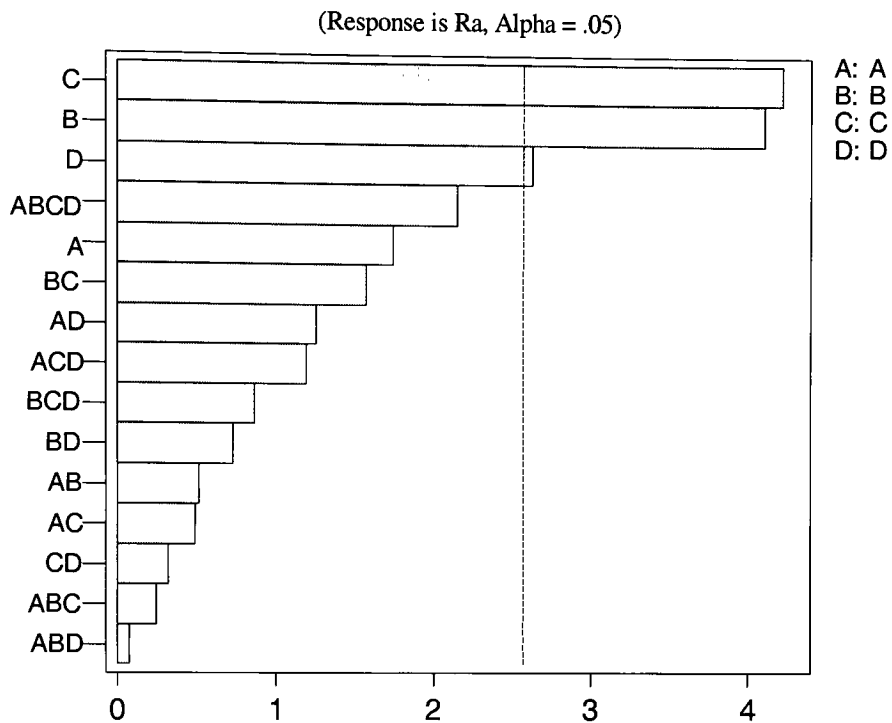


Figure 5.7 Pareto Chart of the Standardized effects (Second Iteration)

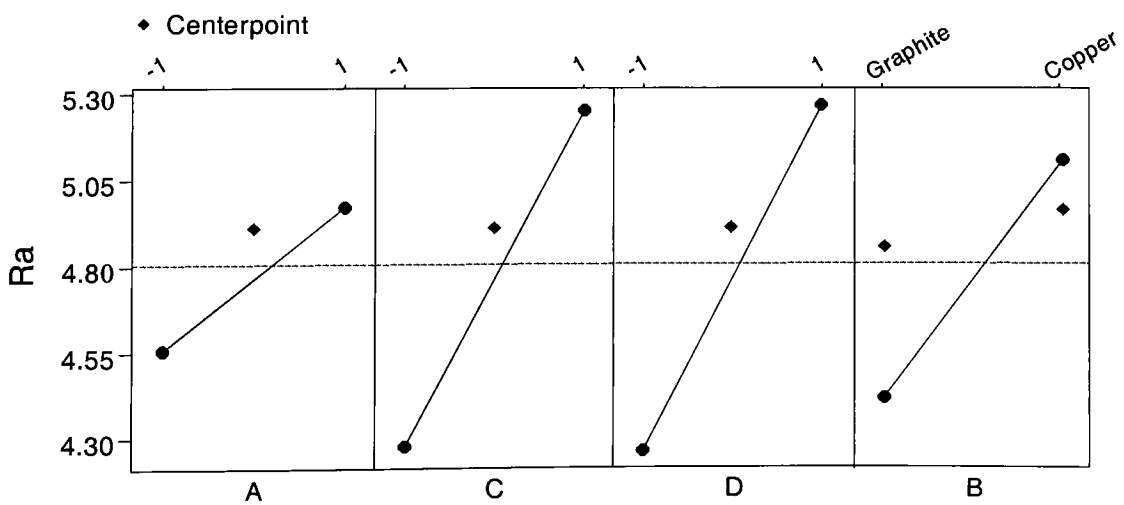


Figure 5.11 Main Effects plots (Second Iteration)

◆ Centerpoint

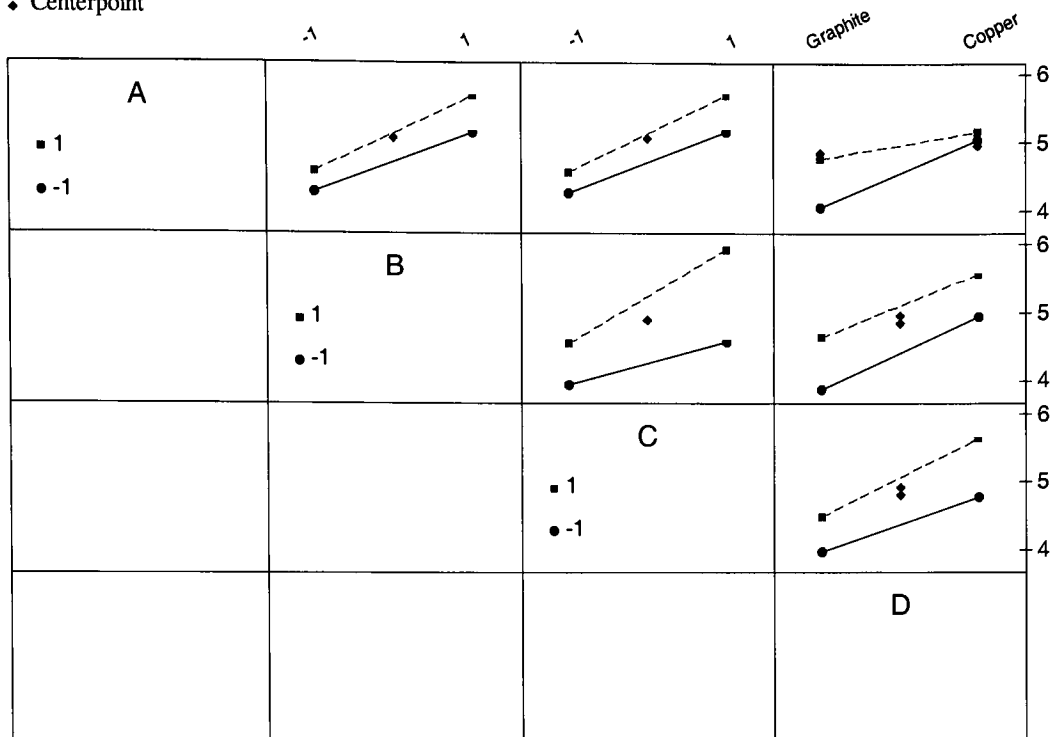


Figure 5.9 Interaction Plots (Second Iteration)

As seen in the pareto chart (figure.) above the second iteration was executed with 22 run design with 6 center points was executed the design showed clearly that pulse duration and average current were two most significant factors. Gap voltage was insignificant factors but it showed opposite results than the previous design result. (i.e. the better surface was obtained at higher voltages). Type of electrode was marginally insignificant. Curvature was also insignificant. Gap voltage was observed to have different trend compared to the results from the previous design, as at higher voltage surface roughness is higher than at lower voltage. Gap voltage is retained in the next design for another review.

It can be seen from the ANOVA table that there is no significant lack of linear fit due to an interaction term and there is no evidence of curvature. Furthermore, there is evidence that the first-order model is significant. Using the DESIGN EXPERT statistical software, we obtain the resulting model (in the coded variables) as

$$\text{Response} = +4.76 + 0.21 \times \text{Gap voltage} + 0.35 \times \text{Pulse duration} + 0.49 \times \text{Average Current} + 0.50 \times \text{Electrode type}$$

The usual diagnostic checks show conformance to the regression assumptions, although the R^2 value is not very high: $R^2 = 0.9447$.

To *minimize* , we use the direction of steepest descent. The engineer selects $\rho = 1$ since a point on the steepest descent direction is one unit (in the coded units) from the origin is desired. Then from the equation above for the predicted (Y) response, the coordinates of the factor levels for the next run are given by:

$$x_1 = \rho \frac{b_1}{\sqrt{\sum_{i=1}^k b_i^2}} = \frac{(1)(0.21)}{\sqrt{(0.21)^2 + (0.35)^2 + (0.49)^2 + (0.5)^2}} = 0.2591$$

Similarly,

$$x_2 = 0.4319, \quad x_3 = 0.5443, \quad x_4 = 0.5554$$

Now we have orthogonally coded factors :

$$x_1 = \frac{X_1 - 70}{50}, \quad x_2 = \frac{X_2 - 14}{4}, \quad x_3 = \frac{X_3 - 15}{5}$$

To minimize the surface roughness descriptor, Ra

for every (0.2591) (50) = 12.95V voltage should be decreased per step

for every (0.5443) (4) = 2.117 μ s pulse duration should be decreased per step

for every (0.5554) (5) = 2.777A average Current should be decreased per step

The step sizes were very small and considering the timeline and machine availability, instead of going one step in the direction of steepest descent, the decision was taken to going 3 steps at a time in the direction of steepest descent. And the succeeding design has the factor levels are decreased 3 times. As explained above to understand the trend of effect of gap voltage on surface roughness. Next step is executed twice with different range of gap voltage, one at higher end i.e. 120V & 140V and second at 10V & 20V.

5.4. 2⁴ Full factorial experiment with center point (Third iteration)

Factor	Code	Low Level(-)	Zero (0)	High Level(+)
Gap Voltage	A	10V	15V	20V
Pulse Duration	B	3μs	5μs	7μs
Average Current	C	4.5A	6A	8A
Electrode Type	D	Graphite		Copper

Table 5.7 Responses of measured parameters for third iteration

#	Treatments	A	B	C	D	Ra (μm)		
						Replicate 1	Replicate 2	Average
1	(1)	-1	-1	-1	-1	2.33	2.97	2.65
2	a	+1	-1	-1	-1	2.66	2.58	2.62
3	b	-1	+1	-1	-1	2.46	2.67	2.57
4	ab	+1	+1	-1	-1	2.16	2.89	2.53
5	c	-1	-1	+1	-1	2.97	2.63	2.80
6	ac	+1	-1	+1	-1	2.49	2.97	2.73
7	bc	-1	+1	+1	-1	2.90	2.35	2.63
8	abc	+1	+1	+1	-1	2.95	2.33	2.64
9	d	-1	-1	-1	+1	2.93	4.51	3.72
10	ad	+1	-1	-1	+1	2.76	3.72	3.24
11	bd	-1	+1	-1	+1	3.30	3.01	3.16
12	abd	+1	+1	-1	+1	3.33	2.29	2.81
13	cd	-1	-1	+1	+1	2.99	2.89	2.94
14	acd	+1	-1	+1	+1	3.10	2.80	2.95
15	bcd	-1	+1	+1	+1	3.66	3.74	3.70
16	abcd	+1	+1	+1	+1	4.05	2.44	3.25
17	0	0	0	0	-1	2.56	2.96	2.76
18	0	0	0	0	+1	2.43	2.17	2.30
19	0	0	0	0	-1	3.11	2.73	2.92
20	0	0	0	0	+1	2.47	3.21	2.84
21	0	0	0	0	-1	2.88	3.17	3.03
22	0	0	0	0	+1	3.05	2.65	2.85
							Overall Avg.	2.89

Table 5.8 Analysis of variance for third iteration

#	TCs	Sum of Squares	DF	Mean Square	F value	P value
1	Constant	4.61	15	4.61	3.39	0.0916
Main effects						
2	A	0.0023	1	0.0023	0.0256	0.881
3	B	1.0360	1	1.0360	11.4244	0.020
4	C	2.3217	1	2.3217	25.6036	0.004
5	D	0.0160	1	0.0160	0.1764	0.690
Two factor interactions						
6	AB	0.0105	1	0.0105	0.1156	0.747
7	AC	0.0610	1	0.0610	0.6724	0.449
8	AD	0.0160	1	0.0160	0.1764	0.690
9	BC	0.0284	1	0.0284	0.3136	0.602
10	BD	0.0907	1	0.0907	1.0000	0.361
11	CD	0.3343	1	0.3343	3.6864	0.113
Three factor interactions						
12	ABC	0.1097	1	0.1097	1.2103	0.320
13	ABD	0.0076	1	0.0076	0.0841	0.783
14	ACD	0.0061	1	0.0061	0.0676	0.807
15	BCD	0.0061	1	0.0061	0.0676	0.807
Four factor interaction						
16	ABCD	0.2439	1	0.2439	2.6896	0.163
Curvature		0.2621	1	0.2621	2.8943	0.149
Pure Error		0.0334	27	0.09608		
Total		5.3313	43			

Table 5.3. Estimated Effects and Coefficient for Ra

Term	Effect	Coefficient	SE Coefficient	T	P
Main Effects					
A	0.0237	0.0119	0.07528	0.16	0.8810
B	0.5087	0.2544	0.07528	3.38	0.0200
C	0.7612	0.3806	0.07528	5.06	0.0040
D	0.2937	0.1469	0.07528	-0.42	0.6900
Two Factor Interactions					
AB	0.0512	0.0256	0.07528	0.34	0.7470
AC	0.1237	0.0619	0.07528	0.82	0.4490
AD	-0.0637	-0.0319	0.07528	-0.42	0.6900
BC	0.0837	0.0419	0.07528	0.56	0.6020
BD	0.1512	0.0756	0.07528	1.00	0.3610
CD	0.2887	0.1444	0.07528	1.92	0.1130
Three Factor Interactions					
ABC	0.1663	0.0831	0.07528	1.10	0.3200
ABD	0.0437	0.0219	0.07528	0.29	0.7830
ACD	-0.0387	-0.0194	0.07528	-0.26	0.8070
BCD	-0.0387	-0.0194	0.07528	-0.26	0.8070
Four Factor Interactions					
ABCD	-0.2463	-0.1213	0.07528	-1.64	0.1630
Curvature		-0.2456	0.14416	-1.70	0.1490

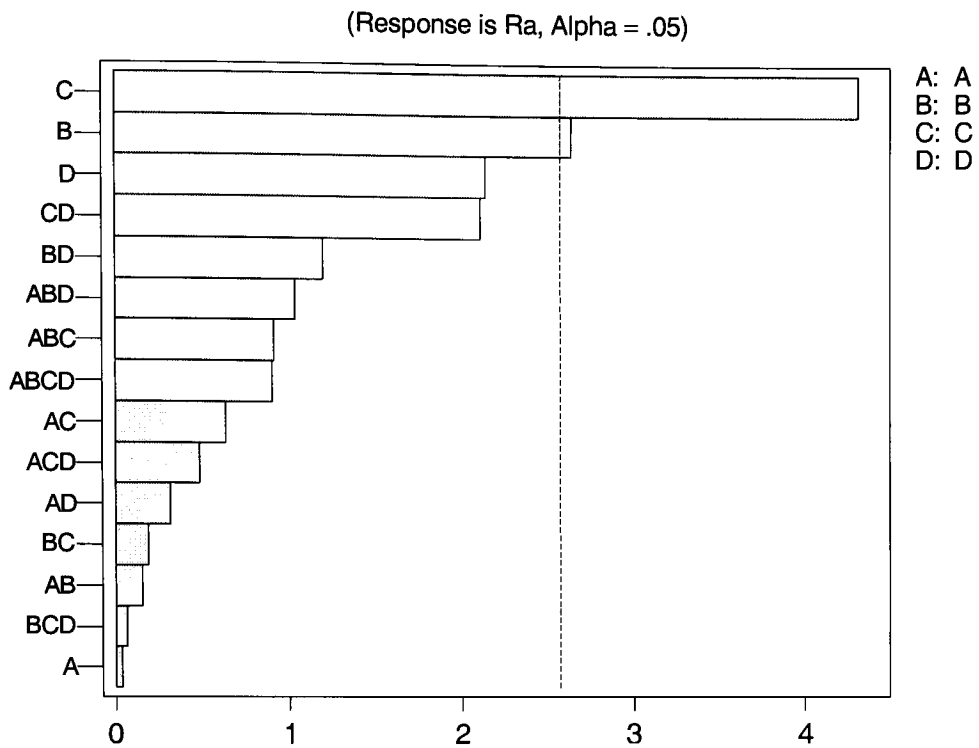


Figure 5.10 Pareto Chart of Standardized Effects (Third Iteration)

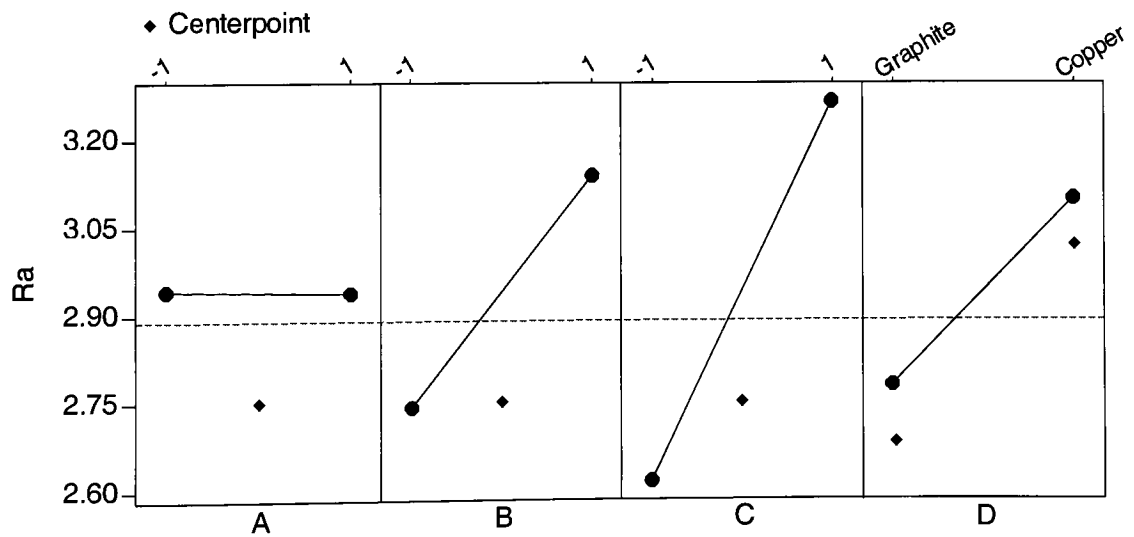


Figure 5.11 Main Effects plots (Third Iteration)

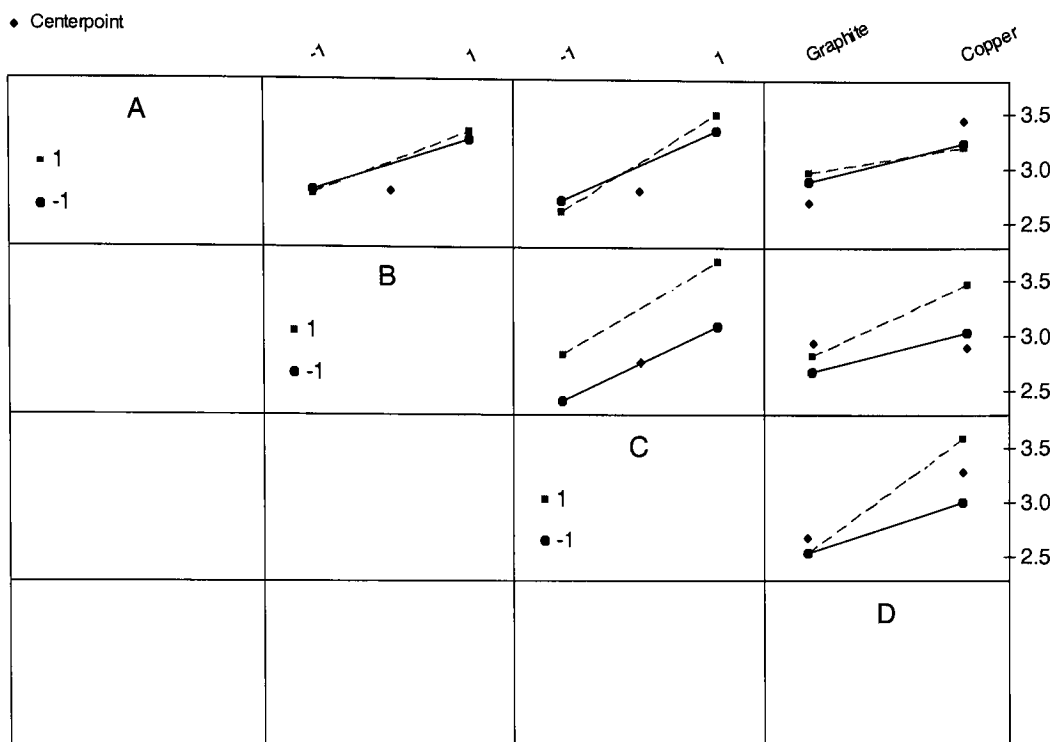


Figure 5.12 Interactions Plot (Third Iteration)

As seen in the (figure 5.10) the pulse duration and average current were found significant. Gap voltage was not significant. In the main effects plot of gap voltage (A) we can observe that there is very small difference in surface roughness from high to low level of gap voltage. Curvature was significant and it was in the direction of minimization showing that the design may be approaching optimal region. Observation from this experiment and the next experiment will be used to conclude about the effect of gap voltage on surface roughness.

It can be seen from the ANOVA table that there is no significant lack of linear fit due to an interaction term and there is no evidence of curvature. Furthermore, there is evidence that the first-order model is significant. Using the DESIGN EXPERT statistical software, we obtain the resulting model (in the coded variables) as

$$\text{Response} = +3.00 + 0.012 \times \text{Gap Voltage} + 0.25 \times \text{Pulse Duration} + 0.38 \times \text{Average Current} + 0.15 \times \text{Electrode Type}$$

The usual diagnostic checks show conformance to the regression assumptions, although the R^2 value is not very high: $R^2 = 0.6421$

To *minimize* , we use the direction of steepest descent. The engineer selects $\rho = 1$ since a point on the steepest descent direction one unit (in the coded units) from the origin is desired. Then from the following equation for the predicted response, the coordinates of the factor levels for the next run are given by:

$$x_1 = \rho \frac{b_1}{\sqrt{\sum_{i=1}^k b_i^2}} = \frac{(1)(0.012)}{\sqrt{(0.012)^2 + (0.15)^2 + (0.25)^2 + (0.38)^2}} = 0.025$$

Similarly,

$$x_2 = 0.522, \quad x_3 = 0.7931, \quad x_4 = 0.3130$$

Now we have orthogonally coded factors :

$$x_1 = \frac{X_1 - 15}{5}, \quad x_2 = \frac{X_2 - 5}{2}, \quad x_3 = \frac{X_3 - 6}{2}$$

To minimize the surface roughness descriptor, Ra

for every (0.025) (5) = 0.125 V voltage should be decreased per step

for every (0.522) (2) = 1.044μs pulse duration should be decreased per step

for every (0.7931) (2) = 1.5862A Average Current should be decreased per step

The step sizes obtained will be considered along with the results from next step to decide the next step. The levels of all the factors except gap voltage is kept the same in the next design.

Gap voltage levels are kept in the higher range (120V and 150V).

5.5. 2⁴ full factorial experiment with center point (Fourth Iteration)

Factor	Code	Low Level(-)	Zero (0)	High Level(+)
Gap Voltage	A	120V	130V	150V
Pulse Duration	B	3μs	5μs	7μs
Average Current	C	4.5A	6A	8A
Electrode Type	D	Graphite		Copper

Table 5.9 Responses of measured parameters for fourth iteration experiment

#	Treatments	A	B	C	D	Ra Avg	Ra Avg	Ra Avg.
						Replicate 1	Replicate 2	
1	(1)	-1	-1	-1	-1	2.27	2.39	2.33
2	a	+1	-1	-1	-1	2.08	2.39	2.24
3	b	-1	+1	-1	-1	3.03	2.85	2.94
4	ab	+1	+1	-1	-1	2.76	2.81	2.79
5	c	-1	-1	+1	-1	2.59	2.35	2.47
6	ac	+1	-1	+1	-1	2.43	2.51	2.47
7	bc	-1	+1	+1	-1	3.42	3.41	3.42
8	abc	+1	+1	+1	-1	3.53	3.86	3.70
9	d	-1	-1	-1	+1	2.73	3.02	2.88
10	ad	+1	-1	-1	+1	2.69	2.79	2.74
11	bd	-1	+1	-1	+1	3.30	3.72	3.51
12	abd	+1	+1	-1	+1	3.24	3.35	3.30
13	cd	-1	-1	+1	+1	2.92	2.83	2.88
14	acd	+1	-1	+1	+1	2.93	2.87	2.90
15	bcd	-1	+1	+1	+1	3.63	3.79	3.71
16	abcd	+1	+1	+1	+1	3.97	3.92	3.95
17	0	0	0	0	-1	2.71	2.90	2.81
18	0	0	0	0	+1	2.51	2.39	2.45
19	0	0	0	0	-1	2.87	3.09	2.98
20	0	0	0	0	+1	2.40	2.91	2.66
21	0	0	0	0	-1	3.03	3.24	3.14
22	0	0	0	0	+1	3.04	3.11	3.08
							Overall Avg.	2.97

Table 5.10 Analysis of variance for fourth iteration experiment

	TCs	Sum of Squares	DF	Mean Square	F value	P value
Main effects						
2	A	0.0023	1	0.0023	0.0256	0.881
3	B	1.0360	1	1.0360	11.4244	0.020
4	C	2.3217	1	2.3217	25.6036	0.004
5	D	0.0160	1	0.0160	0.1764	0.690
Two factor interactions						
6	AB	0.0105	1	0.0105	0.1156	0.747
7	AC	0.0610	1	0.0610	0.6724	0.449
8	AD	0.0160	1	0.0160	0.1764	0.690
9	BC	0.0284	1	0.0284	0.3136	0.602
10	BD	0.0907	1	0.0907	1.0000	0.361
11	CD	0.3343	1	0.3343	3.6864	0.113
Three factor interactions						
12	ABC	0.1097	1	0.1097	1.2103	0.320
13	ABD	0.0076	1	0.0076	0.0841	0.783
14	ACD	0.0061	1	0.0061	0.0676	0.807
15	BCD	0.0061	1	0.0061	0.0676	0.807
Four factor interaction						
16	ABCD	0.2439	1	0.2439	2.6896	0.163
Curvature		0.2621	1	0.2621	2.8943	0.149
Pure Error		0.0334	27	0.09608		
Total			43			

Table 5.11. Estimated Effects and Coefficient for Ra

Term	Effect	Coefficient	SE Coefficient	T	P
Main Effects					
A	-0.0919	-0.0460	0.06672	-0.69	0.522
B	0.4953	0.2476	0.06672	3.71	0.014
C	0.8128	0.4064	0.06672	6.09	0.002
D	0.4506	0.2253	0.06672	3.38	0.020
Two Factor Interactions					
AB	0.0344	0.0172	0.06672	0.26	0.807
AC	0.0536	0.0268	0.06672	0.40	0.705
AD	0.0964	0.0482	0.06672	0.72	0.502
BC	-0.0269	-0.0135	0.06672	-0.20	0.848
BD	-0.0081	-0.0041	0.06672	-0.06	0.954
CD	0.2244	0.1122	0.06672	1.68	0.153
Three Factor Interactions					
ABC	0.0039	0.0020	0.06672	0.03	0.978
ABD	-0.0089	-0.0045	0.06672	-0.07	0.949
ACD	0.0286	0.0143	0.06672	0.21	0.839
BCD	0.1301	0.0515	0.06672	0.77	0.475
Four Factor Interactions					
ABCD	-0.0594	-0.0297	0.06672	-0.45	0.675
Curvature		-0.2500	0.12776	-1.96	0.108

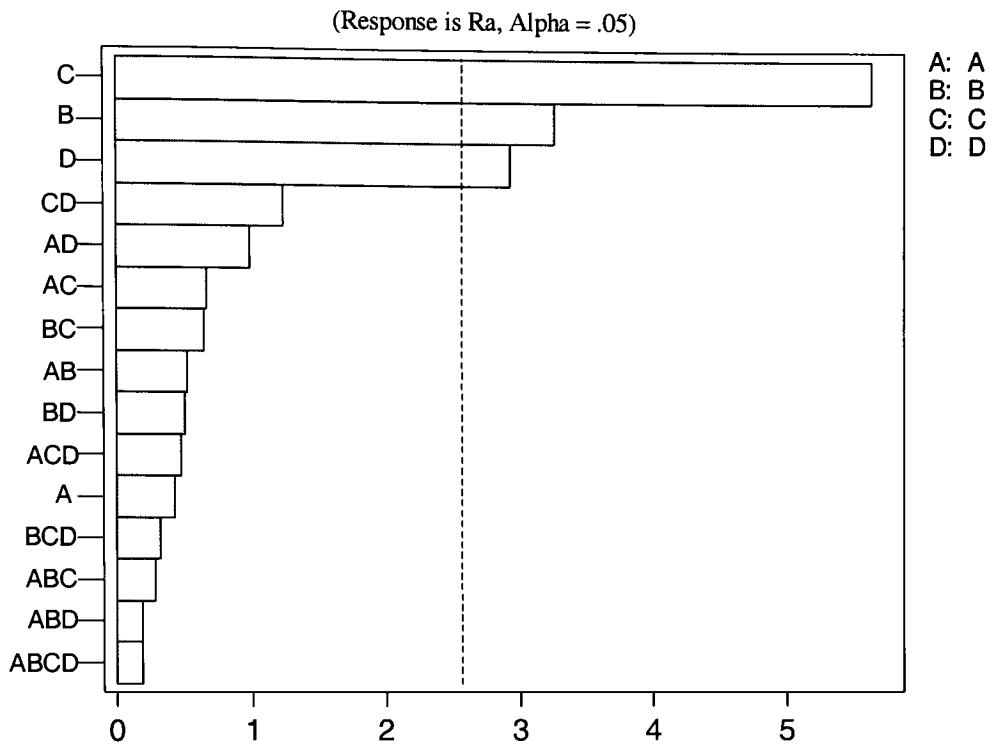


Figure 5.10 Pareto Chart of Standardized Effects (Fourth Iteration)

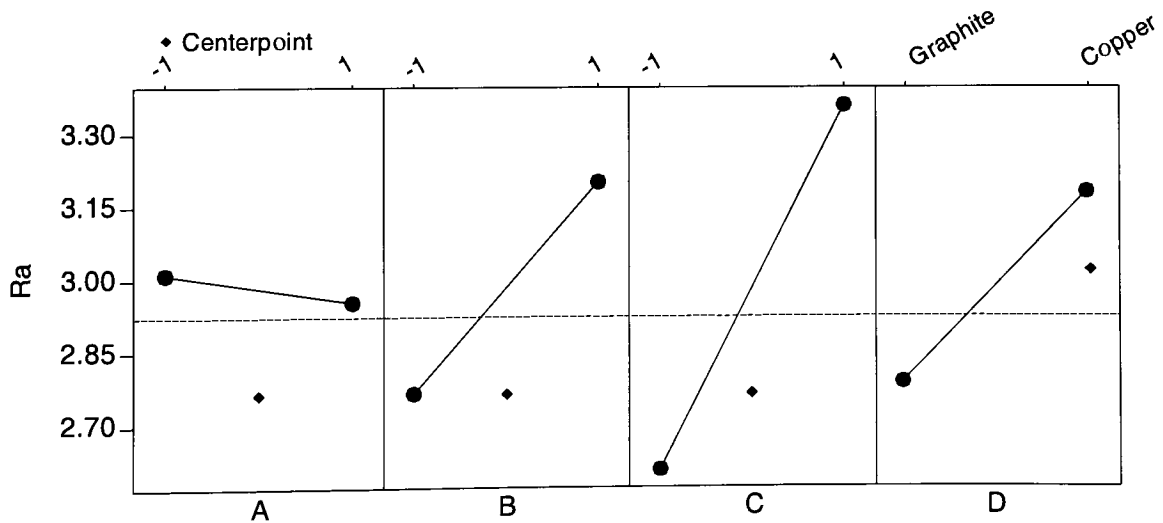


Figure 5.11 Main Effects plots (Fourth Iteration)

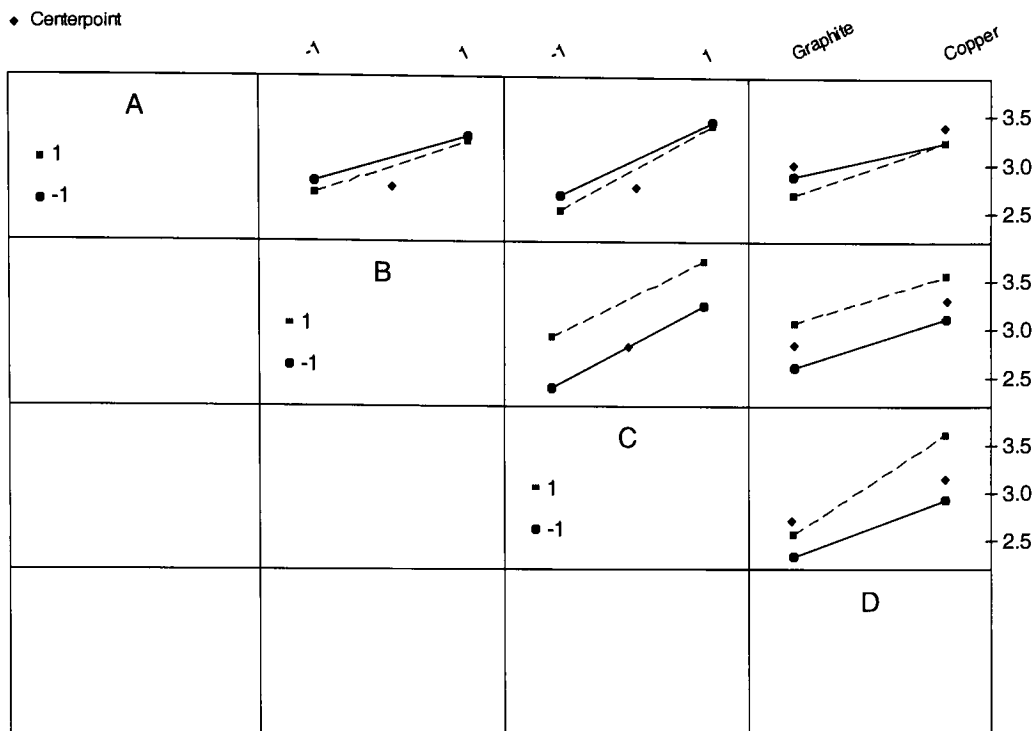


Figure 5.12 Interactions Plot (Fourth Iteration)

This was the second experiment from the set of 2 experiment designed to observe the effect of gap voltage on the surface roughness. It can be observed from ANOVA table and figures above that Pulse Duration and Average Current are found to be most significant. Electrode type is significant factor in this experiment. From figure 5.14 it can be observed that better surface roughness is obtained at higher voltage. Curvature isn't significant in this design.

It can be seen from the ANOVA table that there is no significant lack of linear fit due to an interaction term and there is no evidence of curvature. Furthermore, there is evidence that the first-order model is significant. Using the DESIGN EXPERT statistical software, we obtain the resulting model (in the coded variables) as

$$\text{Response} = +3.01 - 0.046 \times \text{Gap Voltage} + 0.25 \times \text{Pulse Duration} + 0.41 \times \text{Average Current} + 0.23 \times \text{Electrode type}$$

The usual diagnostic checks show conformance to the regression assumptions, although the R^2 value is not very high: $R^2 = 0.8270$.

To *minimize* , we use the direction of steepest descent. The engineer selects $\rho = 1$ since a point on the steepest descent direction is one unit (in the coded units) from the origin is desired. Then from the equation above for the predicted Y response, the coordinates of the factor levels for the next run are given by:

$$x_1 = \rho \frac{b_1}{\sqrt{\sum_{i=1}^k b_i^2}} = \frac{(1)(-0.046)}{\sqrt{(0.046)^2 + (0.25)^2 + (0.41)^2 + (0.23)^2}} = -0.0806$$

Similarly,

$$x_2 = 0.4678, \quad x_3 = 0.7672, \quad x_4 = 0.4233$$

Now we have orthogonally coded factors :

$$x_1 = \frac{X_1 - 130}{20}, \quad x_2 = \frac{X_2 - 5}{2}, \quad x_3 = \frac{X_3 - 6}{2}$$

To minimize the surface roughness descriptor, R_a

for every $(-0.0806) (130) = -10.47$ V voltage should be decreased per step

for every $(0.467) (2) = 0.937$ μ s pulse duration should be decreased per step

for every $(0.7672) (2) = 1.53$ A Average Current should be decreased per step

After considering results from last 2 iterations. It is observed that Higher voltage gives better surface. Most of the literature reviewed agreed with the fact that higher gap voltage gives better surface finish. The electrode type was significant in previous design. Graphite electrode produced better surface than copper electrode in all the previous designs. Travelling through these steps, the surface roughness is improving as we move down the steps. Considering the machine availability issues, by proper observation of results of all the iteration and to do more detailed analysis of the variation of surface roughness in the next step, response surface design (Central Composite Design) is implemented.

5.6. Central Composite Design

Factor	Code	-1.68	-1	0	+1	+1.68
Gap Voltage	A	140	150	160	170	180
Pulse Duration	B	1.5	2	3	4	4.5
Average Current	C	0.5	1.5	2	3	4.5

Table 5.12 Responses of measured parameters for central composite design

#	Treatments	A	B	C	Ra (Avg) Replicate 1	Ra (Avg) Replicate 2	Ra Avg.
1	(1)	-1	-1	-1	2.11	2.11	2.11
2	a	+1	-1	-1	1.80	1.87	1.84
3	b	-1	+1	-1	1.93	1.93	1.93
4	ab	+1	+1	-1	1.95	1.99	1.97
5	c	-1	-1	+1	2.27	2.18	2.23
6	ac	+1	-1	+1	2.17	2.08	2.13
7	bc	-1	+1	+1	2.53	2.60	2.57
8	abc	+1	+1	+1	2.64	2.46	2.55
9	$-\alpha_a$	-1.68	0	0	1.97	1.37	1.67
10	$+\alpha_a$	+1.68	0	0	1.87	1.98	1.93
11	$-\alpha_b$	0	-1.68	0	1.33	1.58	1.46
12	$+\alpha_b$	0	+1.68	0	2.05	2.12	2.09
13	$-\alpha_c$	0	0	-1.68	1.17	1.16	1.17
14	$+\alpha_c$	0	0	+1.68	2.72	2.86	2.79
15	0	0	0	0	2.05	1.96	2.01
16	0	0	0	0	1.99	1.90	1.95
17	0	0	0	0	1.86	1.78	1.82
						Overall Avg.	2.01

Table 5.13 Analysis of variance for central composite design

Treatments	Sum of Square	DF	Mean Square	F value	P Value
Main Effects					
A	0.08306	1	0.08306	5.15	0.8672
B	0.3532	1	0.3532	21.90	0.0034
C	1.7884	1	1.7884	110.88	<0.0001
Quadratic effects					
A ²	0.1733	1	0.1733	10.75	0.5663
B ²	0.0176	1	0.0176	1.09	0.7319
C ²	0.708	1	0.708	43.91	0.0353
Two factor interactions					
AB	0.109	1	0.109	6.76	0.6383
AC	0.0098	1	0.0098	0.61	0.9132
BC	0.4461	1	0.4461	27.66	0.0452
Three factor interaction					
ABC	0.0356	1	0.0356	2.21	0.1590
Pure Error	0.36	25	0.01613		
Total	5.66	39			

Table 5.14. Estimated Effects and Coefficient for Ra

Term	Effect	Coefficient	SE Coefficient	T	P
Main Effects					
A	-0.0857	-0.0437	0.01923	-2.27	0.8672
B	0.1800	0.0900	0.01923	4.68	0.0034
C	0.4050	0.2025	0.01923	10.53	<0.0001
Quadratic effects					
A ²	0.0125	0.0628	0.01923	3.27	0.5663
B ²	0.0398	0.01999	0.01923	1.04	0.7319
C ²	0.2546	0.1273	0.01923	6.62	0.0353
Two factor interactions					
AB	0.1000	0.0500	0.01923	2.60	0.6383
AC	0.0300	0.0150	0.01923	0.78	0.9132
BC	0.2025	0.1012	0.01923	5.26	0.0452
Three factor interaction					
ABC	-0.0575	-0.0287	0.01923	-1.49	0.1590

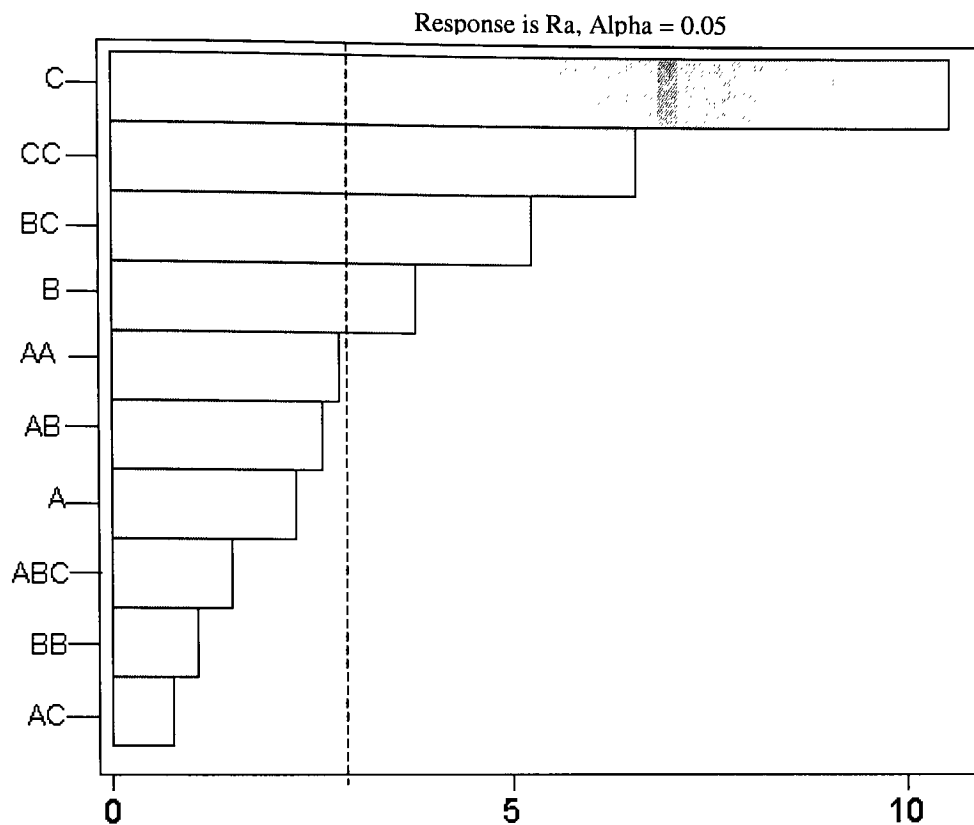


Figure 5.16 Pareto Chart of Standardized Effects (Central Composite Design Experiment)

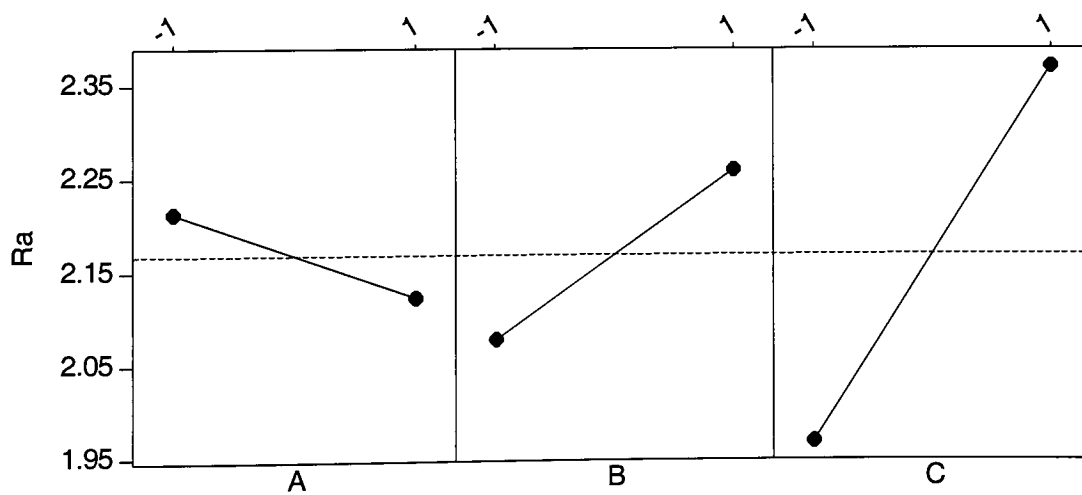


Figure 5.17 Main Effects Plot (Central Composite Design Experiment)

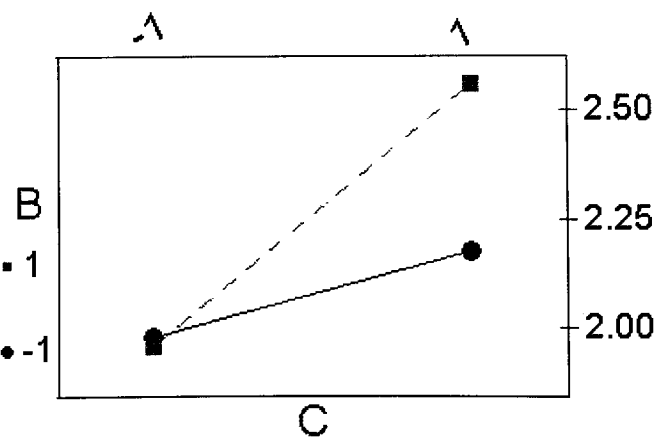
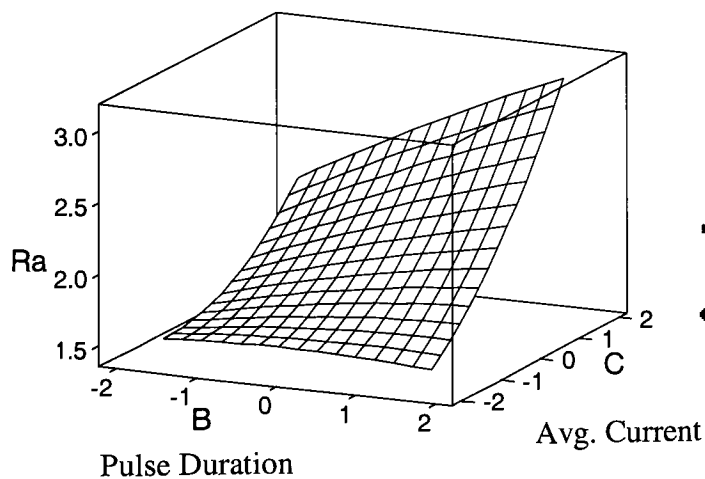
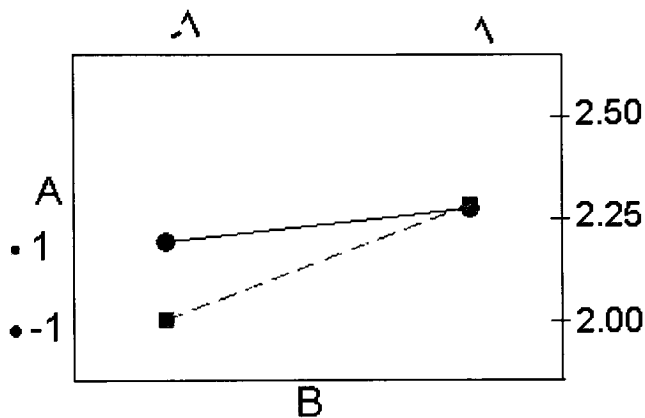
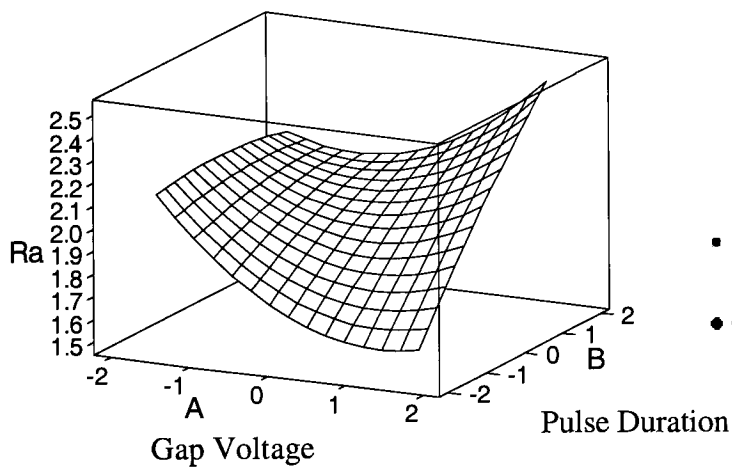
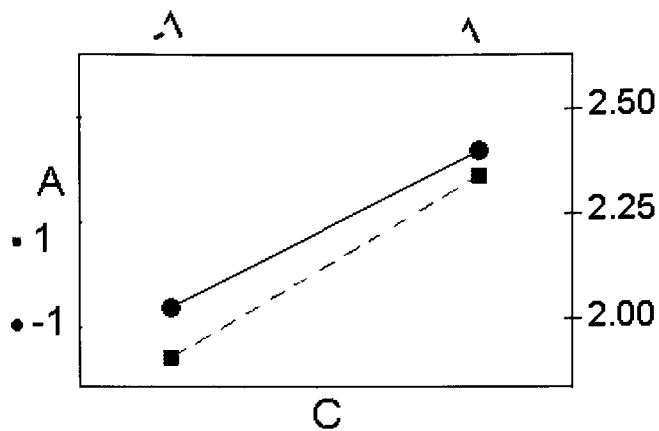
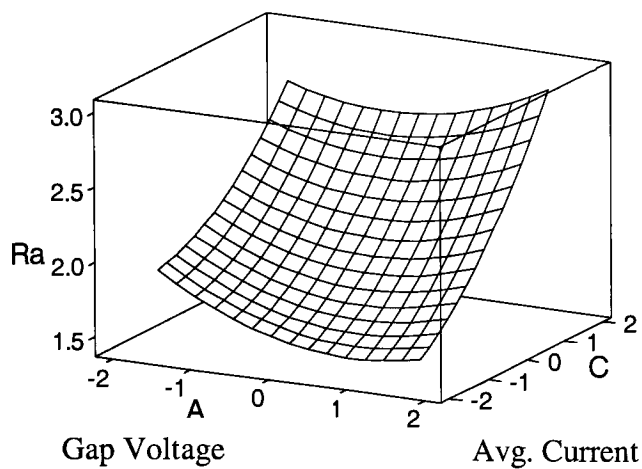


Figure.5.18 Response surfaces for individual two factor interactions

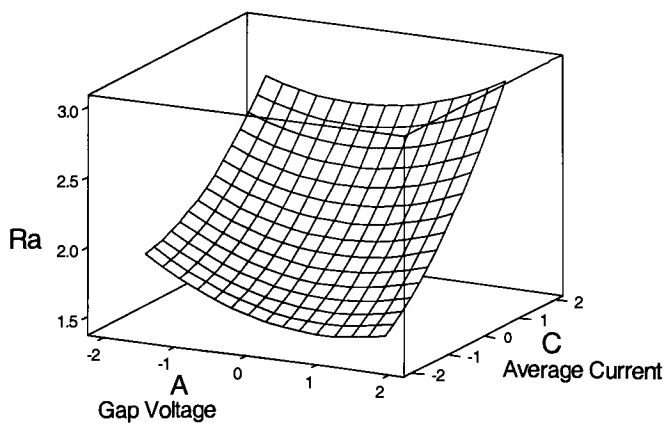
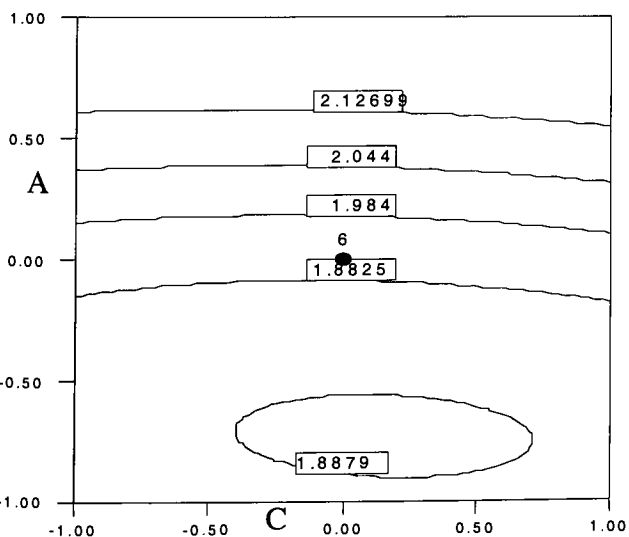
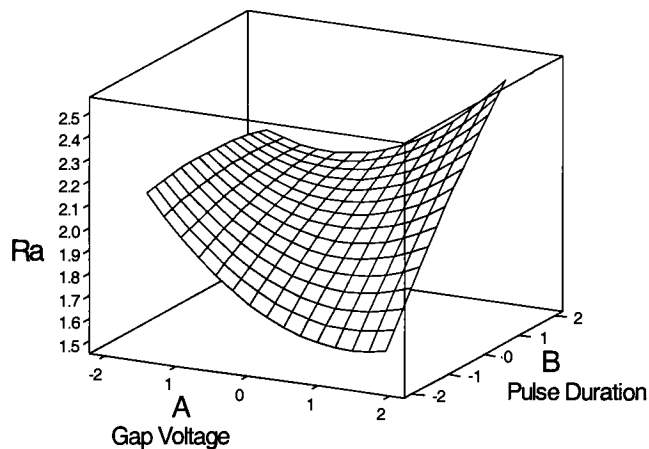
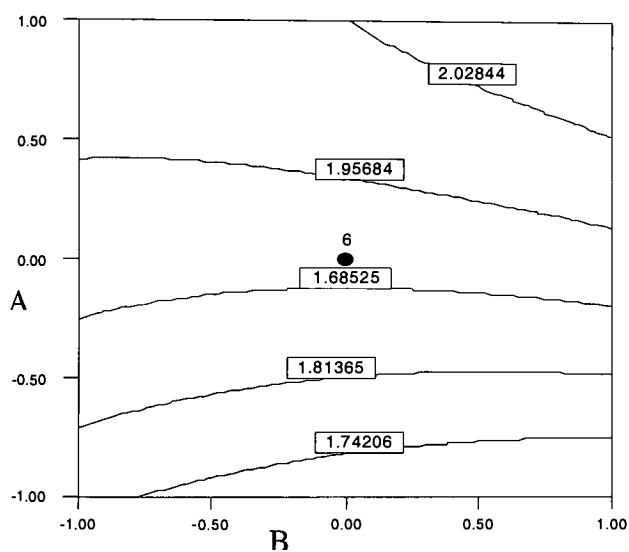
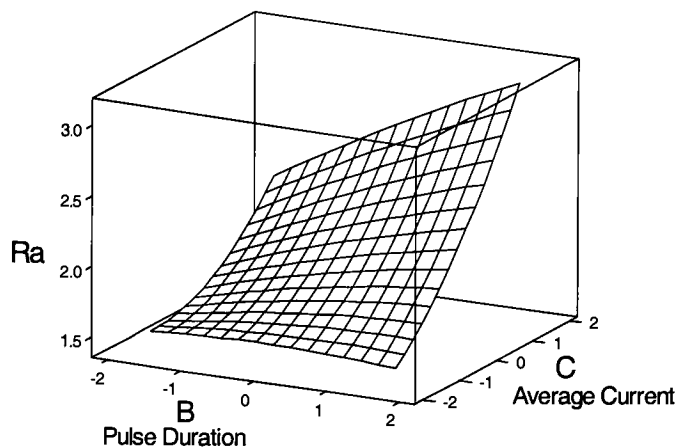
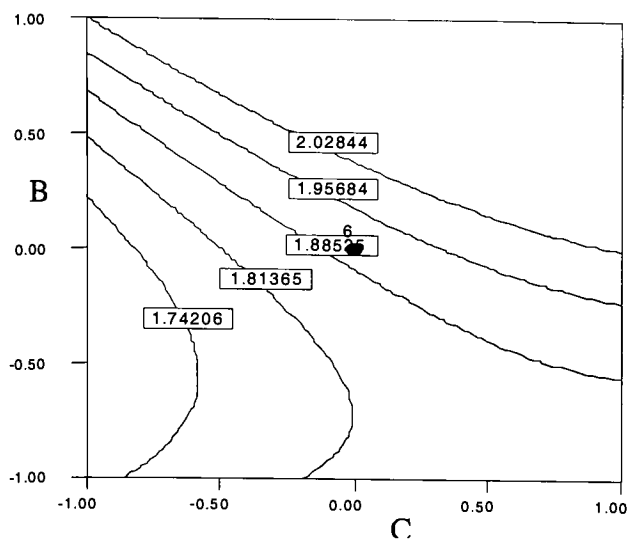


Figure.5.18 Contour and Response surface plots

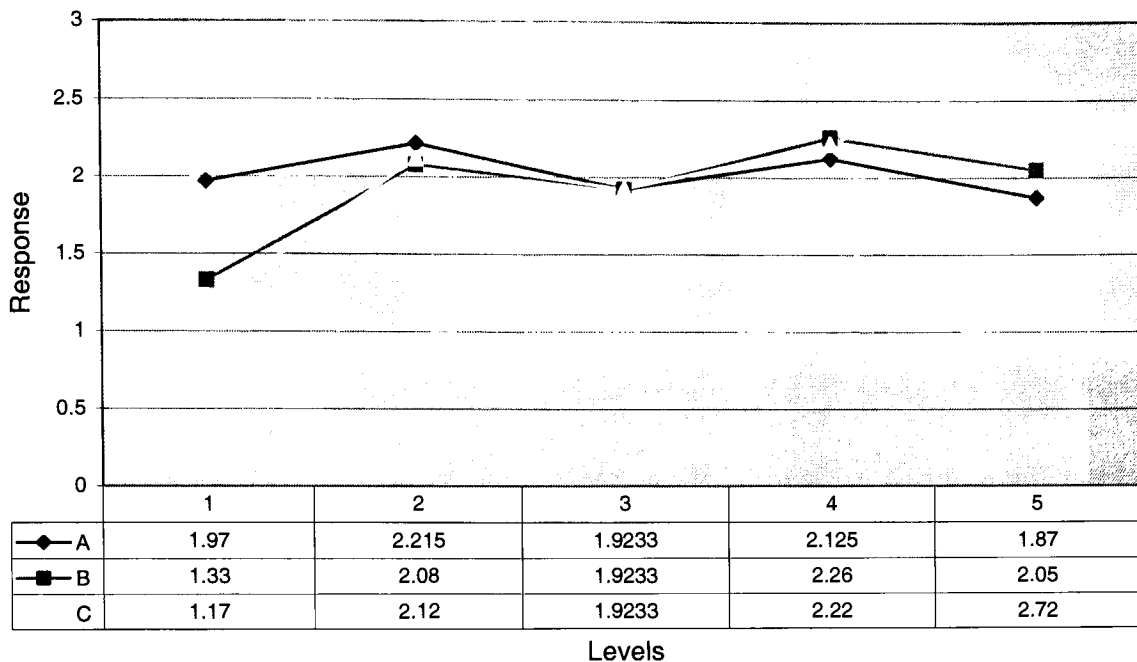


Figure.5.19 Relative effect of change in response of CCD experiment

The goal of this experiment was to fit response surface models to response of surface roughness as a function of three particular controllable factors of EDM process. These factors were gap voltage, average current and pulse duration keeping electrode type constant with graphite electrode. The experiment is designed to allow us to estimate interaction and even quadratic effects, and therefore give an idea of the (local) shape of the response surface which is being investigated.

As we observe from the analysis that factors B and C (i.e Pulse duration and Average current) is significant main effects. Factor C (i.e. Average Current) is having significant quadratic effect and interaction BC (average current and pulse duration) is significant. The contour and response surface plots are plotted to understand the variation of the response in the factorial space. Figure 5.17 and 5.18 shows the response surfaces, interaction plots and contour plots for all 2 factor interactions among gap voltage, average current and pulse duration with respect to the response of surface roughness. Figure 5.19 shows the trend in change of surface roughness at different levels.

First order model predicting surface roughness is as follows:

$$\text{Response} = 2.16 - 0.044 \times \text{Gap Voltage} + 0.090 \times \text{Pulse Duration} + 0.20 \times \text{Average Current} + 0.050 \times \text{Gap Voltage} \times \text{Pulse Duration} + 0.10 \times \text{Pulse Duration} \times \text{Average Current}$$

Second Order model predicting surface roughness is as follows:

$$\text{Response} = 1.91867 + 0.14404 \times \text{Pulse Duration} + 0.32456 \times \text{Average Current} + 0.097142 \times (\text{Average Current})^2 + 0.12358 \times \text{Pulse Duration} \times \text{Average Current}$$

The usual diagnostic checks show conformance to the regression assumptions, although the R^2 value is not very high: $R^2 = 0.8457$.

From the above output, we make the following conclusions. The R^2 is reasonable for fitting surface roughness. The lack of fit test does not have a problem with the model. The Pareto chart of main effects and interaction effects plot provides a visual confirmation of the significant model terms. The interaction plot shows why an interaction term is needed. The model obtained explains the nature of effect on surface roughness.

6. CONCLUSIONS

The objective of this study was to provide information on the relationships between the key input variables and resultant surface roughness and to develop a response model for surface roughness optimization utilizing factorial designs, direction of steepest descent method and response surface methodology (RSM). The results obtained were to be used to recommend process setting to improve process robustness and to get the desired surface roughness. The model produced in this study can accurately predict the surface roughness produced by EDM process at a particular factor level combination. Effect of key process parameters on Aluminium 6061- T3 surface roughness has been observed and the data collected were analysed to calculate the first order model which explains the nature of the effect.

This study has confirmed the assertions made by authors in the literature, regarding the relationship between significant process parameters (gap voltage, average current, pulse duration, electrode type and depth of penetration) and surface roughness. The effect of gap voltage, pulse duration, average current, electrode type and depth of penetration upon surface roughness have been evaluated. Experimental design approach helped in identifying the significant main effects along with its interaction with other factors. Direction of steepest descent method facilitated the progress of the experiments in the direction of interest, which was minimization of surface roughness in this case. Response surface methodology and central composite design experiment with 5 levels helped in analyzing the region of interest more comprehensively at quadratic and cubic levels.

Linear models were developed after each experiment, which constitute the significant main effects and interactions to find the direction of steepest descent and step size in that direction. The levels of the subsequent experimental designs were changed taking into account the machine setting limitations. Finally central composite design was executed to elaborate and to understand the higher order nature of the response. Average current was found to be quadratic in nature and was the only significant quadratic effect. Response model obtained after the analysis will help predict the surface roughness at given factor level combination by substituting the values in the model.

There were lot of limitations involved in this experimental analysis taking into account the number of experiments, the step size adjustments because of machine setting limitations and other irregularities involved during the experimentation.

The experiments yielded following main conclusions:

- The factors, average current and pulse duration have the largest influence on surface roughness. Adjusting these two factors should create the greatest improvement in the general EDM surface characteristics and provide the greatest reduction in surface defects. In all the cases effect of average current on surface roughness was more pronounced than the effect of pulse duration.
- Electrode material has significant influence in finishing operations on wear and surface roughness parameters. At given experimental settings in this research work graphite electrode gave better surface than copper electrode.
- The results shows that graphite electrode can be used in finishing operation while achieving the unprecedented surface quality that was only attainable with copper electrode in such operations.
- Experiments were carried out at two different range of gap voltages as third and fourth interation experiment keeping all the other factor level constant to identify the exact nature of effect and it was observed that better surface was obtained at higher gap voltages.
- Average current showed significant quadratic effect in the central composite design experiment. This significant quadratic effect shows the stochastic nature of the process where there is drastic change in response with small change in the factor level combination. Average current was involved in several significant two factor interaction also in the response surface design.
- Depth of penetration was not having significant effect on surface roughness. It was involved in some two and three interaction effects, which were insignificant.
- Best surface obtained was $0.96\text{ }\mu\text{m}$ at lowest average current value (i.e.0.5amp), $3\mu\text{s}$ pulse duration and 160V gap voltage in the central composite design.

- A higher order nonlinear Response surface model have been developed to represent the effect of process variable on the surface roughness of workpiece machined by Die-sink EDM process. The results obtained can be used to lead to an optimization problem of finding the best set of working parameters yielding the best surface finish. The purpose of fitting the response model is to estimate the response at the certain point of interest.

This research identified the most significant factors which effects the EDM surface roughness. The experimental iterative response surface methodology determined the trend in change of surface roughness with change in factor level combination .The response model obtained could be used to predict the surface roughness at a particular point of interest. The quality of surface roughness obtained is a factor of importance in the evaluation of any machine tool's productivity. Copper electrode was usually used for superfinishing operations but after this study graphite electrode can now be used for finishing operations at the specified factor levels to get surface finish as low as $0.94\mu\text{s}$. As a result this introduces the potential of eliminating the need for post machining after EDM and therefore cost, labor, material and space associated. Limitations associated with copper electrodes can be overcome by graphite electrode in finishing operations. The targeted surface roughness can be obtained using the data obtained by setting the factor level combination for desired surface roughness.

The final response surface design experiment was designed to estimate interaction and even quadratic effects, and therefore give an idea of the (local) shape of the response surface we are investigating. The higher order model obtained will help find improved or optimal process settings, troubleshoot process problems and weak points in the process. Make a product or process more *robust* against external and non-controllable influences.

This research involved exhaustive literature review, experimentation, data collection and statistical analysis to study the stochastic process of electrical discharge machining in detail. The output of this research work was an effort to make this process more robust so that it can be used more affluently by EDM users in more applications in addition to the existing applications.

7. FUTURE WORK

Future research work concentrating on the electro-discharge machined surfaces can focus into considering more factors like workpiece material, type of dielectric, type of flushing(e.g. indirect, inline etc.), Capacitance. More extensive surface analysis can be done using Scanning electron microscope to study several layers which are formed after EDM. Surface obtained after machining can be analysed considering more surface roughness descriptors and results can be compared. Different types of electrodes can be used in the experimentation (e.g. Brass) executed in the present research were based on the five factors. There have been no published research on effect of electro-discharge machining on aluminum as workpiece material.

Response surface methodology is a good tool to optimize the response in the direction of interest, but other algorithms like Artificial Neural Network, Fuzzy logic, etc. can be used to do the same analysis done in this research. Direction of steepest descent was used for minimization of single response i.e. average surface roughness. More responses like material removal rate(MRR), white layer thickness, hole enlargement etc. can be considered for analysis. More work can be done in the area of real time monitoring of the surface modified while machining. Electrode grain size can be altered, as in the present research the grain size was kept constant, More advanced metrology devices can be used to analyze the surface. The work can be done in the field of thermal effects on the surface. There has been comprehensive work in powder suspended dielectric based die-sink EDM, more work is required in that area.

There are number of factors involved in EDM affecting surface roughness. The model obtained after the response surface design can be validated by back tracking verification experiments and by applying various mathematical simulation techniques. The validated mathematical model can be used for future work into simulation of the factors considered for desired surface roughness to be obtained. More comprehensive approach can be used to consider more range of factor level combinations. Significant interactions can be analyzed in greater details.

8. REFERENCES:

1. ASME B46.1(1995), Surface Texture (Surface Roughness, Waviness, and lay). An American National Standard. The American Society of Mechanical Engineers. New York,
2. Barker, T., (1994), Quality by Experimental Design, Marcel Dekker, Inc., New York.
3. Box, George E. P, (1987) Empirical Model-building and Response Surfaces, New York: Wiley.
4. Bruzzone, A.A., Lonardo, P.M. (1999) "Effect of flushing and electrode material on die sinking EDM", Annals of CIRP, v.48, pp.123-126
5. Chen Y., Mahadavian S., (1999) "Parametric study into erosion wear in a computer numerical controlled EDM process", Wear, v.235, pp.350-354
6. Choudhury, I.A.; El-Baradie, M.A., (1999) "Machining assessment of inconel718 by factorial design of experiment with response surface method", Journal of Materials Processing Technology, v.95 n1, pp.30-39
7. Cooke, R. F.; Crookall, J.R., (1973) "An investigation of some statistical aspects of electro-discharge machining", International Journal of Machine Tool Design and Research, v.13, pp.271-286
8. Crookall, J.R.,Khor B.C., (1974) " Electro-discharge machined surfaces", Proceedings of 15th International Machine Tool Design and Research Conference
9. Deng, J.; Lee, T. (2000), "Surface integrity in EDM, ultrasonic machining, and diamond saw cut of ceramic composite", Ceramics International, Volume: 26, pp.825-eoa.
10. Dibitonto D., Eubank P., Patel M., Barrufet M., (1989) "Theoretical models of the electrical discharge machining process", Journal of Applied Physics, v.66, pp.4095-4103
11. Ethz, D., Dauw, D.F., (1995) "About the application of fuzzy-controllers in high performance die-sinking EDM machines" Proceedings of 11th International Symposium on Electro-machining, pp.333-340.
12. Gunaraj, V.; Murugan, N, (1999) "Application of response surface methodology predicting weld quality in submerged arc welding", Journal of Materials Processing Technology, v.88 n1, pp. 266-275
13. Indurkha, G.; Rajurkar, K.P, (1992) "Artificial neural network approach in modeling of EDM process", Proceedings of the 1992 Artificial Neural Networks in Engineering seminar, ANNIE'92, pp. 845-850

14. Jain V. K.; Rajurkar, K. P., (1990) "Multi-objective optimization of electrodischarge machining Process," *Microtechnic*, Vol. 2, pp.33-37.
15. Kahng, C. H.; Rajurkar, K. P., (1977), "Surface characteristic behavior due to rough and fine cutting by EDM, " *Annals of the CIRP*, Vol.26/1, pp. 77-82.
16. Kahng, C. H.; Rajurkar, K. P., (1977) "Fundamental theories of the parameters of EDM process," *SME Technical Paper No. MR77-285*.
17. Konig, W., Sparrer M., (1994), "Electro-polish finishing of three-dimensional geometries produced by means of electro-discharge machining", *Production Engineering*, v.2, n.1., pp.79-82
18. Kruth, J. P., Van Coppenolle B., (1995) "New trends in automatic control of electro-discharge machining", *Proceedings of 4th International conference on monitoring and automatic supervision in manufacturing*, Warsaw, Poland, pp.283-294
19. Kruth, J. P., (1979) "Adaptive control optimization of electro-discharge machining, doctoral thesis, K.U. Leuven, Fac. Applied Sciences, Department of Mechanics, Div PMA.
20. Kunieda M., Yanatori, K., (1997) "Study of debris movement in EDM gap", *International Journal of Electrical Machining*, v.2, pp.43-49
21. Lee, H.T., Yur, J.P., (2000), "Characteristic analysis of EDMed surfaces using the Taguchi approach", *Materials and Manufacturing Processes*, v15, n6, Nov, pp. 781-806.
22. Lloyd, H. K., Warren, R. H., (1965) "Metallurgy of spark-machined surfaces" , *Journal of Iron and Steel institute*, pp.238-247
23. Luc, S., (1998) "Improvement of surface quality in die-sink EDM", doctoral thesis, Kruth J. P., fac. Applied Sciences, Department of metallurgy and material sciencem Div PMA
24. Luo, Y.F., (1998), "Investigation into the actual EDM off-time in SEA machining", *Journal of Materials Processing Technology*, v74, pp.61-68
25. Luo, Y.F.; Chen, C.G., (1990), "Effect of a pulsed electromagnetic field on the surface roughness in superfinishing EDM" , *Precision Engineering*, pp. 97-100
26. Masaki T., Kawata K., Masuzawa T., (1990) "Micro Electro-Discharge machining and its applications", *Proceedings of IEEE Micro Electro Mechanical Systems*
27. Masanori K., Masashiro Y., (1997) "Electro-Discharge Machining in Gas", *Annals Of CIRP*, v.46/1/97, pp.143-146

28. Masuzava, T., Tanaka, K., Nakamura, Y. (1983) " Water-based dielectric solution for EDM", Annals of CIRP, v.38, n.1, pp.119-122
29. Meshcherriakov, G.N., Charugin, N.V., May L.V., (1980) "Physico-chemical surface phenomena in EDM process and metal transfer", Annals of CIRP, v29, n.1, pp.117-122
30. Miller, P.; Guha, A., (1998), "Effects of electrical discharge machining on the surface characteristics of mold materials", Proceedings of ANTEC Conference, pp.857-863
31. Montgomery, D. C, (2000) Design and Analysis of Experiments, 5th Edition, Wiley , New York.
32. Myers, R. H.; Montgomery, D. C., (1995), Response Surface Methodology: Process and Product Optimization, A Wiley, New York.
33. Namiya, H., Mohri N., Saito N., Ootake H., Tsunekawa Y., Takawashi, T., Kobayashi K., (1989) "EDM by suspended powder suspended working fluid", Internation Symposium of Electromachining (IX), pp.5-8
34. Pandit, S. M.; Rajurkar, K. P., (1978) "A mathematical model for electro-discharge machined surface roughness," Trans. and Proc. of the 8th NAMRC, , pp. 339-345.
35. Pandit, S. M.; Rajurkar, K. P., (1980), "Data dependent systems approach to EDM process modeling from surface roughness profiles," Annals of the CIRP, Vol. 29/1, pp. 107-112.
36. Rajurkar, K. P., (1985) "Surface damage and shock waves in EDM, " Trans. and Proc. of the 13th NAMRC, , pp. 379-385.
37. Rajurkar, K. P.; Pandit, S. M., (1982), "Prediction of metal removal rate and surface roughness in electrical discharge machining," Trans.and Proc. of the 10th NAMRC, pp. 444-450.
38. Rajurkar, K. P., (1985) "Modeling and analysis of electro-discharge machining process," Proc. of the VIII Brazilian Congress of Mechanical Engineering.
39. Rebelo, J.C.; Dias, A. M.; Kremer, D.; Lebrun, J.L., (1998), "Influence of EDM pulse energy on the surface integrity of martensitic steels", Journal of Materials Processing Technology, v.84, n1-3 , pp.90-96
40. Rhoades, L.,(1996), "Understanding EDMed surfaces", Cutting tool engineering, v. 48 n3,
41. Scheller, W.L. II, Kanadi, I., (1997) "Effects on workpiece surface finish of EDM electrode grain size", Proceedings of the 1997 6th Annual Industrial Engineering Research Conference, Miami, Florida, pp.856-860

42. Shehata, F., Hanna H., Kohail, A., Mahrous, S., (1996) “ Surface integrity of electro-discharge machined inconel and steel alloys”, Proceedings of the pacific conference on manufacturing, v.2, Seoul, Korea
43. Sherman, J., (1995) “ EDM conquers copper”, Cutting Tool Engineering. V.47,pp.24-31
44. Singh, U. P., Miller, P. P. Urquhart, W. (1985), “Influence of EDM parameters on machining characteristics”, Proceeding of 25th international machine tool design Conference, pp.337-345
45. Soni, J.S., Chakraverti, G. (1997) “Performance evaluation of rotary EDM by experimental design technique”, Defense Science Journal, v47, pp. 65-73
46. Stephen R. Schmidt, Robert G. L., (1994) Understanding Industrial Designed Experiments, Air Academy Press & Associates,
47. Spedding, T.A., Wang, Z.Q., (1997) “Study on modeling of wire EDM process”, Journal of Materials Processing Technology_ v. 69, n1-3, pp. 18-28
48. Tomlison, W.J., Adkin J.R., (1992) “Microstructure and properties of electro-discharge machined surfaces”, Surface Engineering, v.8, n4, pp.183-188
49. Uno Y., Okada A., (1997) “ Surface generation mechanism in electrical discharge machining with silicon powder mixed fluid”, International Journal of Electrical Machining, v.2, pp.13-18
50. Wang, W.M., Liu, J.C., (1986), “Spectrum Analysis of Radio frequency Signal in EDM and its application”, Proceedings of 8th International Symposium on Electro-machining, pp.59-63
51. Williams, R. E.; Rajurkar, K. P., (1991)"Study of wire electrical discharge machined surface characteristics," Journal of Material Processing Technology Vol. 28/1-2, pp. 127-138.
52. Wong, Y.S., Lee, L.c., Lim L.C., (1989) “ EDM induced surface defects on tool steels”, International Symposium on Electromachining, v.9, pp.3-28
53. Wong, Y.S., Lim, L.C., Lee, L.C., (1995) “Effects of flushing on electro-discharge machined surfaces”, Journal of Materials Processing Technology, V.48, n1-4, pp. 299-305.
54. Wong, Y.S., Rahuman, I. (1998) “Near-mirror-finish phenomenon in EDM using powder-mixed dielectric”, Journal of Material Processing Technology, v.79, pp.30-40.

APPENDIX

9. APPENDICES

9.1 Hansvedt MS 50C RAM EDM machine

CNC RAM ELECTRICAL DISCHARGE MACHINE

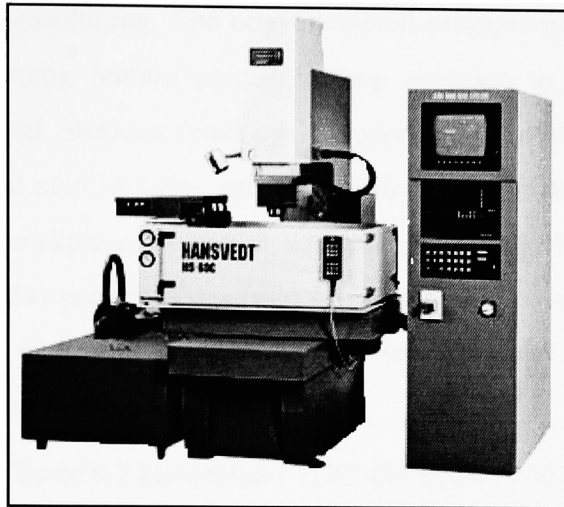


Figure 9.1 Hansvedt MS-50C 5 Axis CNC RAM EDM machine

Table 9.1 Specifications for Hansvedt MS 50c Ram electro-discharge machine

Machine	
Table Dimension	19.7x 13.8"/500x350mm
Worktank Dimensions	32.3x19.7x11.8"/ 820x500x300mm
Table Travel	
X axis	11.8"/300mm
Y axis	7.9"/200mm
Ram travel	11.8"/300mm
Platen to table distance	9.8 to 21.7"/ 250 to 550mm
Electrode weight	132lb/ 60kg
Workpiece Capacity	1,102lb/ 500kg
Net weight	2,205lb/ 1000kg
Dimesion	47.2x53.1x88.5"/ 1200x 1350x2250mm
Power Supply	
Peak Current	50Amp
Electrode Wear	0.20%
Input Power	220VAC
Net Weight	397lb/180kg
Dimensions	22x41x74" / 560 x 1040 x 1880 mm
Dielectric System	
Reservoir Capacity	74US gal/ 280Liter
Filter Type	Paper
Net weight	Built in
Dimensions	Built in

10.2 HEIDE7NHAIN TNC406 EROSION TABLE

The TNC 406 is a shop-floor programmable contouring control with five axes for ram-type electrical discharge machines. It features conversational programming and excellent graphic simulation of workpiece machining. The conversational programming is highly user friendly. Its background-programming feature permits a new program to be created while another program is being executed. Besides fixed cycles, coordinate transformations and parametric programming, the control also includes path functions for spark erosion and edge-finder and centering functions for workpiece alignment with the electrode. Multiple orbit programs and eroding parameters are also present. Files (part programs, erosion tables etc) can be output to peripheral devices and read into the control via the RS-232-C data interface, allowing programs to be created and stored externally.

Table 9.2 Heidenhain TNC 406 Erosion table

PULSE ON & OFF TIME STEP TABLE LIST				LOW VOLTAGE CURRENT STEP TABLE LIST			
Step	On & Off time (μ s)	Step	On & Off time (μ s)	Step	L.V. Current (A)	Step	L.V. Current (A)
1	1.5	13	50	1	0	16	22
2	2	14	75	2	0.5	17	26
3	3	15	100	3	1.5	18	30
4	4	16	150	4	2	19	35
5	5	17	200	5	3	20	40
6	6	18	300	6	3.5	21	45
7	7	19	400	7	4.5	22	50
8	9	20	600	8	5.5	23	55
9	12	21	800	9	6	24	60
10	18	22	1200	10	8	25	75
11	25	23	1600	11	10	26	100
12	36	24	2400	12	12	27	125
				13	16	28	150
				14	18	29	225
				15	20	30	300

9.3 CNC Program for machining

```
01 TOOL DEF 1 L+0 R+0.5  Tool definition is set up
02 TOOL CALL 1 Z U+0 F
03 X +0 R0 F MAX M37
04 Y +0 R0 F MAX M37
05 Z +0 R0 F MAX M37
06 M08
07 M40
08 M48
09 CYCL DEF 1.0 GENERATOR
10 CYCL DEF 1.1 P-TAB 920
11 CYCL DEF 1.2 MAX=25 MIN=1
12 FN 0: Q99 = +13
13 L X+0 Y+0 Z -0.75 R0 F MAX M 36  Tool approach in Z direction (.75 Inch)
14 STOP M02
15 END PGM 1200 INCH
```

Zero correction all direction (X, Y and Z)

Cycle definition settings

9.4 MITUTOYO SJ 401 Surface Roughness Profilometer

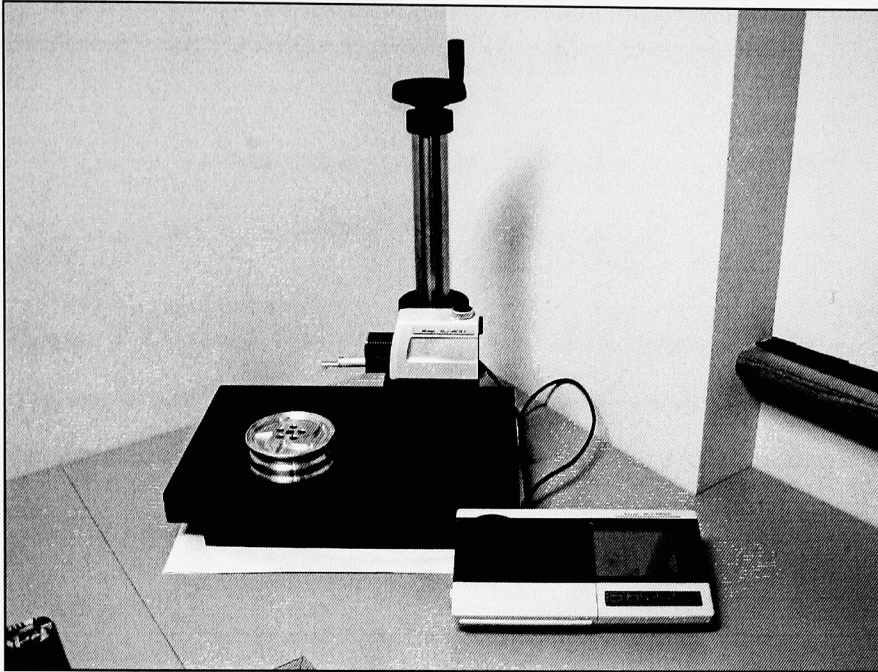


Figure 9.2 Mitutoyo SJ 401 surface roughness profilometer

Table 9.3 Specifications for Mitutoyo SJ 401 surface roughness profilometer

Specification	
Parameters	Ra, Ry, Rz, Rq, S, Sm, Pc, R3z, mr, Rt, Rp, Rpk, Rvk, Rk, Rv, Mrl, Mr2, Lo, Ppi, RAR, Rx, A1, A2, sc
Traversing Range	.5" (12.5mm)
Range (μm)	12000 μ " (300 μm)
Measuring Speed	.01"/s (0.25mm/s) , .02"/s (0.5mm/s) At Return: .03"/s (1mm/s)
Power Supply	AC adapter/Battery (Rechargeable)
Dimensions	
Drive /Detector Unit	5.52X.91X1.02"
Analyzer Unit	12.09x6.50x3.70"
Mass Approx.	3.1lbs (1400g)
Filters	2RC, PC75, GAUSS (GAUSSIAN)
Standards	JIS- B0601-1982, JIS B0601-1994, DIN, ANSI, ISO
Cutoff lengths	0.08mm, 0.25mm, 0.8mm, 2.5mm, 8mm

9.5 Theory for direction of steepest descent step size calculation

The problem of finding the factor settings on the steepest ascent/descent direction that are located a distance ρ from the origin is given by the optimization problem,

$$\begin{aligned} &\text{Maximize } b_0 + b_1x_1 + b_2x_2 + \dots + b_kx_k \\ &\text{subject to : } \sum_{i=1}^k x_i^2 \leq \rho^2 \end{aligned}$$

To solve it, use a Lagrange multiplier approach. First, add a penalty λ for solutions not satisfying the constraint (since we want a direction of steepest ascent, we maximize, and therefore the penalty is negative). For steepest descent we minimize and the penalty term is added instead.

$$\text{Maximize } L = B'x - \lambda (x'x - \rho^2)$$

Compute the partials and equate them to zero

$$\frac{\partial L}{\partial x} = b - 2\lambda x = 0$$

$$\frac{\partial L}{\partial \lambda} = -(x'x - \rho^2) = 0$$

These two equations have two unknowns (the vector x and the scalar λ) and thus can be solved yielding the desired solution:

$$x' = \rho \frac{b}{\|b\|}$$

or, in non-vector notation:

$$x_i' = \rho \frac{b_i}{\sqrt{\sum_{j=1}^k b_j^2}} \quad i = 1, 2, \dots, k$$

From this equation we can see that any multiple ρ of the direction of the gradient ($b / \|b\|$) will lead to points on the steepest ascent direction. For steepest descent, use instead $-b_i$ in the numerator of the equation above.

9.5 Surface Roughness Descriptors: (Source: Mitutoyo SJ 401 Operation Manual)

This section gives the definition of all major surface roughness descriptors which are used in this thesis work. Each parameter explained below are defined as calculated in the sampling length.

Arithmetic Mean Deviation of profile, Ra

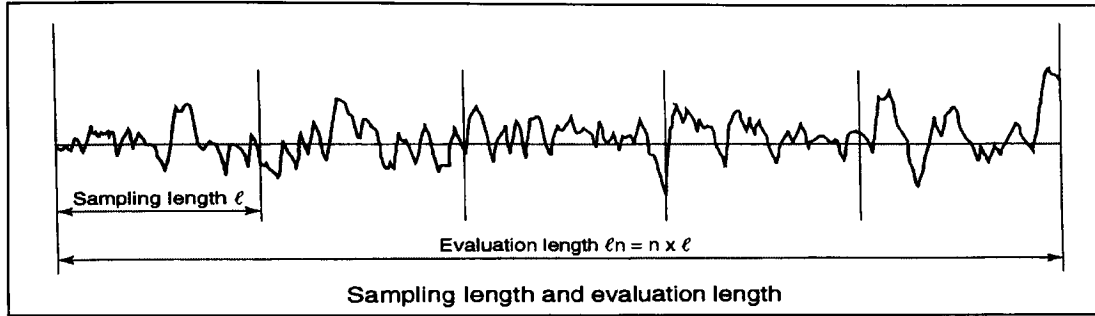


Figure 9.4 Arithmetic mean deviation of profile, Ra

Ra is arithmetic mean of the absolute values of the profile deviations (Y_i) from the mean line.

$$R_a = \frac{1}{N} \sum_{i=1}^N |Y_i|$$

Root mean Square deviation of profile , Rq

Rq is the square-root of the arithmetic mean of the square of profile deviation (Y_i) from the mean line.

$$R_q = \sqrt{\left(\frac{1}{N} \sum_{i=1}^N Y_i^2 \right)}$$

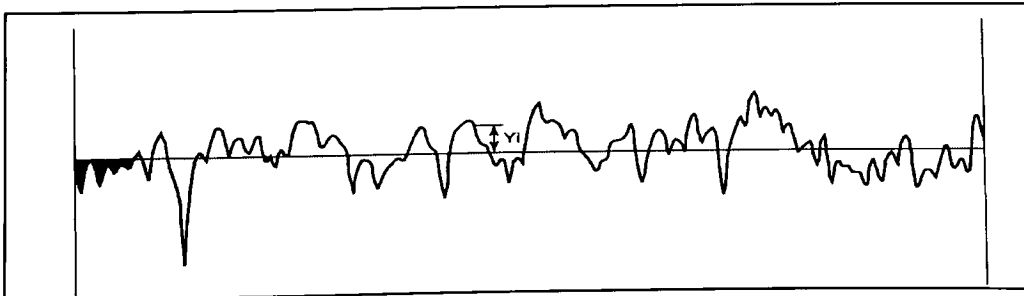


Figure 9.5 Root mean square deviation of profile, Rq

Maximum height of the profile, R_y

R_y is the sum of height Y_p of the highest peak from the mean line and depth Y_v of the deepest valley from the meanline.

$$R_y = Y_p + Y_v$$

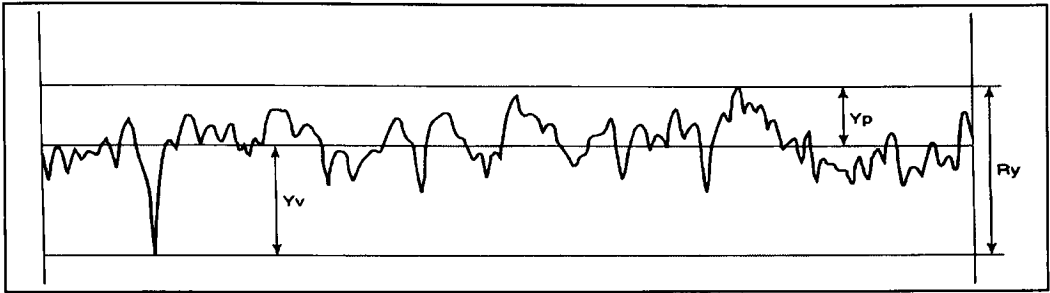


Figure 9.6 Maximum height of the profile, R_y

Ten-point height of irregularities, R_z

Sum of mean height of the five highest of the five highest profile peaks and mean depth of five deepest profile valleys measured from a line parallel to the mean line.

$$R_z = \frac{1}{5} \sum_{i=1}^5 Y_{pi} + \frac{1}{5} \sum_{i=1}^5 Y_{vi}$$

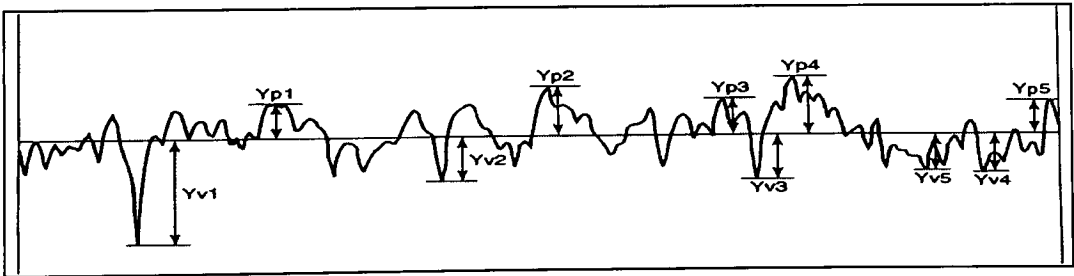


Figure 9.7 Ten-point height of irregularities, R_z

Skewness of the profile, R_{sk}

R_{sk} represents the degree of bias either in the upward or downward direction of an amplitude distribution curve*1. The skewness of a profile, R_{sk} is given by following formula

$$R_{sk} = \frac{1}{R_q^3} * \frac{1}{n} \sum_{i=1}^5 Y_{pi}$$

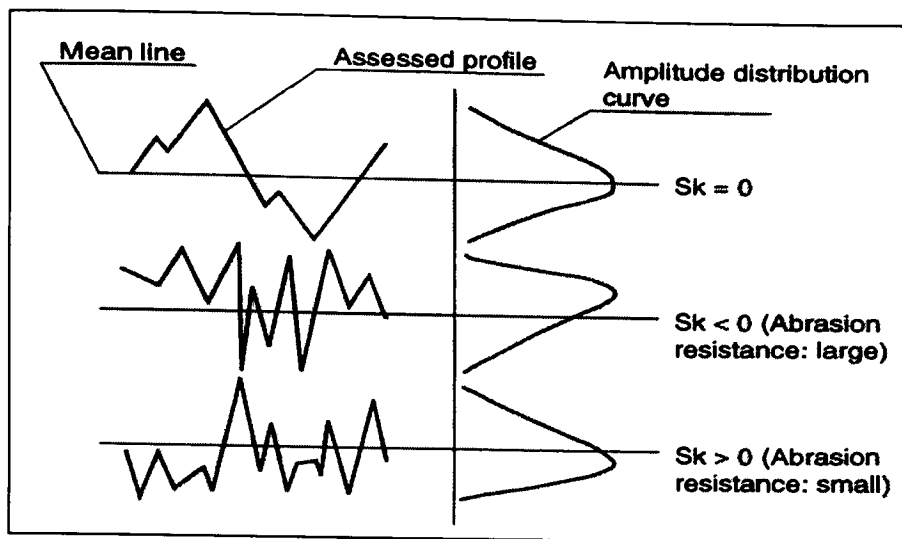


Figure 9.8 Skewness of Profile , Rku

Kurtosis of the profile , Rku

Rku represents the degree of concentration around the mean line of an amplitude distribution curve. The kurtosis of a profile, Rku is given by following formula.7

$$R_{ku} = \frac{1}{R_q^4} * \frac{1}{n} \sum_{i=1}^n Y_i^4$$

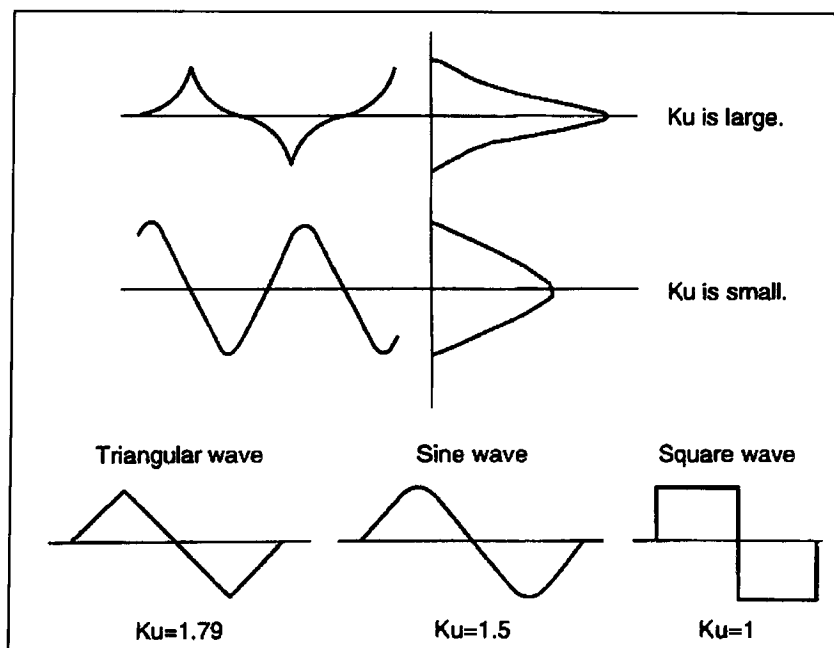


Figure 9.9 Kurtosis of the profile, Rku

Table 9.4. Detailed results of measured responses of Screening experiment (First Iteration)

108

Table 9.5. Detailed results of measured responses of Screening experiment (Second Iteration)

		Ra (μm)				Rv				Rq (μm)				Rku (μm)			
		Rep1	Rep2	Rep3	Avg	Rep1	Rep2	Rep3	Avg	Rep1	Rep2	Rep3	Avg	Rep1	Rep2	Rep3	Avg
1	(1)	5.40	4.43	5.17	5.00	35.10	31.20	39.00	35.10	30.30	24.40	30.00	28.23	6.66	5.57	6.44	6.22
2	a	7.62	7.27	7.09	7.33	53.800	47.00	37.90	46.23	39.40	40.20	34.00	37.87	9.48	9.22	8.70	9.13
3	b	17.92	17.07	17.93	17.64	102.00	3.60	107.30	97.63	81.80	71.60	81.40	78.27	22.14	20.43	21.81	21.46
4	ab	14.41	14.51	16.83	15.25	86.40	88.30	92.60	89.10	65.20	70.50	79.90	71.87	17.31	17.65	20.16	18.37
5	c	8.00	8.84	8.16	8.33	50.80	55.50	49.20	51.83	40.90	46.80	44.10	43.93	9.97	10.85	10.04	10.29
6	ac	8.64	8.71	8.13	8.49	52.00	58.20	49.60	53.27	43.20	43.00	39.70	41.97	10.88	10.75	10.06	10.56
7	bc	15.38	14.32	15.09	14.93	114.90	85.60	95.60	98.70	75.90	68.00	84.10	76.00	19.00	17.57	19.32	18.63
8	abc	14.09	15.06	16.38	15.18	84.10	81.00	102.30	89.13	64.20	70.60	81.20	72.00	17.47	18.72	20.44	18.88
9	d	7.38	8.24	7.61	7.74	49.30	55.30	53.60	52.73	38.40	42.50	44.40	41.77	9.01	10.20	9.98	9.73
10	ad	6.68	6.38	6.81	6.62	50.20	37.70	44.10	44.00	35.40	35.40	38.50	36.43	8.40	7.98	8.47	8.28
11	bd	13.76	13.86	12.05	13.22	81.80	87.50	10.70	93.33	66.00	71.20	65.60	67.60	16.96	17.02	15.81	16.60
12	abd	17.18	16.72	15.64	16.51	118.60	104.20	80.07	100.96	83.60	84.10	72.30	80.00	21.4	22.09	18.77	20.75
13	cd	10.02	9.43	10.42	9.96	60.02	64.50	72.40	55.64	45.00	47.20	51.30	47.83	12.56	11.75	12.93	12.41
14	acd	8.28	8.85	7.78	8.30	53.80	47.60	44.80	48.73	44.40	43.10	41.40	42.97	10.37	10.59	9.68	10.21
15	bcd	20.21	20.77	20.52	20.50	98.30	99.30	1.60	99.73	86.00	85.40	99.50	90.30	24.32	24.84	25.26	24.81
16	abcd	17.64	17.98	18.50	18.04	94.30	113.60	111.70	106.53	77.50	83.60	83.20	81.43	21.21	21.73	23.27	22.07
17	e	8.10	8.20	8.31	8.20	45.30	62.40	48.80	52.17	38.70	41.20	44.80	41.57	9.97	10.28	10.33	10.19
18	ae	8.36	7.79	8.70	8.28	45.50	43.00	42.00	46.90	40.50	38.80	42.40	40.57	10.15	9.44	10.77	10.12
19	be	13.97	13.82	11.85	13.21	80.70	83.50	84.00	82.73	66.40	62.30	64.20	64.30	16.75	16.62	64.2	32.52
20	abe	15.66	14.36	15.91	15.31	83.30	83.70	87.31	84.77	73.50	65.20	72.90	70.53	18.83	17.80	19.18	18.60
21	ce	8.79	9.64	8.25	8.89	55.80	50.90	53.30	53.33	45.00	46.40	46.00	45.80	10.94	11.76	10.34	11.01
22	ace	6.87	7.10	7.57	7.18	47.60	4.40	42.90	44.97	37.70	37.30	37.20	37.40	8.64	8.89	9.48	9.00
23	bce	16.58	15.02	18.00	16.53	105.60	88.40	7.80	100.60	81.60	66.60	77.50	75.23	20.92	18.37	22.29	20.53
24	abce	20.79	19.05	18.81	19.55	116.70	107.20	132.40	118.77	99.90	78.40	86.30	88.20	25.21	23.61	24.18	24.33
25	de	6.60	6.30	6.89	6.60	53.10	39.70	45.40	46.07	37.60	35.90	35.30	36.27	8.42	7.99	8.54	8.32
26	ade	7.75	7.80	8.22	7.92	50.80	67.00	57.60	58.47	40.60	44.00	44.50	43.03	9.83	10.00	10.38	10.07
27	bde	17.08	14.80	17.17	16.37	86.10	89.20	84.00	86.43	77.90	73.60	72.00	74.50	20.49	18.95	20.37	19.94
28	abde	16.38	17.19	18.25	17.27	92.00	111.42	99.30	100.90	76.30	81.90	81.00	79.73	20.38	21.49	22.11	21.33
29	cde	9.06	9.36	8.84	9.09	57.30	56.90	57.50	57.23	47.80	49.30	44.40	47.17	11.21	11.57	10.90	11.23
30	acde	8.51	8.08	9.62	8.74	62.30	42.31	73.40	59.33	48.10	40.30	48.10	45.50	10.84	10.01	12.37	11.07
31	bcde	18.76	20.14	20.44	19.78	116.70	141.3	144.90	134.30	83.10	88.90	94.70	88.90	22.71	25.09	25.41	24.40
32	abcde	21.88	21.15	20.12	21.05	138.50	105.3	105.50	116.43	91.50	97.20	91.60	93.43	27.64	25.74	24.54	25.97

Table 9.6. Detailed results of measured responses of first iteration (first replicate)

ID	Condition	F ₁ (μm)					F ₂					F ₃					R _g (μm)					R _{ku} (μm)							
		Rep1	Rep2	Rep3	Avg	Std	Rep1	Rep2	Rep3	Avg	Std	Rep1	Rep2	Rep3	Avg	Std	Rep1	Rep2	Rep3	Avg	Std	Rep1	Rep2	Rep3	Avg	Std			
1	(1)	4.58	4.96	4.85	4.80	0.15	34.40	30.10	33.70	32.73	0.25	29.00	25.90	28.80	27.90	0.10	5.79	6.01	6.00	5.93	0.06	0.26	0.26	0.48	0.33	3.32	2.61	3.83	3.25
2	a	5.49	4.74	5.38	5.20	0.12	32.10	34.80	34.10	33.67	0.20	29.90	27.70	29.20	28.93	0.15	6.71	5.98	6.57	6.42	0.10	0.17	0.17	-0.06	0.14	2.51	3.06	2.50	2.69
3	b	7.82	8.84	9.65	8.77	0.25	51.40	52.90	49.80	51.37	0.15	42.60	47.40	46.10	45.37	0.10	9.92	11.25	11.98	11.05	0.15	0.43	0.43	0.06	0.32	2.96	3.16	2.52	2.88
4	ab	8.64	7.82	7.11	7.86	0.20	52.20	50.90	51.30	51.47	0.10	47.00	41.10	40.50	42.87	0.15	11.11	9.74	9.02	9.96	0.10	0.01	0.01	0.19	0.26	3.19	2.78	3.05	3.01
5	c	6.87	6.97	7.48	7.11	0.10	67.60	55.30	42.60	55.17	0.15	41.40	39.60	35.50	38.83	0.10	9.63	9.25	8.98	9.29	0.10	-0.14	-0.14	0.18	-0.24	5.90	3.02	2.58	3.83
6	ac	6.77	6.60	6.54	6.64	0.05	46.30	38.90	38.30	41.17	0.10	37.70	36.00	35.90	36.53	0.05	8.40	8.20	8.15	8.25	0.05	0.16	0.16	0.15	0.09	2.87	2.62	2.64	2.71
7	bc	10.04	9.17	10.10	9.77	0.15	51.90	62.30	59.00	57.73	0.10	47.70	49.80	49.40	48.97	0.10	11.98	11.71	12.28	11.99	0.10	0.37	0.47	0.27	0.37	2.35	2.98	2.42	2.58
8	abc	11.30	10.81	7.55	9.89	0.20	65.80	70.30	47.30	61.13	0.15	59.60	56.30	40.70	52.20	0.10	14.09	13.71	9.46	12.42	0.10	0.22	0.22	0.40	0.24	2.83	3.20	2.98	3.00
9	d	6.44	5.99	6.44	6.29	0.10	36.90	36.00	48.00	40.30	0.10	33.20	30.50	36.00	33.23	0.10	7.87	7.22	8.18	7.76	0.10	-0.17	-0.23	-0.09	-0.16	2.50	2.41	2.19	2.37
10	ad	4.91	5.31	6.27	5.50	0.15	30.90	35.70	36.70	34.43	0.10	29.90	27.50	29.20	28.87	0.10	6.23	6.59	7.41	6.74	0.04	0.17	0.17	0.12	0.11	3.07	2.75	2.21	2.68
11	bd	8.23	8.76	8.06	8.35	0.10	51.30	50.10	45.40	48.93	0.10	39.50	41.30	41.30	40.70	0.10	9.97	10.53	9.78	10.09	0.10	-0.10	-0.10	-0.04	-0.01	2.49	2.42	2.47	2.46
12	abd	8.78	7.77	7.74	8.10	0.10	47.00	50.00	59.50	52.17	0.10	43.70	43.00	47.80	44.83	0.10	10.81	9.86	10.13	10.27	0.53	0.37	0.34	0.34	0.41	2.71	3.31	3.50	3.17
13	cd	8.03	8.02	7.95	8.00	0.05	56.40	45.50	49.70	50.53	0.10	43.10	42.00	38.00	41.03	0.10	10.09	9.82	9.70	9.87	0.18	0.37	0.07	0.21	0.21	2.98	2.59	2.47	2.68
14	acd	8.11	8.01	8.02	8.05	0.05	60.70	60.10	48.60	56.47	0.10	42.40	42.50	41.50	42.13	0.10	10.48	10.09	9.93	10.17	-0.33	-0.13	-0.16	-0.21	-0.21	3.58	3.25	2.72	3.18
15	bcd	11.70	11.09	10.07	10.95	0.10	69.10	76.00	58.01	67.70	0.10	55.20	55.20	48.00	52.80	0.10	14.15	14.32	12.37	13.61	0.30	0.32	0.33	0.32	0.32	2.45	3.18	2.58	2.74
16	abcd	11.13	9.94	9.08	10.05	0.08	60.40	57.90	50.30	56.20	0.10	53.00	51.30	42.80	49.03	0.10	13.71	12.35	11.11	12.39	0.47	0.20	-0.05	-0.05	0.21	2.56	2.81	2.33	2.57
17	0	8.10	7.92	6.96	7.66	0.10	51.90	46.20	45.00	47.70	0.10	42.60	39.20	35.70	39.17	0.10	9.93	9.64	8.73	9.43	0.23	0.28	0.14	0.22	0.22	3.09	2.55	2.81	2.82
18	0	8.27	7.76	9.83	8.62	0.10	53.20	43.70	52.10	49.67	0.10	43.60	41.10	44.30	43.00	0.10	10.47	9.65	11.76	10.63	0.39	0.48	0.22	0.36	0.36	2.85	2.85	2.25	2.65
19	0	7.59	6.73	7.74	7.35	0.10	40.30	43.20	60.10	47.87	0.10	37.20	36.30	45.80	39.77	0.10	9.08	8.47	10.32	9.29	0.11	-0.06	0.12	0.06	0.12	2.32	2.76	3.57	2.88
20	0	9.06	7.33	7.47	7.95	0.10	65.10	46.60	48.30	53.33	0.10	49.90	37.30	39.20	42.13	0.10	11.34	9.16	9.26	9.92	0.16	0.27	0.05	0.16	0.16	5.90	3.02	2.58	3.83
21	0	8.01	8.15	8.30	8.15	0.05	45.70	55.50	57.60	52.93	0.10	41.00	43.90	46.60	43.83	0.10	9.90	11.40	10.44	10.58	-0.01	0.06	0.39	0.15	0.15	2.81	3.07	3.12	3.00
22	0	8.18	9.51	8.70	8.80	0.10	58.30	65.90	49.70	57.97	0.10	45.20	46.90	44.50	45.53	0.10	10.75	12.23	10.53	11.17	-0.29	0.34	0.14	0.06	0.06	3.41	3.70	2.54	3.22

Table 9.7. Detailed results of measured responses of first iteration experiment (second replicate)

ID	TCs	Ra (µm)					Rz (µm)					Rq (µm)									
		Rep1	Rep2	Rep3	Avg		Rep1	Rep2	Rep3	Avg		Rep1	Rep2	Rep3	Avg						
1	(1)	4.29	4.26	4.33	4.29		37.00	31.70	33.90	34.20		30.30	28.40	29.90	29.53		Rep1	Rep2	Rep3	Avg	
2	a	5.49	5.33	5.28	5.37		38.80	45.00	32.90	38.90		29.70	31.40	28.00	29.70		0.01	0.42	-0.23	0.07	
3	b	7.82	7.44	8.68	7.98		48.30	55.60	53.00	52.30		42.80	39.50	50.00	44.10		0.21	0.30	0.19	0.23	
4	ab	7.42	7.41	7.61	7.48		41.10	42.50	51.50	45.03		36.50	37.20	40.50	38.07		0.46	0.14	0.21	0.27	
5	c	6.67	7.41	7.29	7.12		43.40	55.40	42.60	47.13		35.20	39.60	35.50	36.77		0.43	0.27	0.23	0.31	
6	ac	6.82	6.42	7.15	6.80		47.30	43.30	53.70	48.10		38.00	34.90	40.60	37.83		-0.09	-0.14	0.18	-0.02	
7	bc	10.54	9.83	9.66	10.01		49.50	64.80	72.20	62.17		46.90	46.90	47.50	47.10		-0.40	-0.18	0.14	-0.15	
8	abc	8.36	10.04	8.86	9.09		54.90	62.90	61.40	59.73		42.60	48.40	53.40	48.13		0.31	0.00	0.56	0.21	
9	d	6.67	7.41	7.29	7.12		43.40	55.40	42.60	47.13		35.20	39.60	35.50	36.77		0.07	0.00	0.18	-0.02	
10	ad	6.82	6.42	7.15	6.80		47.30	43.30	53.70	48.10		38.00	34.90	40.60	37.83		-0.40	-0.18	0.14	-0.15	
11	bd	9.57	9.88	9.54	9.66		56.50	59.80	55.60	57.30		41.40	49.50	46.50	45.80		0.41	0.33	0.14	0.02	
12	abd	7.09	6.55	6.98	6.87		48.30	39.10	51.00	46.13		41.00	34.70	40.80	38.83		0.09	0.57	0.29	0.32	
13	cd	7.18	6.84	7.34	7.12		41.40	52.30	47.40	47.03		35.00	37.40	41.10	37.83		0.19	0.42	0.07	0.23	
14	acd	7.94	7.42	7.86	7.74		51.00	52.20	51.00	51.40		43.70	39.70	45.50	42.97		-0.01	-0.02	-0.36	-0.13	
15	bcd	10.62	9.95	9.88	10.15		75.10	57.20	51.50	61.27		56.40	48.80	44.20	49.80		0.40	0.45	-0.09	0.25	
16	abcd	11.04	12.14	12.18	11.79		64.30	76.90	58.80	66.67		52.00	58.20	47.80	52.67		0.40	0.20	0.65	0.42	
17	0	7.56	7.76	7.30	7.54		44.60	51.90	48.00	48.17		39.50	41.90	37.20	39.53		0.26	0.44	0.28	0.33	
18	0	8.69	9.97	9.56	9.41		49.60	75.50	52.50	59.20		41.40	53.90	45.10	46.80		0.38	-0.53	-0.04	-0.06	
19	0	7.31	7.16	7.71	7.39		44.10	44.30	49.10	45.83		37.50	37.80	42.21	39.17		0.30	0.14	0.40	0.28	
20	0	9.28	9.31	9.77	9.45		54.40	58.70	67.30	60.13		45.80	45.50	51.90	47.73		0.24	0.05	-0.05	0.08	
21	0	8.23	8.79	8.92	8.65		53.90	60.10	51.40	55.13		41.60	43.70	48.20	44.50		0.72	-0.10	-0.11	0.17	
22	0	9.38	10.28	9.48	9.71		58.50	68.00	55.30	60.60		48.30	48.70	49.30	48.77		-0.35	-0.22	0.44	-0.04	
																	0.261	0.325	0.289	0.292	

Table 9.8. Detailed results of measured responses of second experiment (first replicate)

		Ra (µm)												Rz (µm)												Rku (µm)			
		Rep1	Rep2	Rep3	Avg	Rep1	Rep2	Rep3	Avg	Rep1	Rep2	Rep3	Avg	Rep1	Rep2	Rep3	Avg	Rep1	Rep2	Rep3	Avg	Rep1	Rep2	Rep3	Avg				
1	(1)	3.92	3.48	3.56	3.65	21.40	22.00	20.40	21.27	16.30	15.10	15.10	15.50	4.71	4.42	4.42	4.52	-0.01	0.02	0.04	0.02	2.51	3.09	2.62	2.74				
2	a	3.30	3.34	3.90	3.51	19.90	19.80	22.10	20.60	14.60	13.90	16.00	14.83	4.12	4.11	4.88	4.37	0.04	-0.12	0.09	0.00	2.87	2.90	2.71	2.83				
3	b	4.92	4.14	5.05	4.70	30.90	22.90	28.10	27.30	20.20	15.80	19.40	18.47	6.24	5.14	6.27	5.88	0.08	-0.27	-0.29	-0.16	2.82	2.64	2.71	2.72				
4	ab	5.34	4.19	4.93	4.82	30.90	22.90	28.10	27.30	20.20	15.80	19.40	18.47	6.24	5.14	6.28	5.89	0.08	-0.27	-0.29	-0.16	2.82	2.64	2.71	2.72				
5	c	4.92	4.14	5.05	4.70	30.90	22.90	28.10	27.30	20.20	15.80	19.40	18.47	6.24	5.14	6.27	5.88	0.08	-0.27	-0.29	-0.16	2.82	2.64	2.71	2.72				
6	ac	5.19	4.85	5.56	5.20	28.10	29.00	30.90	29.33	19.60	19.50	20.10	19.73	6.4	6.09	6.84	6.44	0.11	-0.05	-0.04	0.01	2.78	2.88	2.56	2.74				
7	bc	5.58	5.22	5.44	5.41	30.00	27.80	25.40	27.73	19.60	19.10	18.50	19.07	6.76	6.28	5.75	6.26	0.14	0.15	-0.15	0.05	2.51	2.34	2.50	2.45				
8	abc	5.57	5.48	5.68	5.58	28.90	30.80	31.20	30.30	21.70	20.10	21.70	21.17	6.81	6.69	6.93	6.81	-0.06	-0.17	0.14	-0.03	2.63	2.67	2.49	2.60				
9	d	4.12	3.88	3.82	3.94	23.60	24.50	23.30	23.80	16.80	16.00	16.50	16.43	5.06	4.97	4.81	4.95	0.08	-0.14	-0.25	-0.10	2.69	2.95	3.03	2.89				
10	ad	4.6	3.72	4.21	4.18	22.30	20.00	23.90	22.10	16.70	14.50	16.20	15.80	5.43	4.5	5.12	5.02	0.29	0.02	0.06	0.12	2.20	2.36	2.65	2.40				
11	bd	4.97	5.06	5.66	5.23	27.90	32.50	33.80	31.40	17.61	22.10	22.80	20.84	6.15	7.5	7.41	7.02	-0.19	0.14	0.08	0.01	2.55	2.64	2.66	2.62				
12	abd	5.31	4.84	5.57	5.24	34.50	28.70	31.40	31.53	20.0	18.60	20.20	19.60	6.87	5.95	6.94	6.59	0.37	0.38	0.38	0.38	3.44	3.42	2.85	3.24				
13	cd	4.84	4.86	5.13	4.94	26.70	23.60	28.70	26.33	17.80	16.60	20.00	18.13	5.93	5.08	6.38	5.80	-0.23	-0.30	-0.05	-0.19	2.68	2.63	2.65	2.65				
14	acd	4.54	4.66	4.89	4.70	25.40	28.20	25.10	26.23	18.00	18.40	18.40	18.27	5.56	5.72	5.94	5.74	-0.01	0.04	-0.02	0.00	2.54	2.72	2.40	2.55				
15	bcd	5.37	4.83	5.61	5.27	30.20	29.00	29.60	29.60	18.00	17.80	20.20	18.87	6.77	6.14	6.80	6.57	0.47	0.27	0.01	0.25	2.95	2.99	2.40	2.78				
16	abcd	5.97	5.69	5.55	5.74	35.20	30.40	33.80	33.13	20.90	19.70	21.40	20.67	7.56	7.01	7.10	7.22	0.10	0.34	-0.16	0.09	3.21	2.81	2.97	3.00				
17	0	3.8	4.22	5.25	4.42	23.00	24.10	28.00	25.03	16.40	17.10	20.10	17.87	4.78	5.22	6.43	5.48	-0.02	0.05	0.26	0.10	2.85	2.56	2.55	2.65				
18	0	4.49	4.92	4.21	4.54	26.00	27.60	24.20	25.93	18.34	18.80	17.0	18.05	5.57	6.04	5.22	5.61	-0.12	0.16	-0.15	-0.04	2.93	2.63	2.70	2.75				
19	0	4.25	4.53	4.64	4.47	24.60	25.30	24.50	24.80	16.80	18.00	18.70	17.83	5.2	5.53	5.71	5.48	-0.04	0.25	0.23	0.15	2.60	2.62	2.50	2.57				
20	0	4.76	4.78	4.66	4.73	26.40	26.40	30.30	27.70	18.40	17.80	18.20	18.13	5.81	5.8	6.041	5.88	-0.12	0.09	0.35	0.11	2.55	2.52	3.21	2.76				
21	0	5.42	6.1	5.71	5.74	32.30	31.20	31.80	31.77	19.70	21.20	20.50	20.47	6.86	7.45	5.43	6.58	0.00	-0.12	-0.16	-0.09	2.99	2.55	2.67	2.74				
22	0	4.81	5.36	5.19	5.12	28.00	29.20	28.10	28.43	19.10	19.90	19.60	19.53	6.1	6.58	6.4	6.36	-0.04	0.23	0.11	0.10	2.96	2.81	2.78	2.85				

Table 9.9. Detailed results of measured responses of second iteration experiment (second replicate)

Tos	Rav (mm)					Risk (µm)					Rku (µm)				
	Rep1	Rep2	Rep3	Avg	Rep1	Rep2	Rep3	Avg	Rep1	Rep2	Rep3	Avg	Rep1	Rep2	Rep3
1	3.44	3.66	3.75	3.62	20.30	21.40	20.50	20.73	14.30	15.40	15.00	14.90	2.56	3.07	2.32
2	3.86	4.03	3.83	3.91	21.80	22.90	21.50	22.07	16.30	16.50	16.10	16.30	2.92	2.88	2.41
3	4.79	4.96	4.66	4.80	27.00	27.40	27.80	27.40	18.20	18.90	0.00	12.37	2.87	2.62	2.41
4	4.97	4.73	4.48	4.73	27.80	26.80	23.30	25.97	18.10	18.90	16.50	17.83	2.87	2.62	2.41
5	3.87	3.64	3.99	3.83	22.66	24.50	24.70	23.95	16.30	15.50	17.80	16.53	2.87	2.62	2.41
6	4.34	4.66	5.09	4.70	25.40	25.80	27.90	26.37	16.90	17.90	18.80	17.87	2.83	2.86	2.26
7	5.14	5.80	5.67	5.54	29.90	31.00	33.00	31.30	19.40	21.20	20.90	20.50	2.56	2.32	2.20
8	5.43	5.96	5.92	5.77	30.10	35.20	30.80	32.03	21.20	22.90	21.30	21.80	2.68	2.65	2.19
9	4.14	4.45	3.60	4.06	23.40	26.00	21.50	23.63	16.70	17.40	14.90	16.33	2.74	2.93	2.73
10	4.27	4.26	4.21	4.25	25.30	27.70	29.20	27.40	17.90	18.80	19.70	18.80	2.25	2.34	2.35
11	5.45	5.42	5.67	5.51	30.30	28.90	32.70	30.63	19.90	17.80	20.50	19.40	2.60	2.62	2.36
12	4.93	5.05	4.31	4.76	27.30	25.00	26.10	26.13	18.20	18.00	18.50	18.23	3.49	3.40	2.55
13	5.02	4.99	4.98	5.00	26.40	27.90	26.40	26.90	18.60	18.40	18.40	18.47	2.73	2.61	2.35
14	4.86	4.68	4.97	4.84	25.90	27.70	29.20	27.60	17.90	18.80	19.70	18.80	2.59	2.70	2.10
15	5.53	5.68	5.72	5.64	31.60	31.10	34.80	32.50	19.90	19.60	21.20	20.23	3.00	2.97	2.10
16	7.38	6.69	6.44	6.84	41.70	37.50	34.20	37.80	28.90	24.10	24.60	25.87	3.26	2.79	2.67
17	4.33	4.61	4.63	4.52	26.30	25.20	27.10	26.20	18.30	17.50	17.70	17.83	2.90	2.54	2.25
18	4.39	4.82	4.95	4.72	27.40	26.10	28.50	27.33	17.50	17.30	18.40	17.73	2.98	2.61	2.40
19	4.64	4.81	4.60	4.68	27.50	26.80	26.00	26.77	18.00	19.40	17.60	18.33	2.65	2.60	2.20
20	5.61	5.55	5.20	5.45	29.30	34.00	28.80	30.70	20.50	21.70	20.00	20.73	2.60	2.50	2.91
21	5.31	5.17	5.62	5.37	25.70	27.90	29.30	27.63	18.70	17.60	20.10	18.80	3.04	2.53	2.37
22	4.78	4.92	4.46	4.72	26.10	28.80	25.20	26.70	18.60	19.80	18.20	18.87	3.01	2.79	2.48

Table 9.11. Detailed results of measured responses of fourth Iteration experiment (second replicate)

#	T ₅	R ₁ (µm)				R ₂ (µm)				R ₃ (µm)				R ₄ (µm)				R ₅ (µm)			
		Rep1	Rep2	Rep3	Avg	Rep1	Rep2	Rep3	Avg	Rep1	Rep2	Rep3	Avg	Rep1	Rep2	Rep3	Avg	Rep1	Rep2	Rep3	Avg
1	(1)	2.35	2.44	2.03	2.27	15.70	15.10	15.00	15.27	11.50	11.40	11.00	11.30	3.25	3.01	2.87	3.04	0.29	0.51	0.32	0.37
2	a	2.12	2.09	2.03	2.08	13.60	14.30	15.20	14.37	10.30	10.10	10.80	10.40	2.63	2.66	2.88	2.72	0.31	0.12	0.05	0.16
3	b	2.74	2.78	2.66	2.73	16.90	16.70	19.70	17.77	12.40	13.90	12.30	12.87	3.48	3.42	3.95	3.62	0.39	0.05	0.38	0.27
4	ab	2.50	2.47	3.11	2.69	16.30	17.60	19.30	17.73	11.40	12.40	10.30	11.37	3.45	3.32	2.98	3.25	0.24	0.19	0.35	0.26
5	c	3.17	2.99	2.93	3.03	19.30	18.50	17.10	18.30	14.50	13.40	12.90	13.60	3.92	3.74	3.59	3.75	0.10	0.17	0.63	0.30
6	ac	2.68	2.96	2.64	2.76	17.20	16.50	17.00	16.90	12.70	13.40	12.10	12.73	3.40	3.64	3.30	3.45	0.00	0.23	0.33	0.19
7	bc	3.36	3.33	3.20	3.30	19.70	21.30	21.50	20.83	14.80	14.30	14.10	14.40	4.13	4.12	4.05	4.10	0.24	0.06	0.20	0.17
8	abc	3.36	3.09	3.27	3.24	22.00	22.80	24.00	22.93	15.50	16.40	16.20	16.03	4.26	4.82	4.68	4.59	0.27	0.05	0.08	0.13
9	d	2.61	2.47	2.70	2.59	17.40	16.40	14.50	16.10	11.90	11.40	11.30	11.53	3.35	3.13	3.24	3.24	0.25	0.06	0.12	0.14
10	ad	2.44	2.55	2.31	2.43	16.80	15.90	13.90	15.53	11.50	11.60	10.70	11.27	3.45	3.22	2.97	3.21	0.00	0.24	0.09	0.11
11	bd	3.16	2.66	2.95	2.92	19.10	16.40	18.60	18.03	13.50	11.60	12.50	12.53	3.57	3.59	3.76	3.64	0.57	0.07	-0.17	0.16
12	abd	2.90	2.86	3.02	2.93	18.10	17.40	19.60	18.37	12.80	12.60	13.70	13.03	3.62	3.53	3.83	3.66	-0.10	0.21	0.27	0.13
13	cd	3.52	3.40	3.33	3.42	22.50	21.50	20.80	21.60	15.50	14.20	15.00	14.90	4.46	4.20	4.24	4.30	0.22	0.54	0.11	0.29
14	acd	3.90	3.35	3.35	3.53	22.90	22.30	19.80	21.67	15.50	15.30	14.50	15.10	4.29	4.15	4.15	4.20	0.22	0.26	0.08	0.19
15	bcd	3.35	3.78	3.77	3.63	22.00	22.80	24.00	22.93	15.50	16.40	16.20	16.03	4.26	4.82	4.68	4.59	0.26	0.33	0.09	0.23
16	abcd	3.87	3.99	4.04	3.97	23.40	24.30	23.90	23.87	15.70	16.00	16.60	16.10	4.80	4.97	5.04	4.94	0.09	0.05	0.01	0.05
17	0	2.73	2.68	2.73	2.71	16.50	16.90	16.90	16.77	12.00	12.20	12.20	12.13	3.41	3.36	3.39	3.39	0.17	0.44	0.19	0.27
18	0	2.45	2.34	2.75	2.51	14.90	15.70	17.20	15.93	11.30	11.50	12.60	11.80	3.02	3.18	3.40	3.20	0.32	0.09	-0.09	0.11
19	0	2.79	2.89	2.94	2.87	18.10	17.00	17.90	17.67	12.20	12.30	12.50	12.33	3.57	3.59	3.76	3.64	-0.15	-0.19	-0.31	-0.22
20	0	2.45	2.39	2.37	2.40	15.40	18.80	18.30	17.50	11.10	13.20	12.70	12.33	3.04	3.62	3.60	3.42	0.34	0.11	0.20	0.22
21	0	3.09	2.94	3.07	3.03	18.30	19.40	19.60	19.10	13.40	13.60	13.90	13.63	4.12	3.70	3.91	3.91	0.34	0.27	0.03	0.21
22	0	2.95	3.09	3.08	3.04	19.20	19.70	17.50	18.80	13.80	13.90	13.60	13.77	3.77	3.86	3.79	3.81	0.11	0.37	0.27	0.25

Table 9.12. Detailed results of measured responses of central composite design(first replicate)

TCS		Rz (µm)			Ra (µm)			Rsk (µm)			Rku (µm)														
		Rep1	Rep2	Rep3	Avg	Rep1	Rep2	Rep3	Avg	Rep1	Rep2	Rep3	Avg	Rep1	Rep2	Rep3	Avg								
1	(1)	2.15	2.16	2.04	2.12	12.9	14.5	13.1	13.50	9.3	9.7	8.7	9.23	2.65	2.76	2.55	2.65	-0.11	2.96	2.58	2.55	2.70			
2	a	1.94	1.63	1.84	1.80	11.7	11.4	13.2	12.10	8.9	8.3	8.8	8.67	2.4	2.08	2.42	2.30	0.12	0.27	-0.22	0.06	3.42	2.81	2.75	2.99
3	b	2.01	2	1.8	1.94	13	14.2	11.1	12.77	9	9	8.2	8.73	2.51	2.6	2.24	2.45	0.23	0.12	-0.1	0.08	3.12	3.33	3.24	3.23
4	ab	1.94	1.92	2.01	1.96	12.8	11.4	14	12.73	8.8	8.6	10.1	9.17	2.44	2.35	2.57	2.45	-0.21	-0.26	-0.2	-0.22	3.01	2.96	2.85	2.94
5	c	2.25	2.36	2.22	2.28	14	15.1	14.5	14.53	10.5	11.3	9.8	10.53	2.79	2.98	2.77	2.85	-0.15	-0.18	-0.01	-0.11	2.54	2.78	2.79	2.70
6	ac	2.28	2.14	2.09	2.17	15	14	13.4	14.13	11	10	10	10.33	3.02	2.74	2.61	2.79	0.14	0.16	0.21	0.17	2.23	2.12	2.11	2.15
7	bc	2.41	2.62	2.27	2.43	14.3	17.4	13.8	15.17	10.7	11.8	10.2	10.90	2.9	3.31	2.81	3.01	-0.18	0.26	0.1	0.06	2.65	3.25	2.93	2.94
8	abc	2.55	2.66	2.71	2.64	14.2	15.7	14.8	14.90	10.6	10.9	11	10.83	2.92	3.16	2.94	3.01	-0.23	-0.08	-0.23	-0.18	2.75	2.96	3.35	3.02
9	-αa	2	1.96	1.97	1.98	13.5	11.6	11.7	12.27	9.8	8.8	8.9	9.17	2.49	2.31	2.43	2.41	-0.23	-0.34	-0.02	-0.20	3.55	2.67	2.35	2.86
10	+αa	1.87	1.97	1.79	1.88	12.5	12.2	12.2	12.30	9	9.3	8.6	8.97	2.35	2.43	2.24	2.34	-0.21	-0.05	-0.28	-0.18	2.76	3.03	3.35	3.05
11	-αb	1.31	1.36	1.32	1.33	11.7	12.2	12.6	12.17	8.6	8.6	8.6	8.60	2.18	2.2	2.27	2.22	-0.22	-0.19	0.03	-0.13	2.76	2.72	3.12	2.87
12	+αb	2.06	2.09	2.01	2.05	14.5	13.2	13.4	13.70	9.9	9.7	9.1	9.57	2.59	2.61	2.54	2.58	0.23	0.34	0.16	0.24	3.01	3.11	2.72	2.95
13	-αc	1.29	1.13	0.94	1.17	9.7	9.9	10.9	10.17	7.1	6.8	7.3	7.07	1.86	1.79	2	1.88	0.21	-0.12	0.11	0.07	2.92	3.01	3.11	3.01
14	+αc	2.89	2.62	2.65	2.72	15.9	15.2	15.3	15.47	11.5	11.4	11.3	11.40	3.07	3.12	3.12	3.10	-0.08	0.12	0.21	0.08	2.77	2.93	3.03	2.91
15	0	1.98	2.04	2.15	2.06	13.1	13.9	13.5	13.50	9.3	9.5	9.3	9.37	2.48	2.58	2.72	2.59	-0.2	-0.51	-0.31	-0.34	2.87	3.65	3.4	3.31
16	0	2	2.03	1.96	2.00	13.4	13.5	12.1	13.00	9.1	9.4	9.3	9.27	2.44	2.58	2.46	2.49	-0.5	-0.32	0.18	-0.21	3.25	4.36	2.63	3.41
17	0	1.92	1.74	1.94	1.87	12.8	11.5	13.7	12.67	8.8	8.7	9.4	8.97	2.38	2.17	2.46	2.34	0.11	0.13	0.21	0.15	3.12	3.42	3.56	3.37
18	0	1.88	1.98	2.03	1.96	12.5	12.9	12.8	12.73	9.5	9.7	9.5	9.57	2.35	2.5	2.56	2.47	0.2	-0.13	-0.05	0.01	3.1	2.93	2.72	2.92
19	0	1.82	1.93	1.97	1.91	12.2	12.6	12.2	12.33	9.1	9.5	9.1	9.23	2.27	2.44	2.44	2.38	0.19	-0.16	-0.1	-0.02	3.24	3.25	2.77	3.09
20	0	1.71	1.82	1.83	1.79	11.4	14	11.9	12.43	8.1	8.9	9	8.67	2.12	2.32	2.26	2.23	-0.01	-0.02	-0.3	-0.11	2.54	3.13	2.65	2.77

		Rep1	Rep2	Rep3	Avg	Rep1	Rep2	Rep3	Avg	Rep1	Rep2	Rep3	Avg	Rep1	Rep2	Rep3	Avg	Rku (µm)							
1	(1)	2.15	2.16	2.04	2.12	12.90	14.50	13.10	13.50	9.30	9.70	8.70	9.23	2.65	2.76	2.55	2.65	-0.11	0.32	0.43	0.21	2.17	3.37	3.45	3.00
2	a	1.77	1.88	1.96	1.87	12.20	13.10	12.10	12.47	8.80	8.70	9.20	8.90	2.28	2.56	2.35	2.40	-0.11	0.22	-0.02	0.03	3.17	2.98	2.94	3.03
3	b	2.01	2.00	1.80	1.94	13.00	14.20	11.10	12.77	9.00	9.00	8.20	8.73	2.51	2.6	2.24	2.45	-0.5	0.32	-0.15	-0.11	2.97	2.76	2.99	2.91
4	ab	2.10	1.96	1.91	1.99	14.60	12.10	11.50	12.73	9.50	8.70	8.70	8.97	2.71	2.42	2.36	2.50	0.13	-0.09	0.46	0.17	3.13	2.84	2.85	2.94
5	c	2.01	2.25	2.28	2.18	14.50	12.50	13.30	13.43	10.20	10.00	9.40	9.87	2.59	2.52	2.78	2.63	0.09	0.17	0.16	0.14	3.14	3.05	2.98	3.06
6	ac	2.02	2.24	1.99	2.08	14.10	14.50	13.80	14.13	10.20	10.00	9.70	9.97	2.55	2.78	2.54	2.62	-0.19	0.2	-0.17	-0.05	3.00	3.12	4.56	3.56
7	bc	2.62	2.59	2.61	2.61	16.10	16.10	17.20	16.47	11.40	11.40	11.00	11.27	3.03	3.03	3.12	3.06	-0.11	-0.33	0.19	-0.08	2.67	3.1	2.95	2.91
8	abc	2.42	2.48	2.50	2.47	15.50	16.50	15.50	15.83	11.10	11.40	11.60	11.37	3.05	3.11	3.13	3.10	-0.22	-0.07	0.01	-0.09	2.83	2.86	2.48	2.72
9	-αa	1.33	1.48	1.30	1.37	11.80	12.70	14.10	12.87	9.20	9.10	9.80	9.37	2.37	2.40	2.52	2.43	-0.43	-0.11	-0.09	-0.21	3.12	3.21	3.44	3.26
10	+αa	1.94	2.06	1.96	1.99	12.80	12.90	12.20	12.63	9.10	9.70	9.10	9.30	2.45	2.57	2.44	2.49	-0.01	0.08	0.01	0.03	2.52	2.58	2.94	2.68
11	-αb	1.54	1.59	1.62	1.58	10.90	11.70	11.90	11.50	8.20	8.80	8.70	8.57	2.16	2.33	2.38	2.29	0.03	-0.11	-0.04	-0.04	2.62	3.44	2.78	2.95
12	+αb	2.33	2.02	2.03	2.13	14.80	13.90	14.00	14.23	11.00	10.90	9.50	10.47	2.92	2.89	2.56	2.79	0.01	0.00	0.3	0.10	2.15	2.19	2.23	2.19
13	-αc	1.34	1.23	1.23	1.27	10.70	10.30	10.30	10.43	7.60	7.40	7.40	7.47	2.04	1.93	2.04	2.00	-0.2	0.11	-0.34	-0.14	2.45	2.67	2.87	2.66
14	+αc	2.90	2.86	2.82	2.86	15.10	15.90	15.90	15.63	11.70	12.30	11.90	11.97	3.17	3.28	3.16	3.20	-0.04	-0.11	-0.09	-0.08	3.01	3.10	3.20	3.10
15	0	1.88	1.98	2.03	1.96	12.50	12.90	12.80	12.73	9.50	9.70	9.50	9.57	2.35	2.50	2.56	2.47	-0.23	0.22	0.00	0.00	2.87	2.81	2.78	2.82
16	0	1.82	1.93	1.97	1.91	12.20	12.60	12.20	12.33	9.10	9.50	9.10	9.23	2.27	2.44	2.44	2.38	-0.05	-0.06	0.05	-0.02	3.01	3.73	3.29	3.34
17	0	1.71	1.82	1.83	1.79	11.40	14.00	11.90	12.43	8.10	8.90	9.00	8.67	2.12	2.32	2.26	2.23	0							